

ChE 430

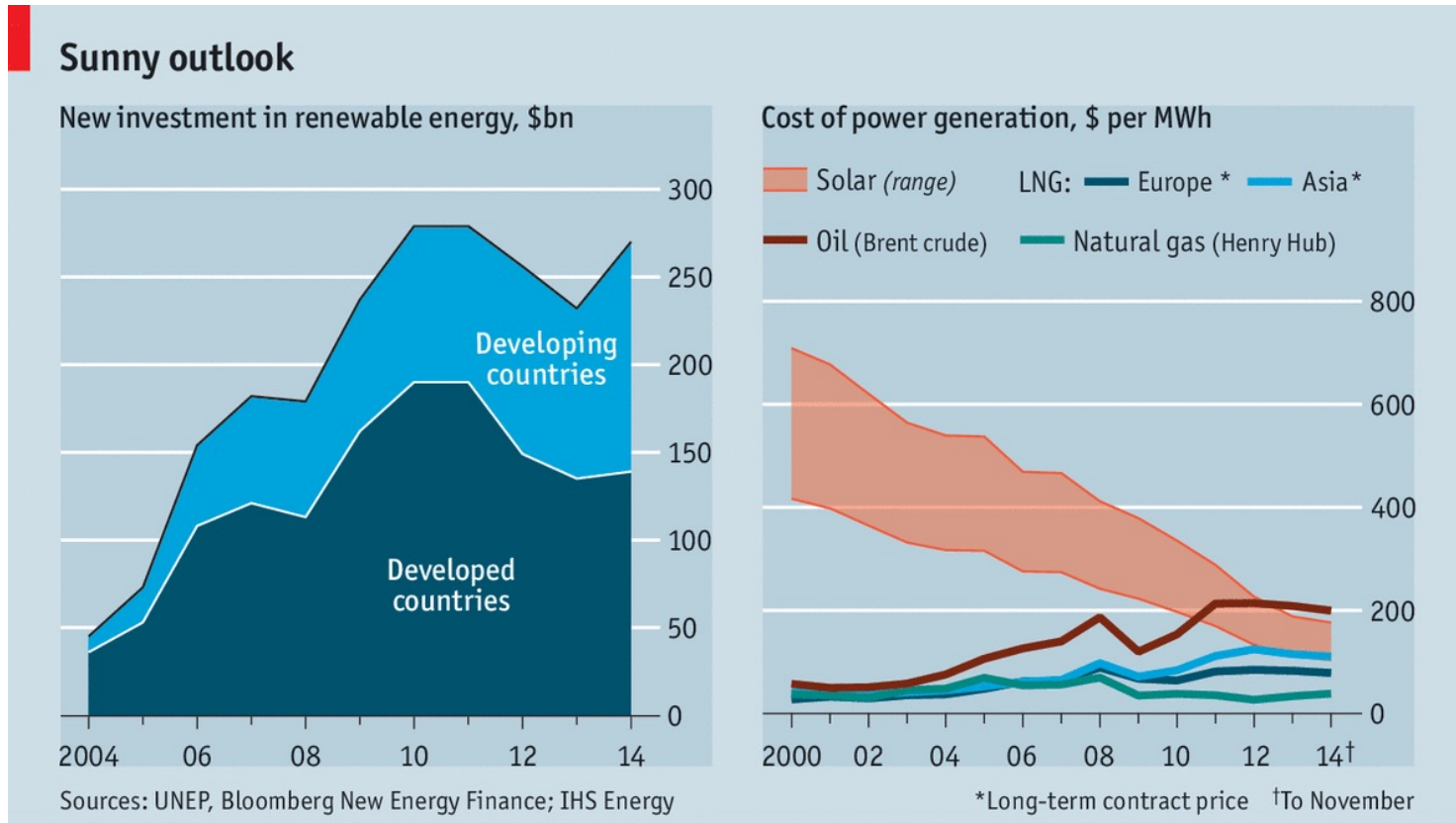
Colloidal synthesis of nanoparticles and their energy applications

MODULE 8: ELECTROLYZERS and FUEL CELLS

- 8.0. Introduction and motivation
- 8.1. Storing energy in chemical bonds
- 8.2 Water electrolyzers
- 8.3 CO₂ electrolyzers
- 8.4. Fuel cells

8.0. Introduction and motivation

Solar Energy is becoming very competitive



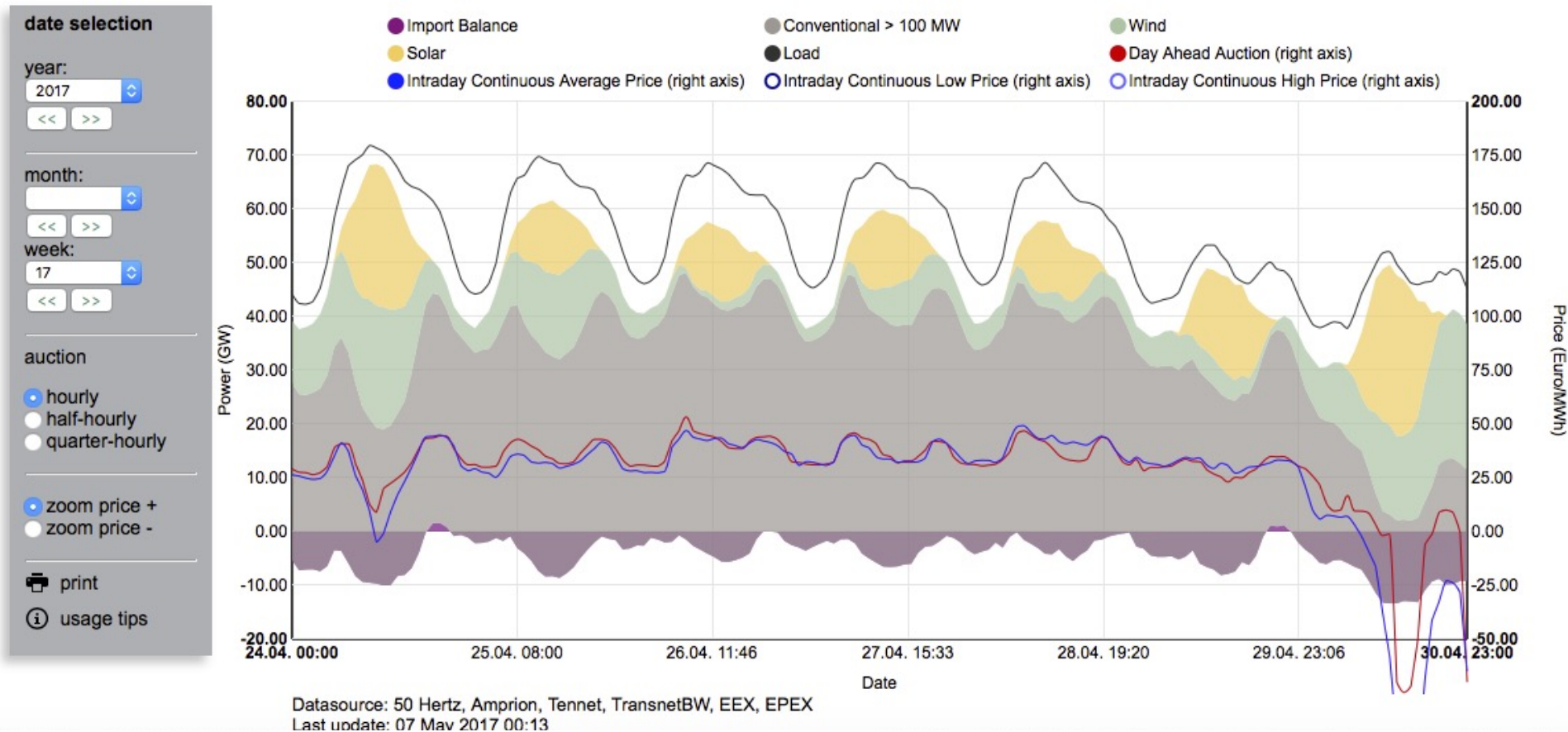
Economist.com

The
Economist

8.0. Introduction and motivation

The electricity market: the cost of electricity can go negative!

Electricity production and spot prices in Germany in week 17 2017



8.0. Introduction and motivation

The electricity market: the cost of electricity can go negative!

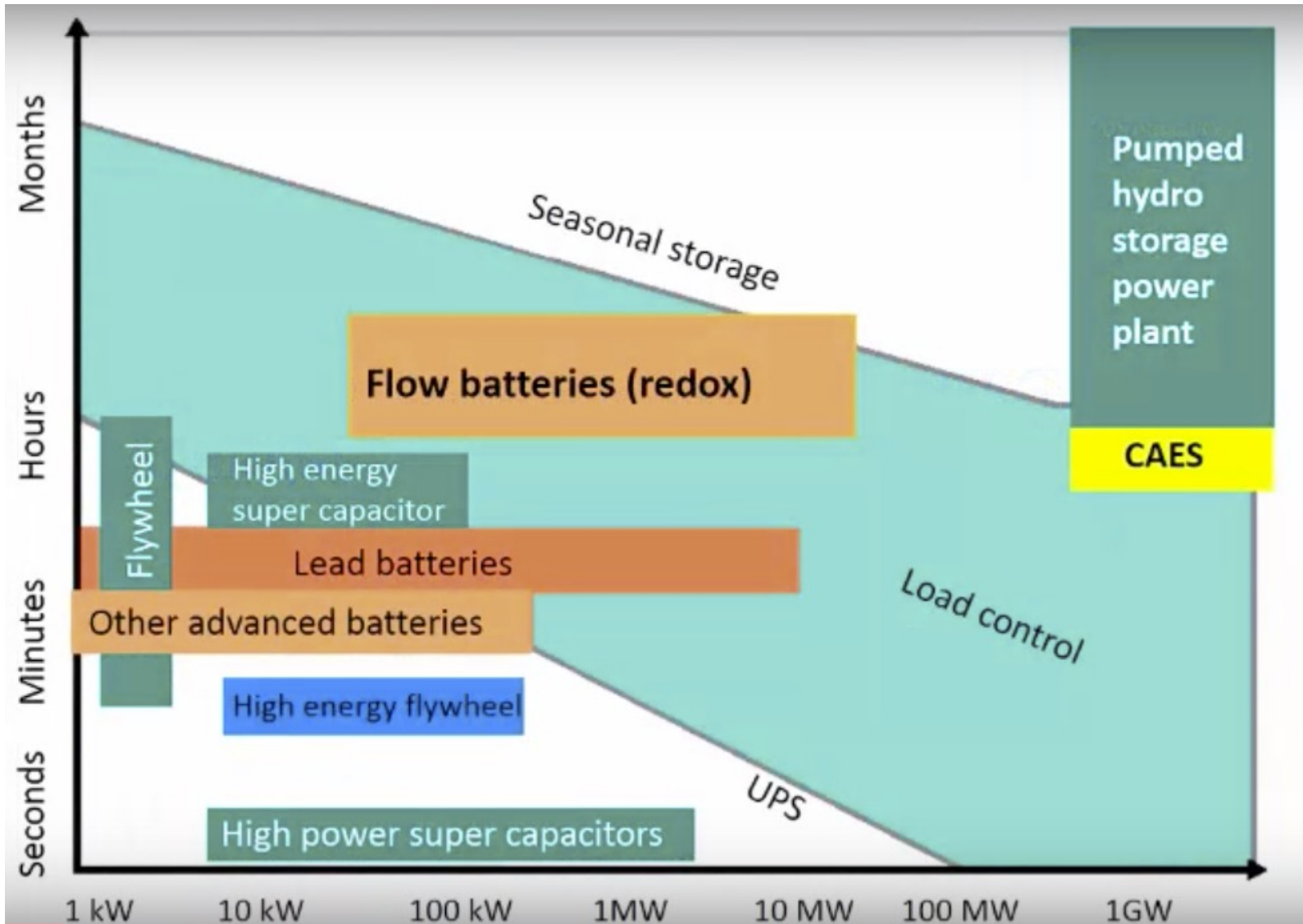
Germany Had To Pay People To Use Electricity Over The Holidays

The country had too much renewable energy to use it all.

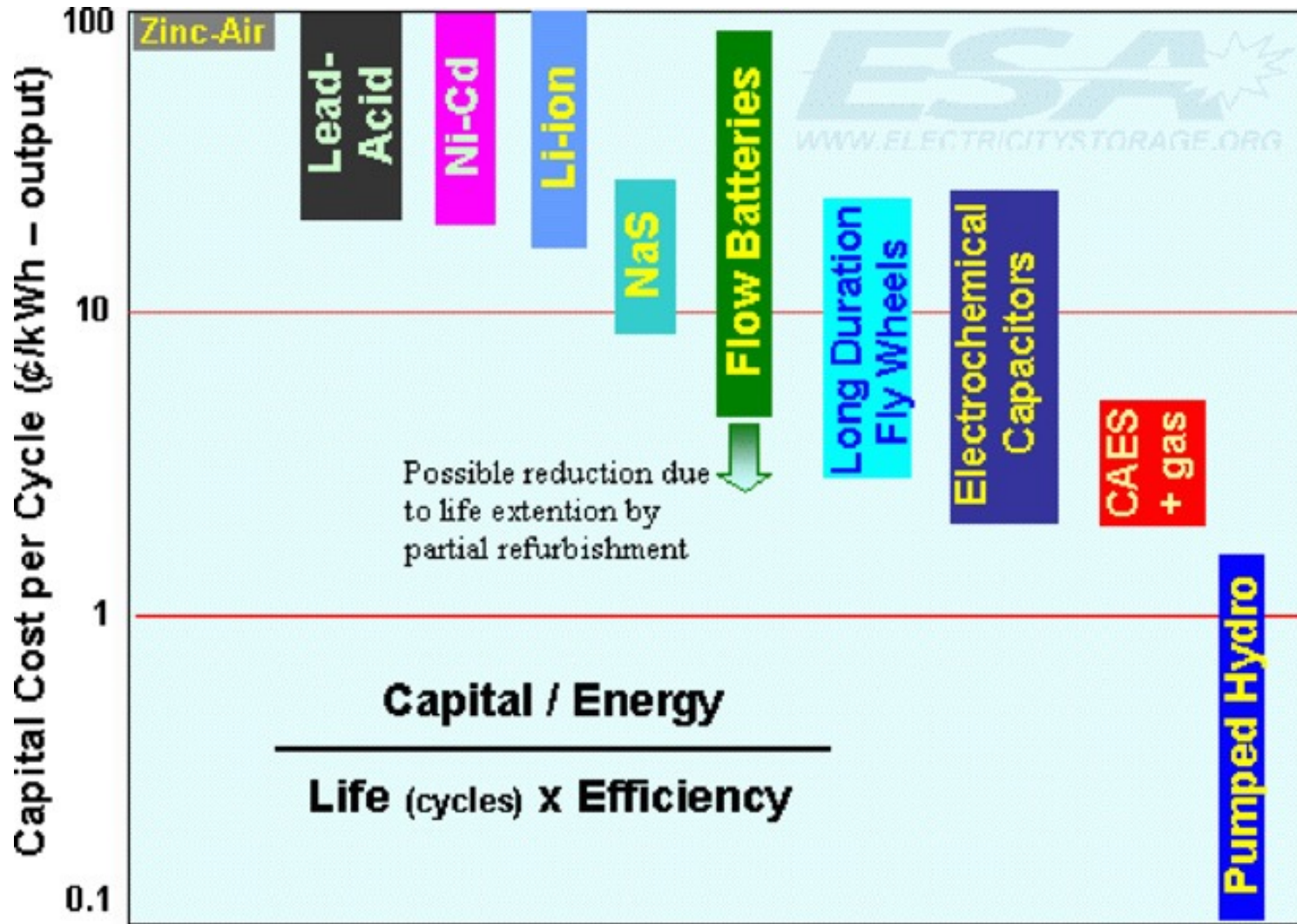
https://www.huffingtonpost.ca/2018/01/06/germany-had-to-pay-people-to-use-electricity-over-the-holidays_a_23325975/

8.0. Introduction and motivation

Energy Storage



8.0. Introduction and motivation

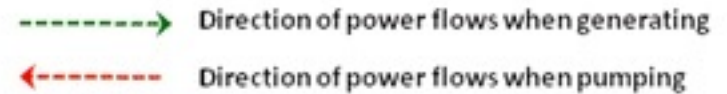
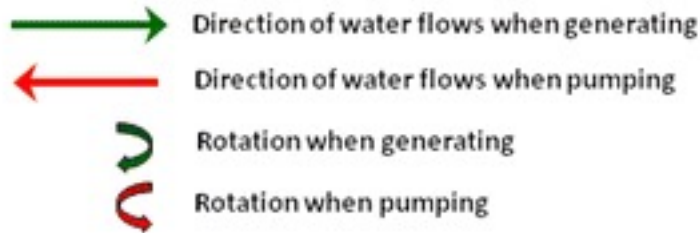
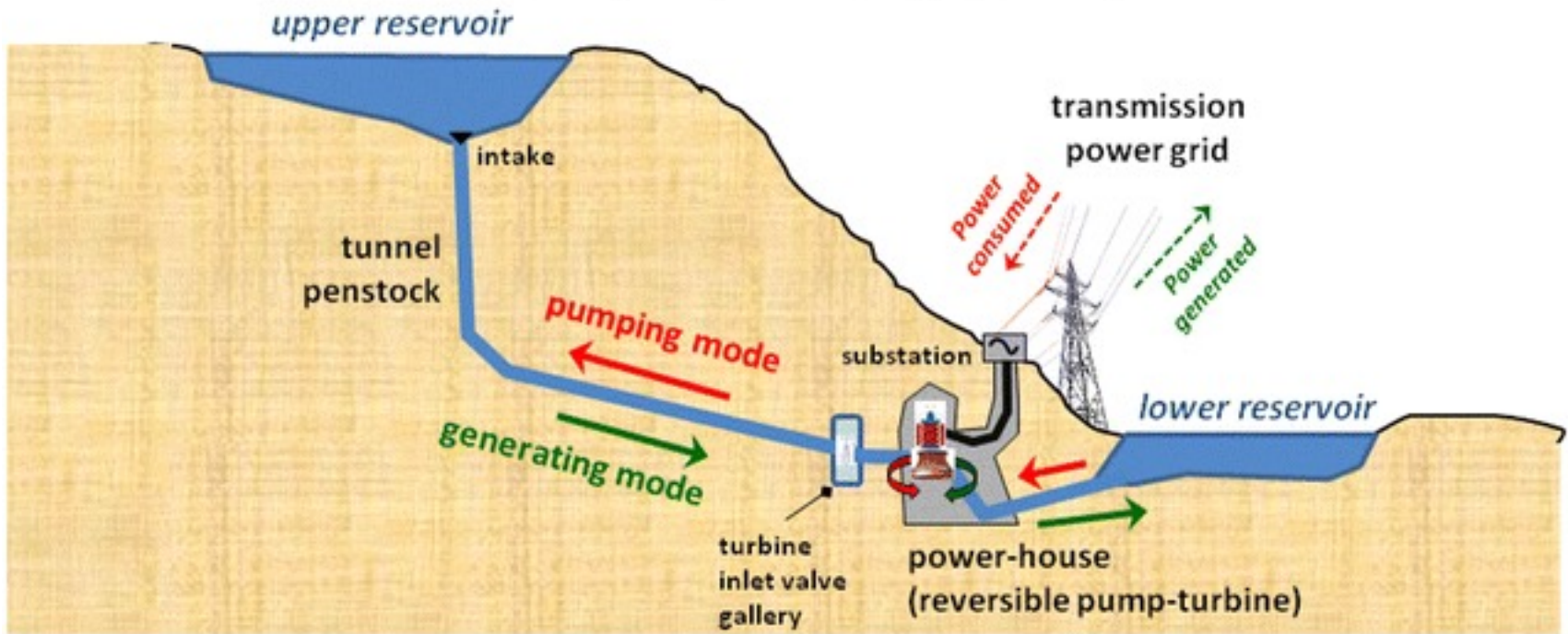


Carrying charges, O&M and replacement costs are not included

8.0. Introduction and motivation

Pump Hydro

Principle of a pumped-storage power plant



<https://www.youtube.com/watch?v=lwKOGaVkZvl> for more info

8.0. Introduction and motivation

Does it still make sense?



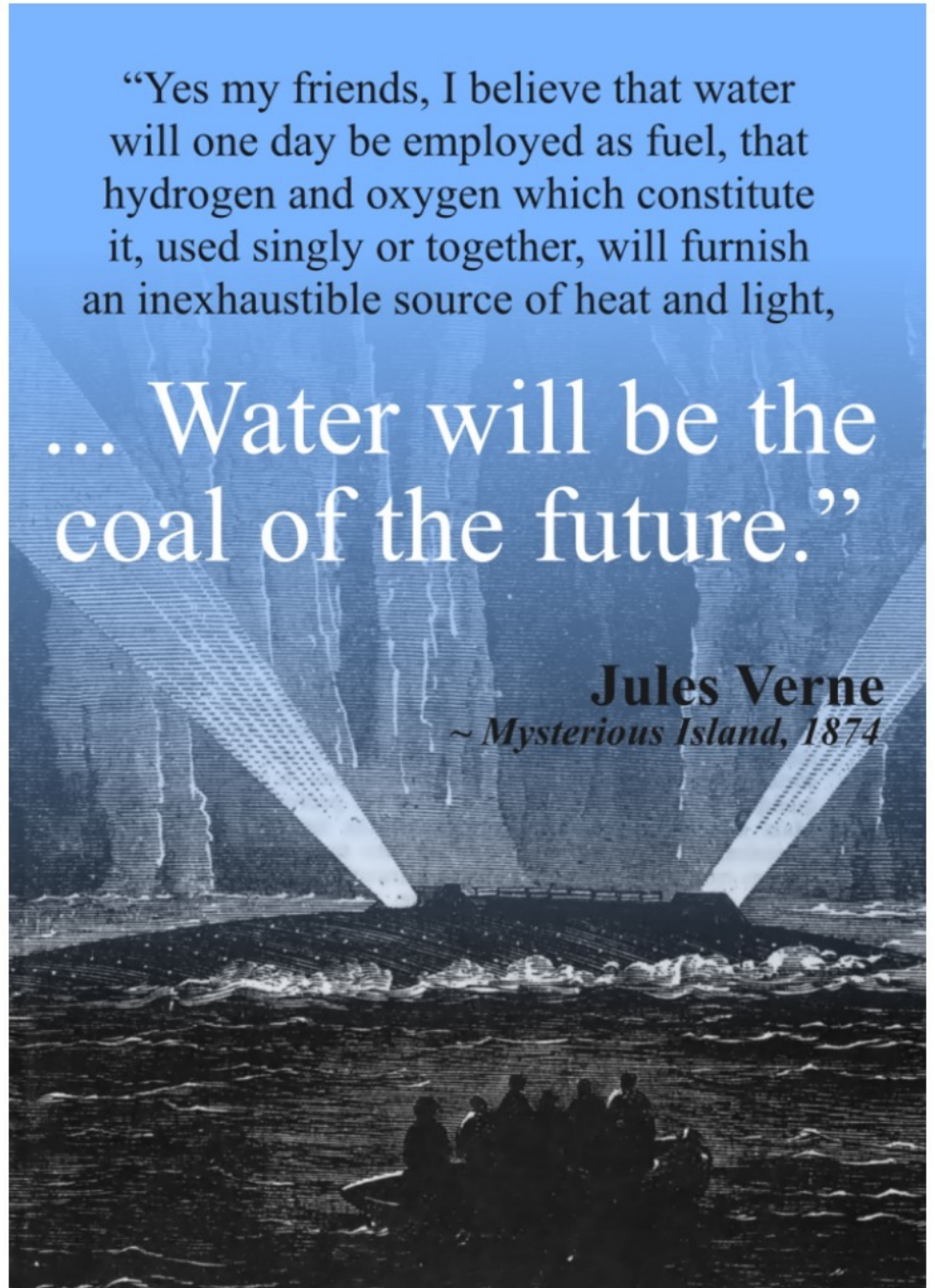
8.0. Introduction and motivation

CAN WE STORE ENERGY IN
CHEMICAL BONDS?

“Yes my friends, I believe that water will one day be employed as fuel, that hydrogen and oxygen which constitute it, used singly or together, will furnish an inexhaustible source of heat and light,

... Water will be the
coal of the future.”

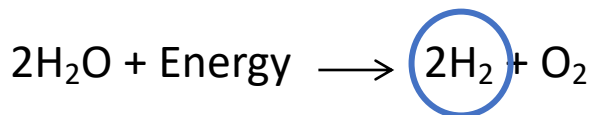
Jules Verne
~ *Mysterious Island, 1874*



8.1. Storing energy in chemical bonds

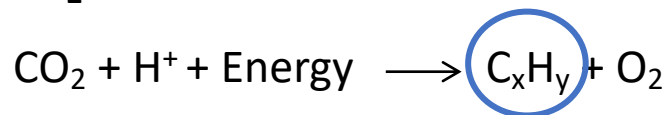
Energy storage in chemical bonds: the reactions

WATER SPLITTING

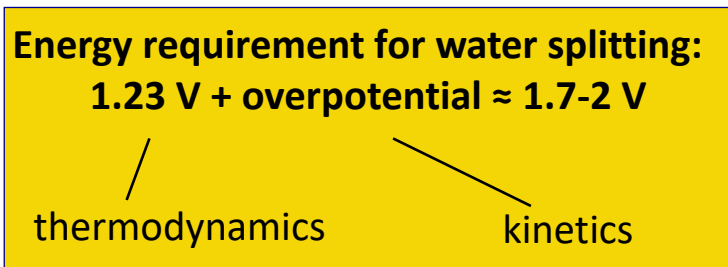
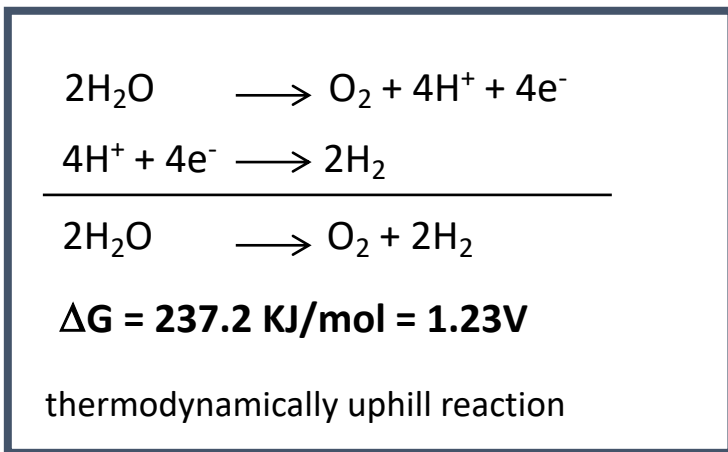


Storable energy carrier

CO₂ REDUCTION



Storable fuels or chemicals

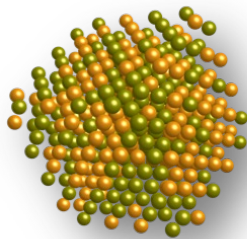
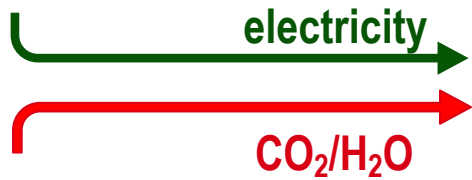


Half-electrochemical thermodynamic reactions	Electrode potentials (V vs. SHE) under standard conditions
$\text{CO}_2(\text{g}) + 4\text{H}^+ + 4\text{e}^- = \text{C}(\text{s}) + 2\text{H}_2\text{O}(\text{l})$	0.210
$\text{CO}_2(\text{g}) + 2\text{H}_2\text{O}(\text{l}) + 4\text{e}^- = \text{C}(\text{s}) + 4\text{OH}^-$	-0.627
$\text{CO}_2(\text{g}) + 2\text{H}^+ + 2\text{e}^- = \text{HCOOH}(\text{l})$	-0.250
$\text{CO}_2(\text{g}) + 2\text{H}_2\text{O}(\text{l}) + 2\text{e}^- = \text{HCOO}^-(\text{aq}) + \text{OH}^-$	-1.078
$\text{CO}_2(\text{g}) + 2\text{H}^+ + 2\text{e}^- = \text{CO}(\text{g}) + \text{H}_2\text{O}(\text{l})$	-0.106
$\text{CO}_2(\text{g}) + 2\text{H}_2\text{O}(\text{l}) + 2\text{e}^- = \text{CO}(\text{g}) + 2\text{OH}^-$	-0.934
$\text{CO}_2(\text{g}) + 4\text{H}^+ + 4\text{e}^- = \text{CH}_2\text{O}(\text{l}) + \text{H}_2\text{O}(\text{l})$	-0.070
$\text{CO}_2(\text{g}) + 3\text{H}_2\text{O}(\text{l}) + 4\text{e}^- = \text{CH}_2\text{O}(\text{l}) + 4\text{OH}^-$	-0.898
$\text{CO}_2(\text{g}) + 6\text{H}^+ + 6\text{e}^- = \text{CH}_3\text{OH}(\text{l}) + \text{H}_2\text{O}(\text{l})$	0.016
$\text{CO}_2(\text{g}) + 5\text{H}_2\text{O}(\text{l}) + 6\text{e}^- = \text{CH}_3\text{OH}(\text{l}) + 6\text{OH}^-$	-0.812
$\text{CO}_2(\text{g}) + 8\text{H}^+ + 8\text{e}^- = \text{CH}_4(\text{g}) + 2\text{H}_2\text{O}(\text{l})$	0.169
$\text{CO}_2(\text{g}) + 6\text{H}_2\text{O}(\text{l}) + 8\text{e}^- = \text{CH}_4(\text{g}) + 8\text{OH}^-$	-0.659
$2\text{CO}_2(\text{g}) + 2\text{H}^+ + 2\text{e}^- = \text{H}_2\text{C}_2\text{O}_4(\text{aq})$	-0.500
$2\text{CO}_2(\text{g}) + 2\text{e}^- = \text{C}_2\text{O}_4^{2-}(\text{aq})$	-0.590
$2\text{CO}_2(\text{g}) + 12\text{H}^+ + 12\text{e}^- = \text{CH}_2\text{CH}_2(\text{g}) + 4\text{H}_2\text{O}(\text{l})$	0.064
$2\text{CO}_2(\text{g}) + 8\text{H}_2\text{O}(\text{l}) + 12\text{e}^- = \text{CH}_2\text{CH}_2(\text{g}) + 12\text{OH}^-$	-0.764
$2\text{CO}_2(\text{g}) + 12\text{H}^+ + 12\text{e}^- = \text{CH}_3\text{CH}_2\text{OH}(\text{l}) + 3\text{H}_2\text{O}(\text{l})$	0.084
$2\text{CO}_2(\text{g}) + 9\text{H}_2\text{O}(\text{l}) + 12\text{e}^- = \text{CH}_3\text{CH}_2\text{OH}(\text{l}) + 12\text{OH}^-$	-0.744

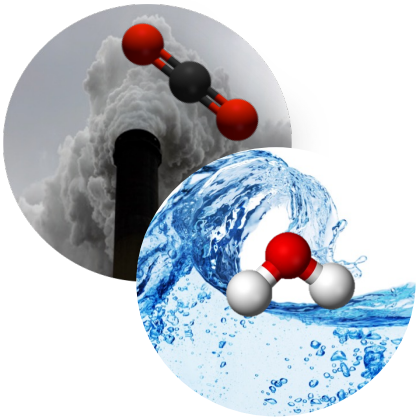
**Energy requirement for CO₂ reduction
> 2 V**



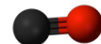
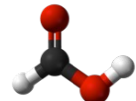

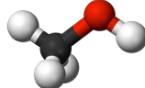
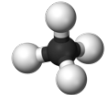

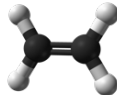
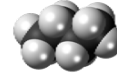

8.1. Storing energy in chemical bonds

Energy storage in chemical bonds: the reactions



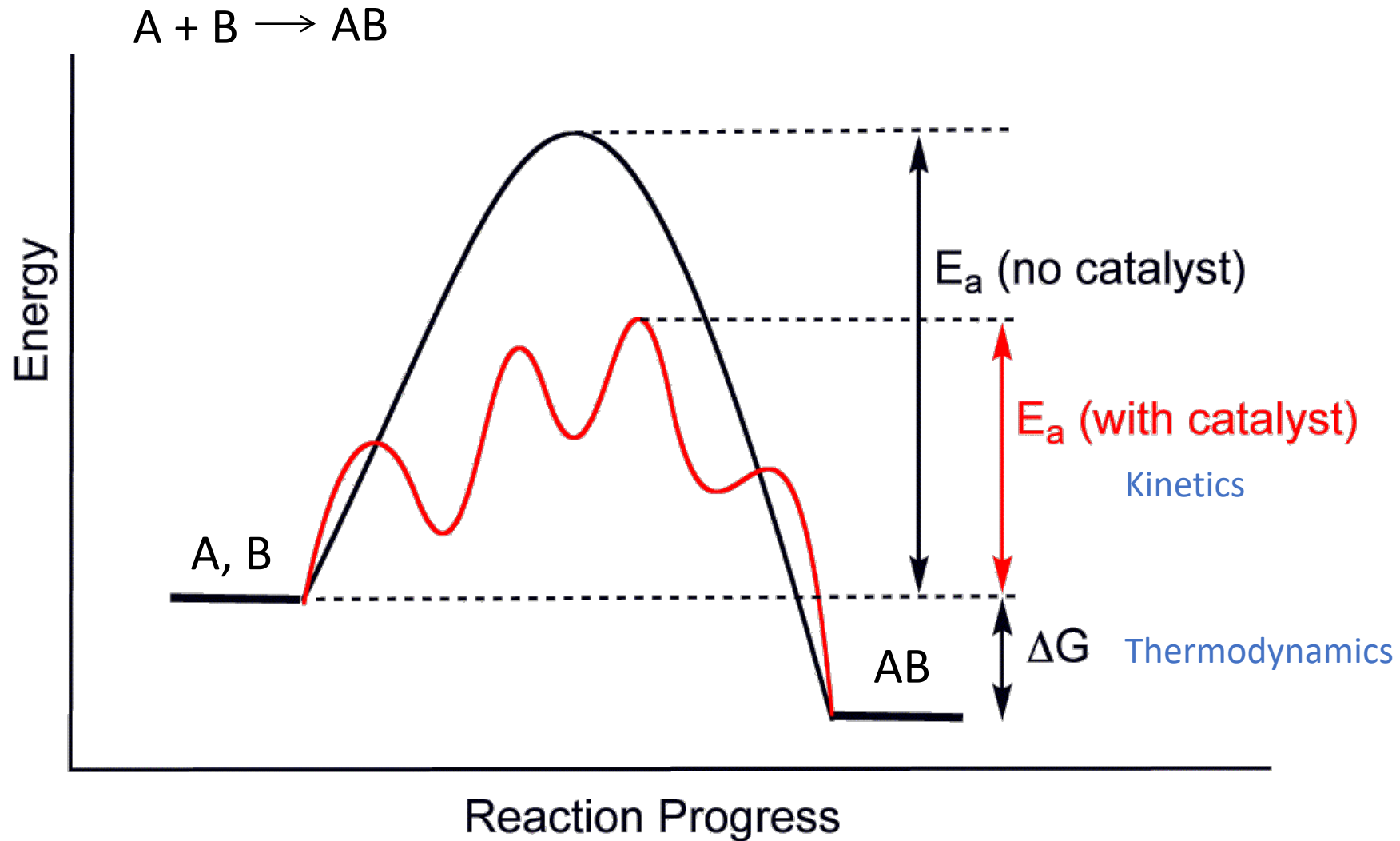
CATALYST
breaks bonds and
lets other bonds form



	H₂ (Hydrogen)	Synthetic Rubber 
	CO (Carbon monoxide)	
	HCOOH (Formic acid)	Fuels 
	CH₃OH (Methanol)	
	CH₄ (Methane)	Lubricants 
	C₂H₄ (Ethylene)	
	C₄H₁₀ (Butane)	Plastic 

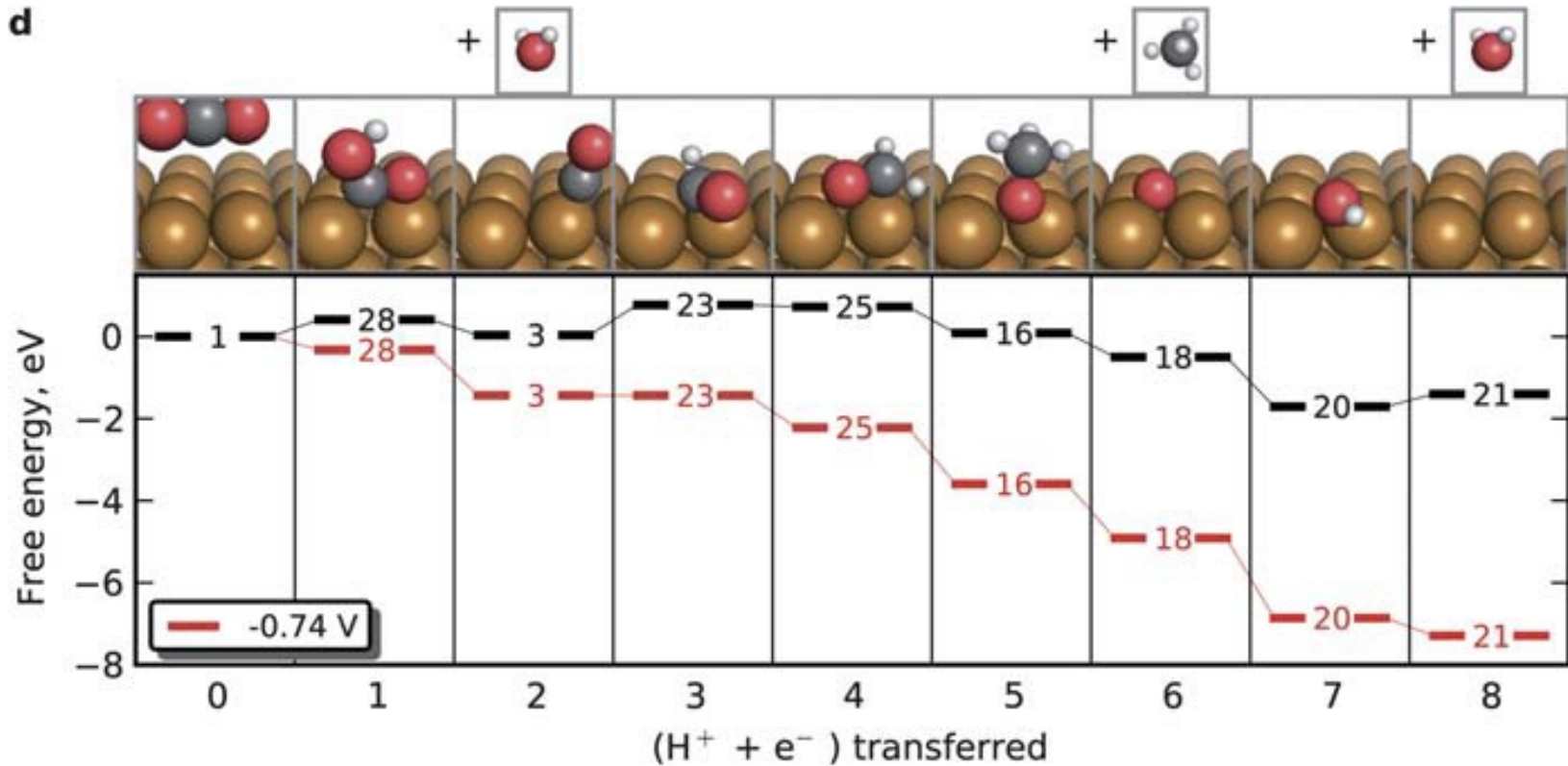
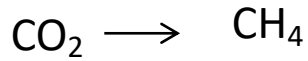
8.1. Storing energy in chemical bonds

Catalysis



8.1. Storing energy in chemical bonds

Catalysis



Just focus on the black pathway which represents the free energy path in the absence of applied potential (red pathway)

8.1. Storing energy in chemical bonds

Electrolyzer

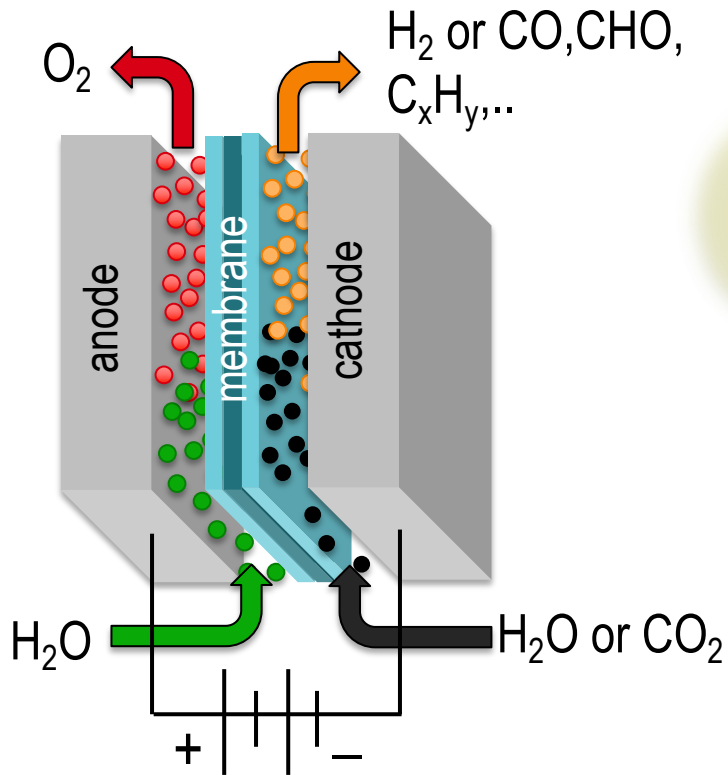
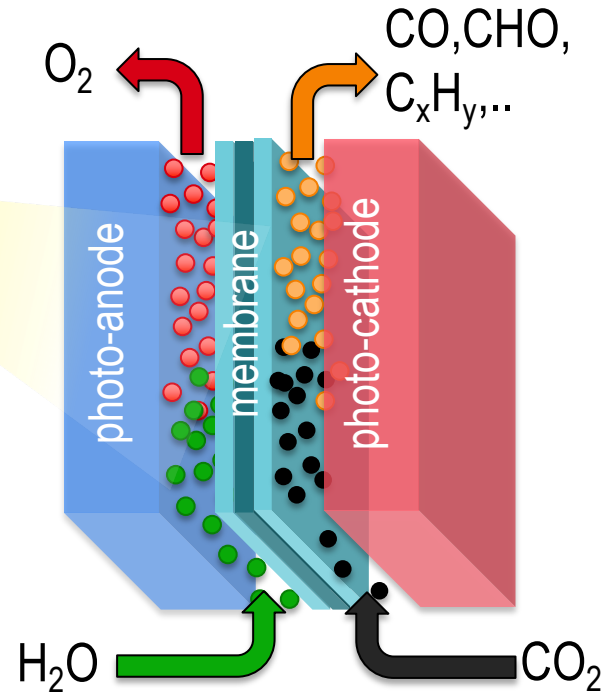


Photo-electrochemical cell

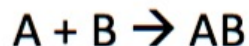


A **fuel cell** does the opposite operation of an electrolyzer as it turns fuels into electricity.

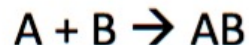
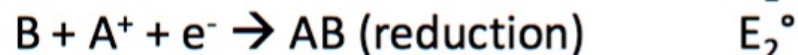
8.1. Storing energy in chemical bonds

Chemistry \longrightarrow Electrochemistry

Equilibrium Thermodynamics



$$\Delta G = -100 \text{ kJ/mol}$$



$$\Delta G^\circ = -100 \text{ kJ/mol} = -nFE^\circ_{\text{cell}}$$

Where: n = # of electrons transferred (overall rxn)



F = Faraday's constant = 96,485 C/mol

$E^\circ_{\text{cell}} = \Delta E^\circ \dots$ can be confusing!

See next slides on how to use tables of standard electrochemical potentials to calculate this.

8.1. Storing energy in chemical bonds

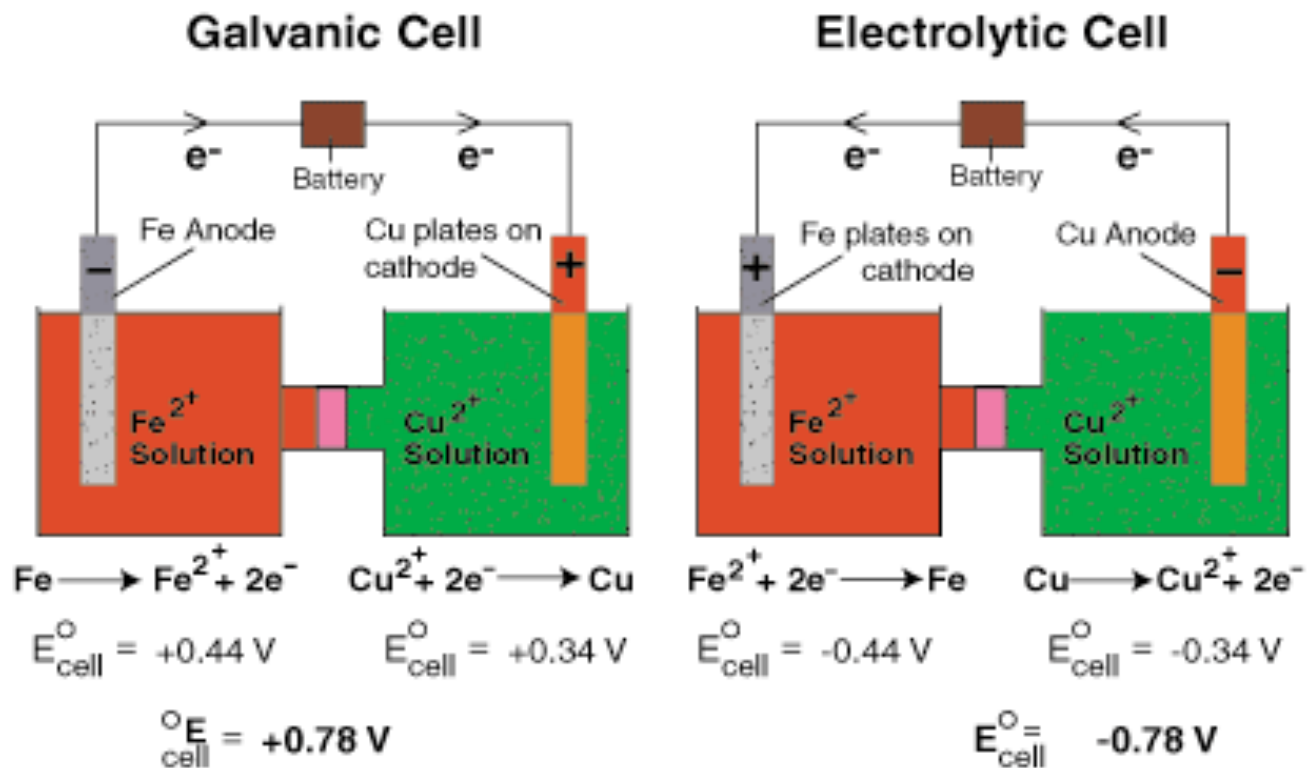
Equilibrium potentials

	Reduction Half-Reaction	E° (V)	
 <p>Stronger oxidizing agent</p>	$F_2(g) + 2 e^- \longrightarrow 2 F(aq)$	2.87	 <p>Weaker reducing agent</p>
	$H_2O_2(aq) + 2 H^+(aq) + 2 e^- \longrightarrow 2 H_2O(l)$	1.78	
	$MnO_4^-(aq) + 8 H^+(aq) + 5 e^- \longrightarrow Mn^{2+}(aq) + 4 H_2O(l)$	1.51	
	$Cl_2(g) + 2 e^- \longrightarrow 2 Cl^-(aq)$	1.36	
	$Cr_2O_7^{2-}(aq) + 14 H^+(aq) + 6 e^- \longrightarrow 2 Cr^{3+}(aq) + 7 H_2O(l)$	1.33	
	$O_2(g) + 4 H^+(aq) + 4 e^- \longrightarrow 2 H_2O(l)$	1.23	
	$Br_2(l) + 2 e^- \longrightarrow 2 Br^-(aq)$	1.09	
	$Ag^+(aq) + e^- \longrightarrow Ag(s)$	0.80	
	$Fe^{3+}(aq) + e^- \longrightarrow Fe^{2+}(aq)$	0.77	
	$O_2(g) + 2 H^+(aq) + 2 e^- \longrightarrow H_2O_2(aq)$	0.70	
	$I_2(s) + 2 e^- \longrightarrow 2 I^-(aq)$	0.54	
	$O_2(g) + 2 H_2O(l) + 4 e^- \longrightarrow 4 OH^-(aq)$	0.40	
	$Cu^{2+}(aq) + 2 e^- \longrightarrow Cu(s)$	0.34	
	$Sn^{4+}(aq) + 2 e^- \longrightarrow Sn^{2+}(aq)$	0.15	
	$2 H^+(aq) + 2 e^- \longrightarrow H_2(g)$	0	
	$Pb^{2+}(aq) + 2 e^- \longrightarrow Pb(s)$	-0.13	
	$Ni^{2+}(aq) + 2 e^- \longrightarrow Ni(s)$	-0.26	
$Cd^{2+}(aq) + 2 e^- \longrightarrow Cd(s)$	-0.40		
$Fe^{2+}(aq) + 2 e^- \longrightarrow Fe(s)$	-0.45		
$Zn^{2+}(aq) + 2 e^- \longrightarrow Zn(s)$	-0.76		
$2 H_2O(l) + 2 e^- \longrightarrow H_2(g) + 2 OH^-(aq)$	-0.83		
$Al^{3+}(aq) + 3 e^- \longrightarrow Al(s)$	-1.66		
$Mg^{2+}(aq) + 2 e^- \longrightarrow Mg(s)$	-2.37		
$Na^+(aq) + e^- \longrightarrow Na(s)$	-2.71		
$Li^+(aq) + e^- \longrightarrow Li(s)$	-3.04		
<p>Weaker oxidizing agent</p>			<p>Stronger reducing agent</p>

E^0 are the redox potential measured under standard conditions (25°C, 1atm pressure, 1mol/L solution) against the hydrogen electrode (vs RHE)

8.1. Storing energy in chemical bonds

Example Let's consider one redox reaction involving copper and iron



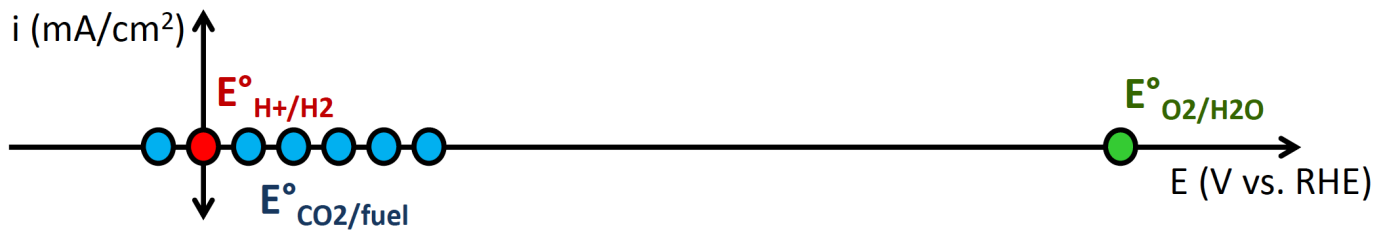
Oxidation occurs at the ANODE
Reduction occurs at the CATHODE

8.1. Storing energy in chemical bonds

Thermodynamic consideration for water splitting and CO₂ reduction

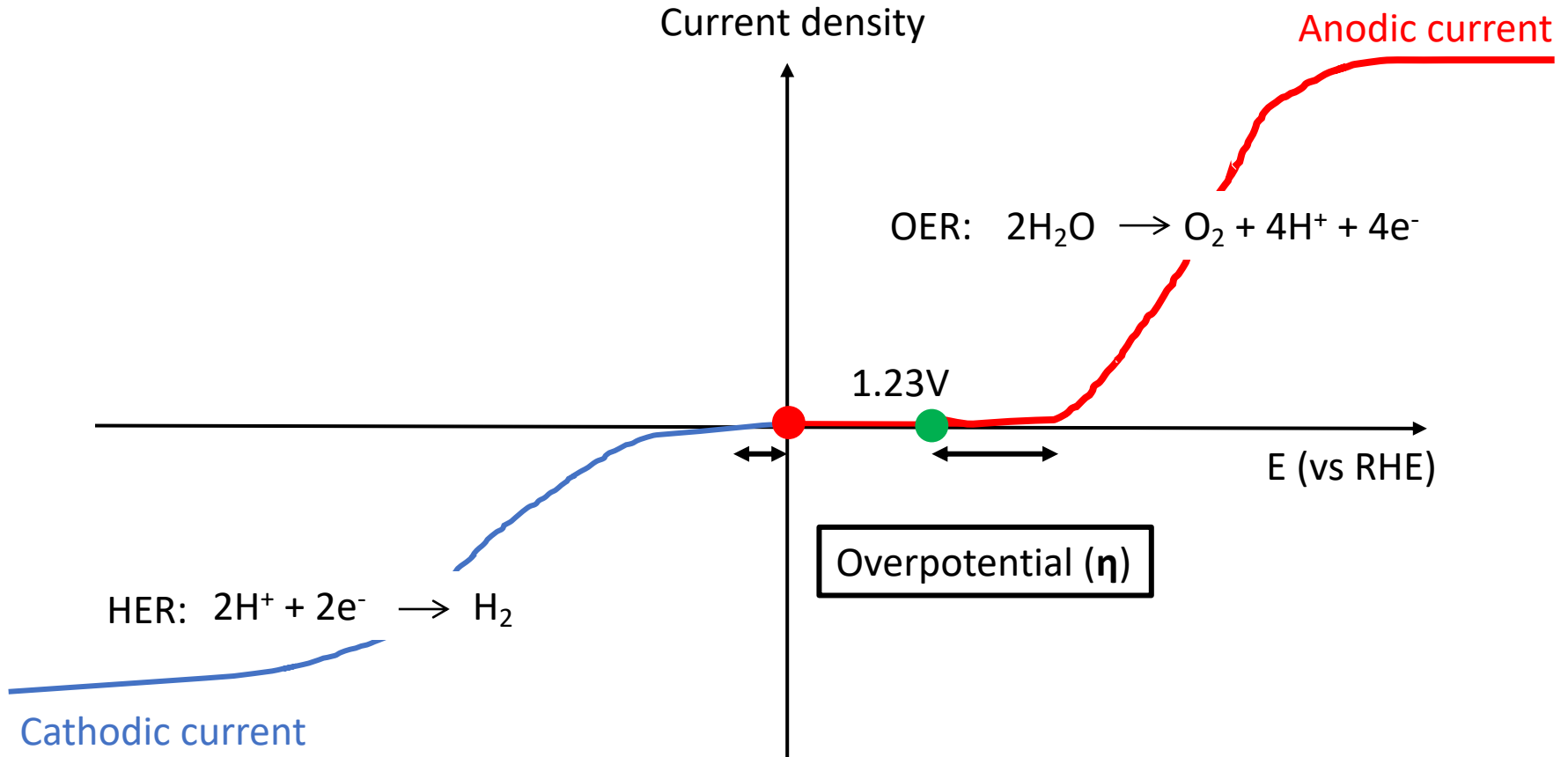
Y. Hori, "Electrochemical CO₂ reduction on metal electrodes" *Modern Aspects of Electrochemistry*, Number 42, edited by C. Vayenas et. al., Springer, NY (2008)

			E ⁰ vs. RHE	
	2H ⁺ + 2e ⁻	↔ H ₂	0.00 V	
}	CO ₂ + 2H ⁺ + 2e ⁻	↔ CO + H ₂ O	- 0.11 V	All values are close to the H ₂ evolution potential (0.00 V).
	CO ₂ + 6H ⁺ + 6e ⁻	↔ CH ₃ OH + H ₂ O	+ 0.02 V	
	CO ₂ + 8H ⁺ + 8e ⁻	↔ CH ₄ + 2H ₂ O	+ 0.16 V	
	2CO ₂ + 12H ⁺ + 12e ⁻	↔ C ₂ H ₄ + 4H ₂ O	+ 0.07 V	
	2CO ₂ + 12H ⁺ + 12e ⁻	↔ C ₂ H ₅ OH + 3H ₂ O	+ 0.08 V	
	3CO ₂ + 18H ⁺ + 18e ⁻	↔ C ₃ H ₇ OH + 5H ₂ O	+ 0.09 V	
	O ₂ + 4H ⁺ + 4e ⁻	↔ 2H ₂ O	+ 1.23 V	



8.1. Storing energy in chemical bonds

Reaction kinetics of water splitting and current vs voltage curves



SIMPLE DEFINITION OF OVERPOTENTIAL: is the potential difference between a half reaction's thermodynamically determined redox potential and the potential at which the redox reaction actually occurs. However, because the onset potential can be ascribed to the production of an arbitrarily defined current density, then the onset potential might not be the best parameter to compare catalysts.

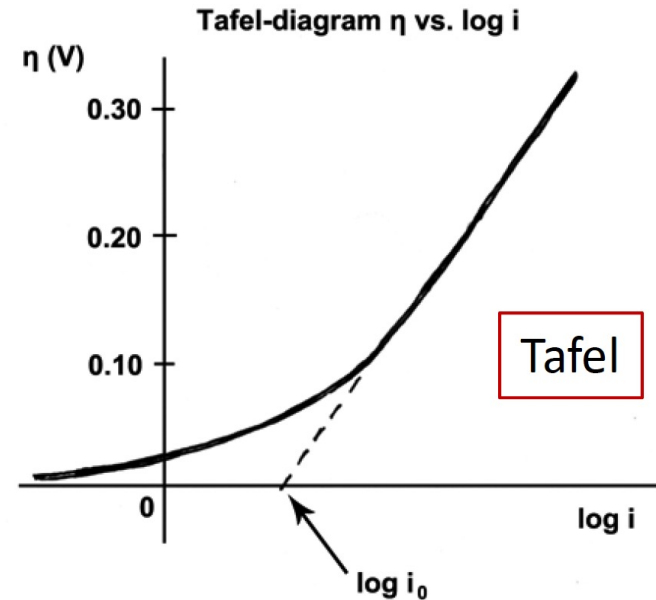
8.1. Storing energy in chemical bonds

Figures of merit for electrocatalyst activity

There are four primary figures of merit:

- Exchange Current density, i_0 (mA/cm_2)
- Tafel slope, b (mV/decade)
- Current density at a given overpotential:
 $i_{E(\text{V vs RHE})}$ (mA/cm_2)
- Overpotential needed to reach a given current density:
 $\eta_{i=10\text{mA}/\text{cm}^2}$ (mV)

↑
relevant for solar fuels but you find different arbitrary values in the literature



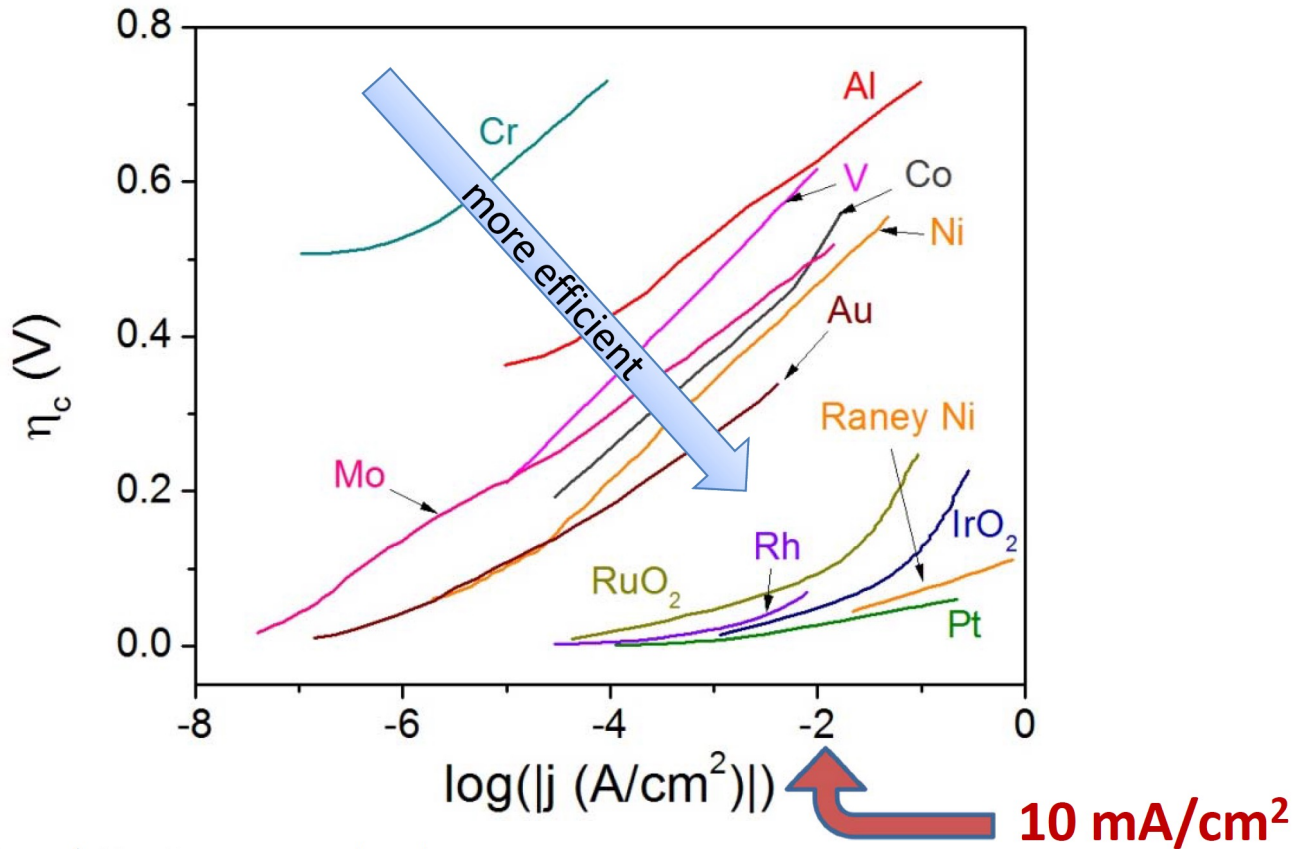
There are three ways to report current densities:

- Per geometric surface area (cm_{geo}^2)
- Per surface area (cm_{real}^2)
- Per electrochemically active surface area (cm_{ECSA}^2)
(more difficult to determine but also more useful)

NB. Sometime current density is indicated also as J

8.1. Storing energy in chemical bonds

Tafel plots for various HER catalysts



Comparison of exchange current density for proton reduction reaction in 1 mol/kg H₂SO₄^[1]

Electrode material ↕	Exchange current density -log ₁₀ (A/cm ²) ↕
Palladium	3.0
Platinum	3.1
Rhodium	3.6
Iridium	3.7
Nickel	5.2
Gold	5.4
Tungsten	5.9
Niobium	6.8
Titanium	8.2
Cadmium	10.8
Manganese	10.9
Lead	12.0
Mercury	12.3

.F., et al. *NanoLetters* 11, 10 (2011)

The exchange current density reflects the electron transfer rate between the electrode and the analyte.

8.1. Storing energy in chemical bonds

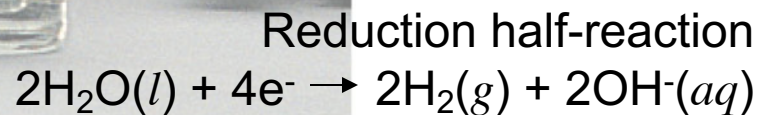
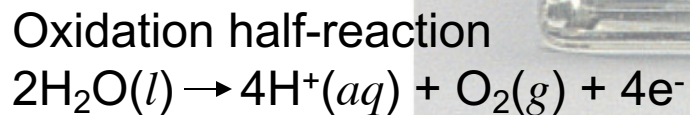
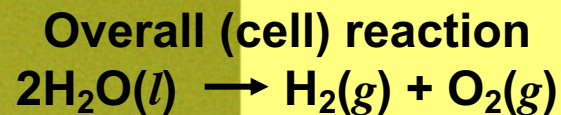
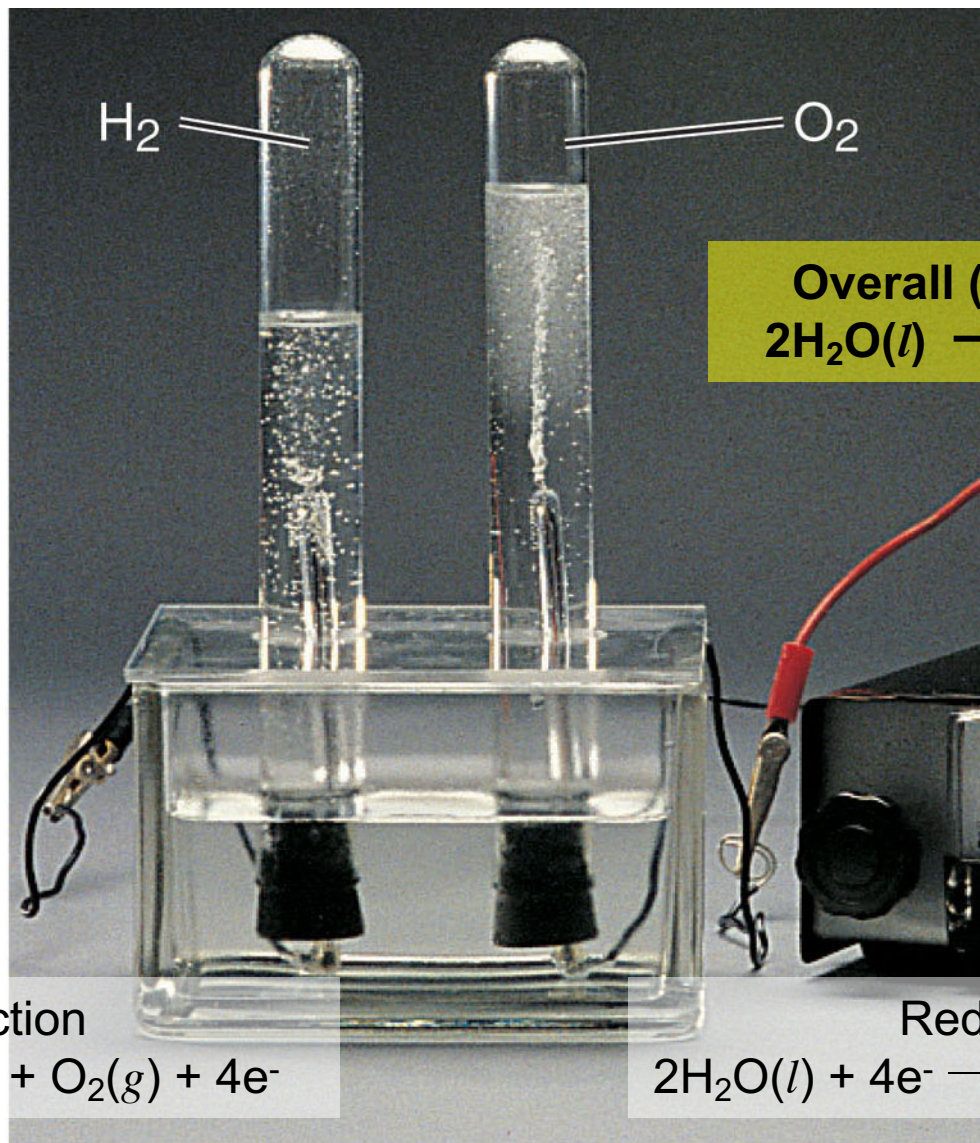
Faradaic efficiency

$$\begin{aligned}\text{Faradaic efficiency} &= \frac{\text{experimental gas evolution}}{\text{theoretical gas evolution}} = \\ &= \frac{\sum (\text{mol}_i \times n_i) \times F}{I \times t} \times 100\%\end{aligned}$$

$$\text{i.e. } FE_{HER} = \frac{\text{mol}(H_2) \times 2 \times 96,485 \text{ C/mol}}{I \times t \text{ (C)}} \times 100$$

8.2. Water Electrolyzers

The
electrolysis of
water.

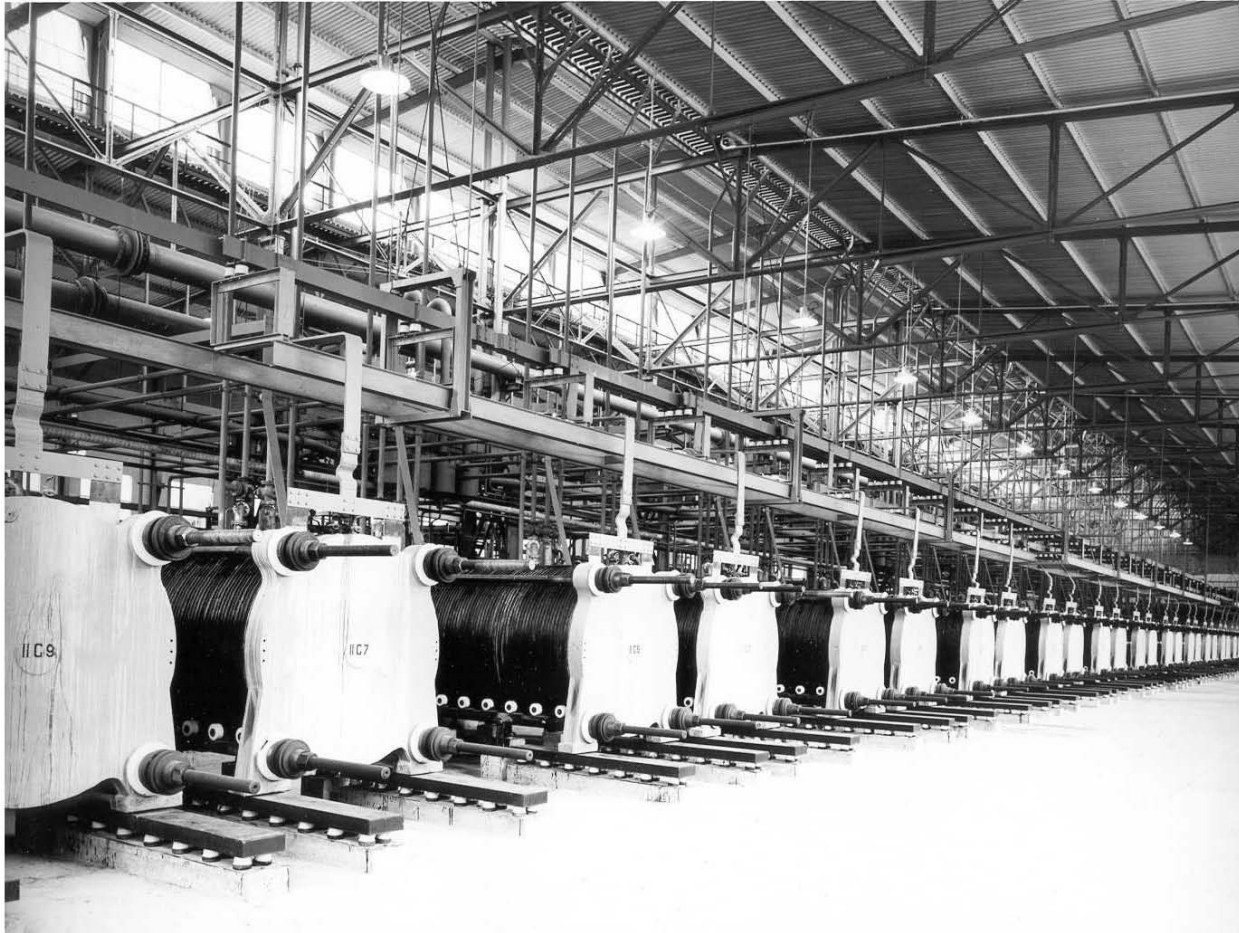


8.2. Water Electrolyzers

The **hydrogen economy** is a proposed system of delivering energy using hydrogen. The term hydrogen economy was coined by **John Bockris** during a talk he gave in 1970 at General Motors (GM) Technical Center. Hydrogen advocates promote hydrogen as a potential fuel for motive power (including cars and boats), the energy needs of buildings and portable electronics.

Free hydrogen does not occur naturally in quantity, but can be generated by steam reformation of hydrocarbons, **water electrolysis** or by other methods. A small part (4% in 2006) is produced by electrolysis using electricity and water, consuming approximately 50 kilowatt-hours of electricity per kilogram of hydrogen produced. Hydrogen production is a large and growing industry. Globally, some 50 million metric tons of hydrogen, equal to about 170 million tons of oil equivalent, were produced in 2004. The growth rate is around 10% per year. There are two primary uses for hydrogen today. **About half is used in the Haber process to produce ammonia (NH₃), which is then used directly or indirectly as fertilizer. The other half of current hydrogen production is used to convert heavy petroleum sources into lighter fractions suitable for use as fuels.**

8.2. Water Electrolyzers



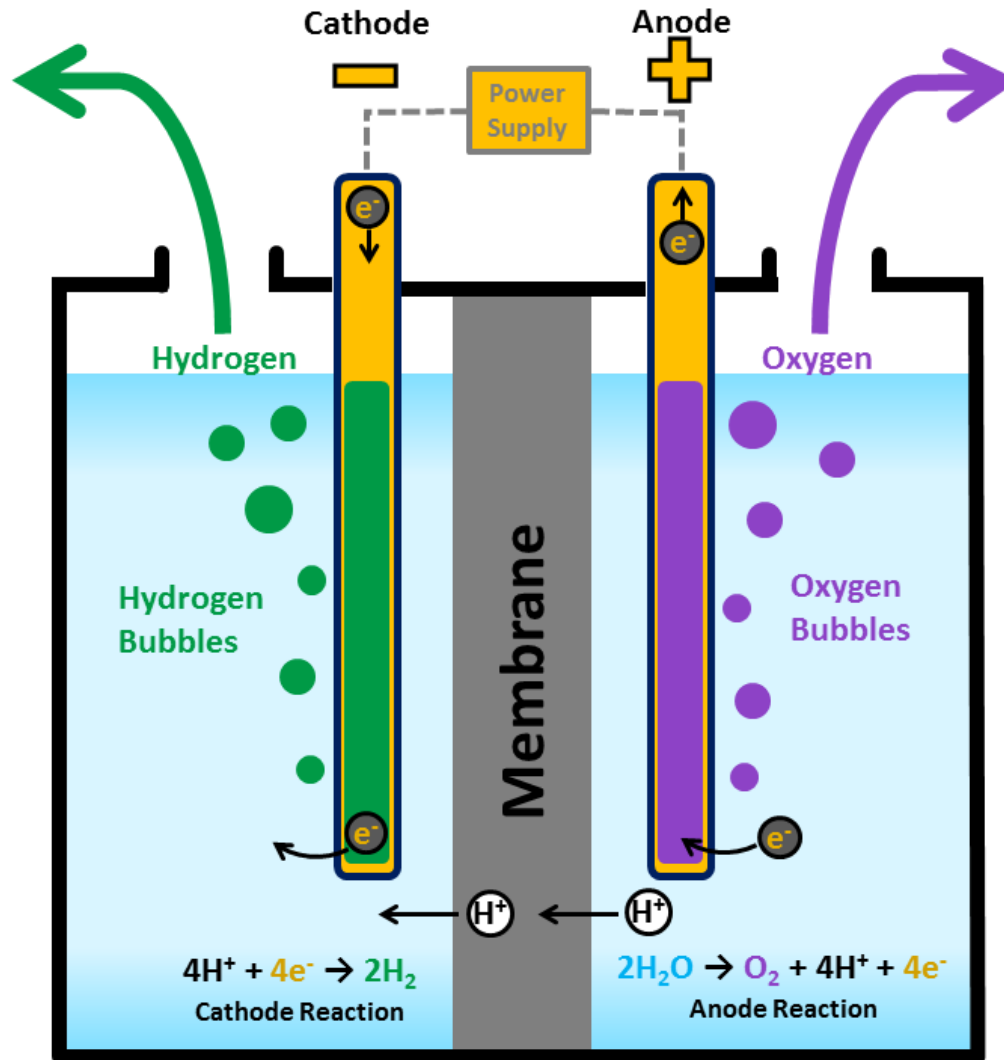
**Norsk Hydro's 30,000 Nm³/h (~150 MW)
Electrolyzer Plant (1948 - 90)**

Connected to a hydroelectric plant, generating about 70,000 kg/day, enough for 3,500,000 miles/day for FCVs.

The US would need ~ 3000 of these for 250 million FCVs

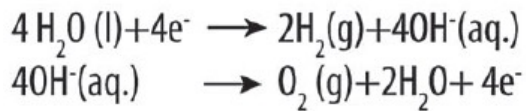
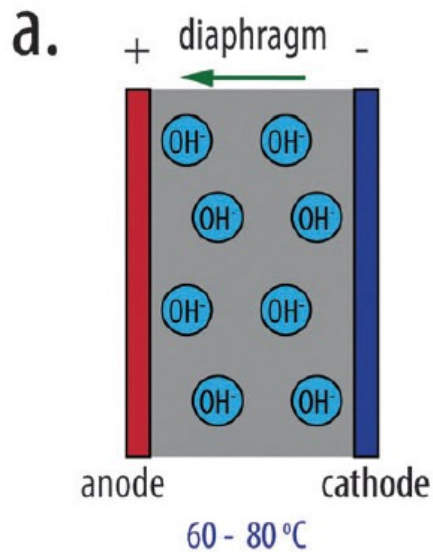
8.2. Water Electrolyzers

We need a membrane to separate hydrogen and oxygen!

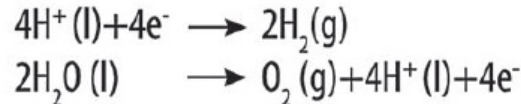
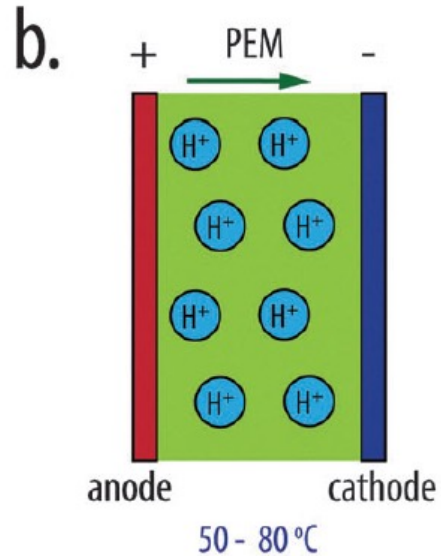


8.2. Water Electrolyzers

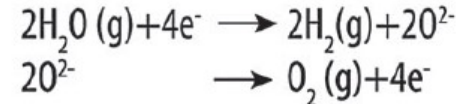
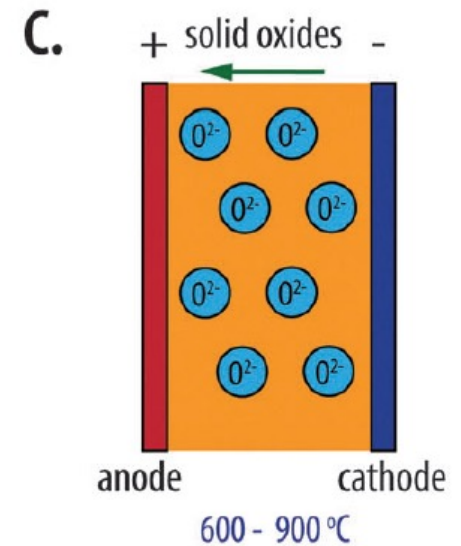
ALKALINE WATER ELECTROLYZER



PEM WATER ELECTROLYZER



HIGH T SOLID-OXIDE WATER ELECTROLYZER



8.2. Water Electrolyzers

Features of cell technologies.

Feature	AEL	PEMEL	SOEL
Maturity	Mature	Early phase of commercialization	Development
Temperature (°C)	40–90 [71]	20–100 [71]	600–1000 [40]
Pressure (bar)	< 30 [71]	< 100 [66]	–
Voltage (V)	1.8–2.4 [71]	1.8–2.2 [71]	0.95–1.3 [32]
Efficiency (%)	62–82 [71]	67–82 [71]	
Current density (A cm ⁻²)	< 0.5 [72] 0.2–0.4 [65]	< 2 [32] 1.0–2.0 [65]	< 1 [32]
Cold start up time (min)	15 [32] 20 [65]	< 15 [32] 5 [65]	> 60 [32]
Degradation rate (mV h ⁻¹)	< 3 [71] 2 [73]	< 14 [71] 5 [73]	–
Life time (stack)	< 90,000 [32] < 75,000 [65]	< 62,000 [65]	–

8.2. Water Electrolyzers

- **POLYMER ELECTROLYTE MEMBRANE (PEM) ELECTROLYZERS**

The electrolyte is a polymer and H⁺ are transported through the membrane)

- **ALKALINE ELECTROLYZERS**

NaOH or KOH solutions are used as electrolyte and OH⁻ is transported through the membrane (Zirfon, Perl)

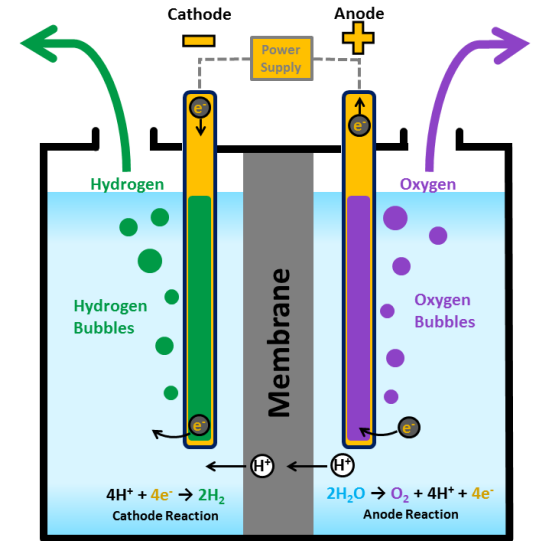
- **SOLID OXIDE ELECTROLYZERS**

Solid oxide electrolyzers, which use a solid ceramic material as the electrolyte that selectively conducts negatively charged oxygen ions (O²⁻) at elevated temperatures, generate hydrogen in a slightly different way.

- **Water at the cathode combines with electrons from the external circuit to form hydrogen gas and negatively charged oxygen ions.**

- **The oxygen ions pass through the solid ceramic membrane and react at the anode to form oxygen gas and generate electrons for the external circuit.**

Solid oxide electrolyzers must operate at temperatures high enough for the solid oxide membranes to function properly (about 700°–800°C, compared to PEM electrolyzers, which operate at 70°–90°C, and commercial alkaline electrolyzers, which operate at 100°–150°C). The solid oxide electrolyzers can effectively use heat available at these elevated temperatures (from various sources, including nuclear energy) to decrease the amount of electrical energy needed to produce hydrogen from water.



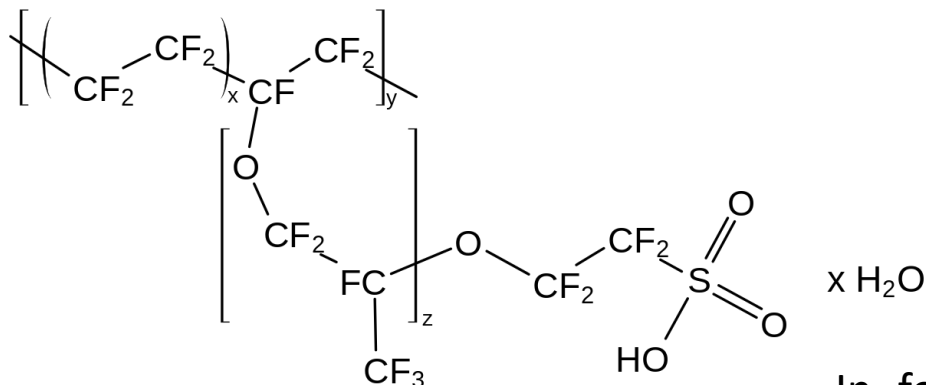
R&D Challenges:

- Reducing capital cost
- Improve faradaic efficiencies
- Integrating compression for hydrogen storage

8.2. Water Electrolyzers

PEM Electrolyzers

NAFION is basically the only commercially available proton conductive membrane because of its high proton conductivity and chemical/mechanical stability,

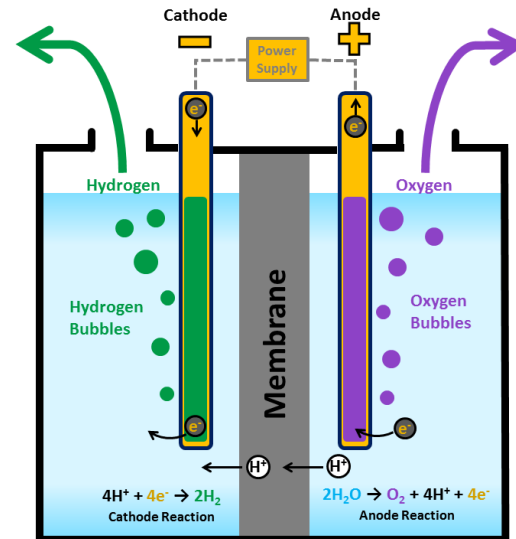


Pt is used as HER catalyst

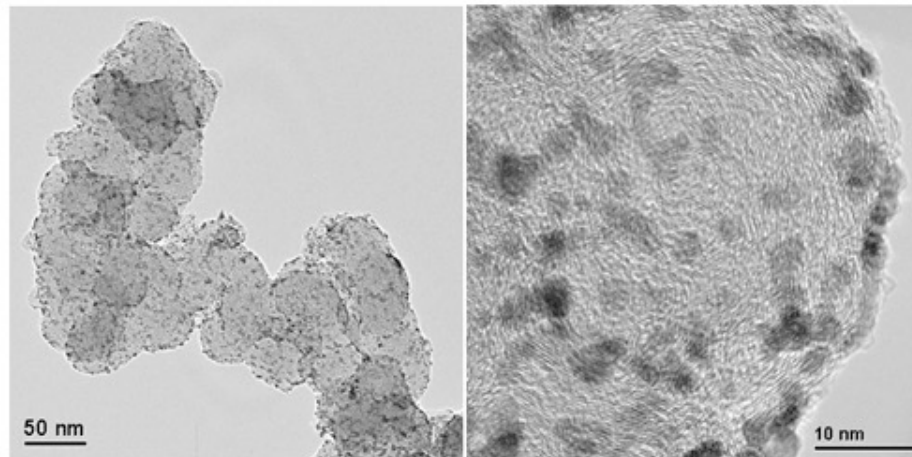
IrO₂ is used as OER catalyst

Advantage: operating flexibility (T and P)

Disadvantage: the use of precious metals as catalysts



In form of Pt nanoparticles supported on **Vulcan** (carbon black) from Sigma Aldrich



8.2. Water Electrolyzers

Alkaline Electrolyzers

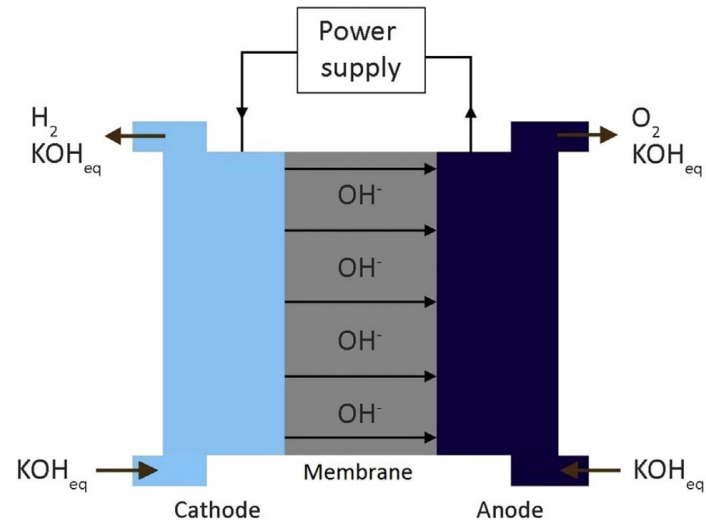
ZIRFON PERL is used as the membrane. It is a nanocomposites which include ZrO_2 nanoparticles and has a symmetrical pore structure with porosity of 50% and pore size around 150nm

Steel is used as electrode for the cathode and **Ni/Pt** as HER catalyst

Nickel is used as electrode for the anode and **Ni/Co/Fe** as OER Catalyst

Advantages: it is the cheapest and more mature technology

Disadvantage: the use of the corrosive KOH and NaOH electrolyte

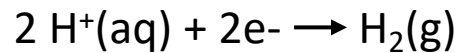


8.2. Water Electrolyzers

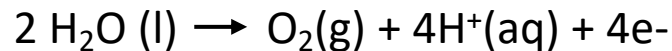
What happens when the pH changes?

For pH < 7

Cathode (reduction):

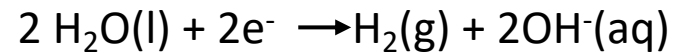


Anode (oxidation):

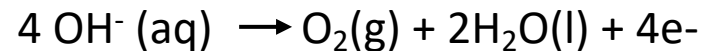


For pH > 7

Cathode (reduction):



Anode (oxidation):

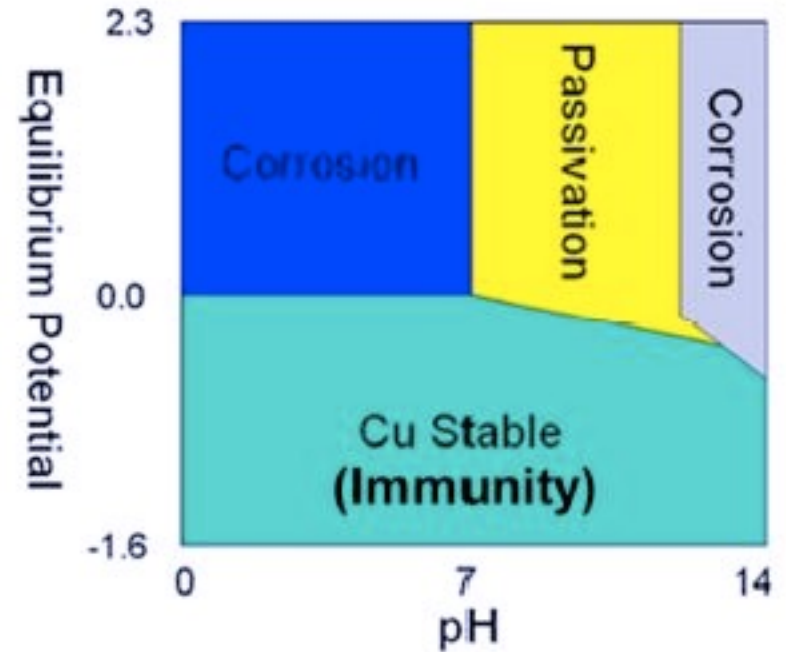
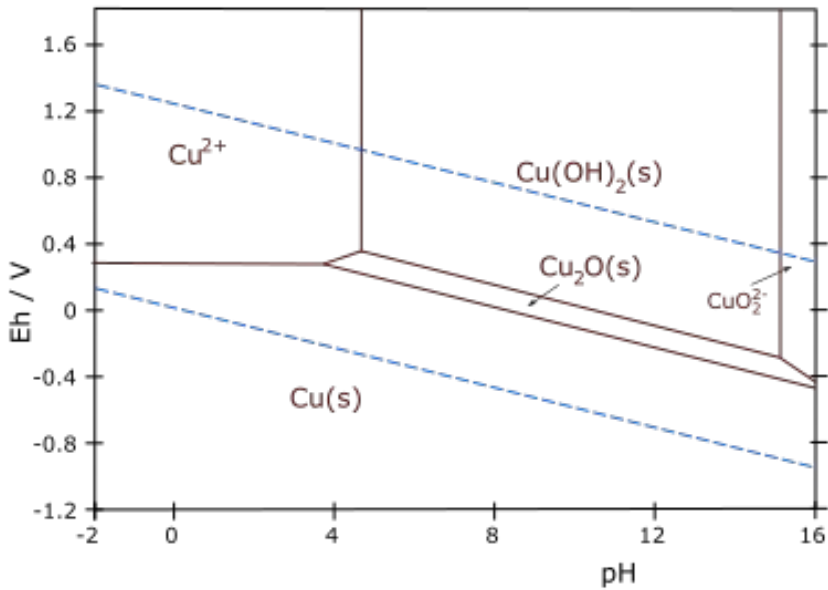


8.2. Water Electrolyzers

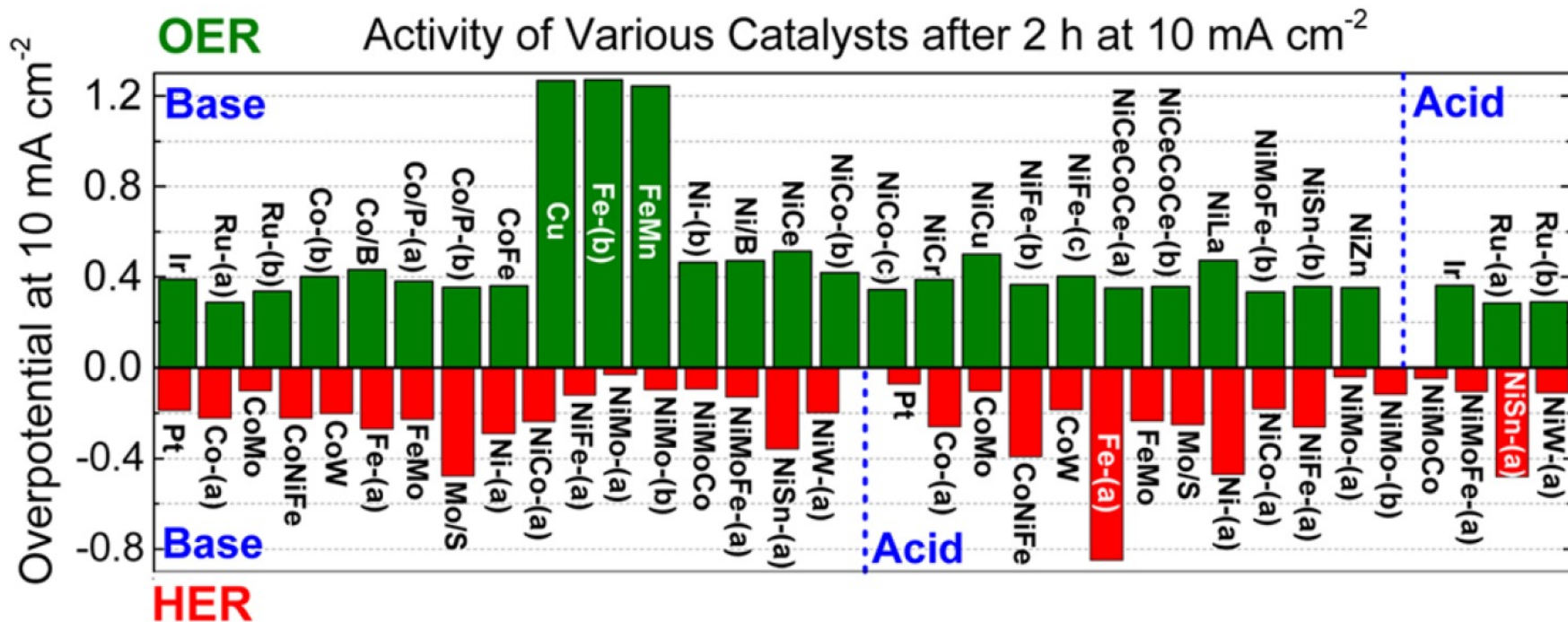
What happens when the pH changes?

Catalyst stability!

Pourbaix diagram



8.2. Water Electrolyzers



Pt, Ru, Ir are the best catalysts for OER and HER. Great, all noble metals!

On the OER side: more non-noble metal catalysts stable in acid are needed

On the HER side: alternative to noble metals? Sulfides or Oxides are good options

8.2. Water Electrolyzers

EARTH ABUNDANT CATALYSTS FOR HER

Catalyst	Advantages	Disadvantages
Precious metals (Pt, Pd)	Best known catalysts.	Expensive (\$65/gram for Pt).
Common metals (Al, V)	Inexpensive.	Poor activity.
Nickel alloys (NiMo, NiAl)	Inexpensive, stable in base, very active.	Lower activity than precious metals, unstable in acidic electrolyte.
Molybdenum sulfides (MoS ₂)	Inexpensive, stable in acid, very active.	Lower activity than precious metals, unstable in base.

Another class of Earth-abundant catalysts for HER active in acidic conditions are metal phosphides, including Ni₂P, CoP, Fe₂P, MoP, WP. Colloidal chemistry has contributed quite a bit to this with the work from Schaak's group at Penn State.

Schaak et al. *Chem. Mater.* (2016)

8.2. Water Electrolyzers

Catalyst characterization before echem

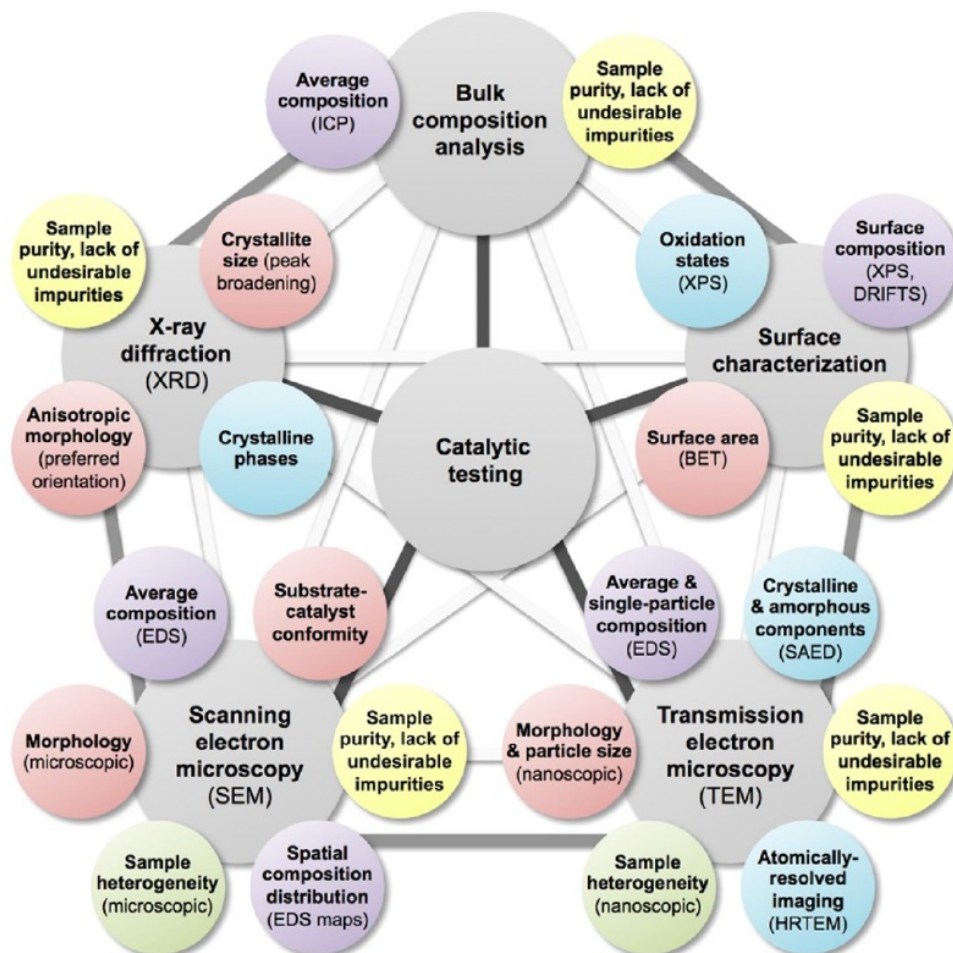


Figure 5. Representative, nonexhaustive summary of materials-characterization data that can be used to understand the key characteristics that underpin the observed catalytic performance, including important aspects of surface and bulk structure, composition, and morphology. Color-coding shows complementary types of information that are provided by different characterization techniques.

8.2. Water Electrolyzers

BENCHMARK: Pt

FOR REFERENCE: Platinum is so far the best catalyst for HER, with the lowest overpotential of -18 mV at -10 mA/cm² and -26 mV at -20 mA/cm²

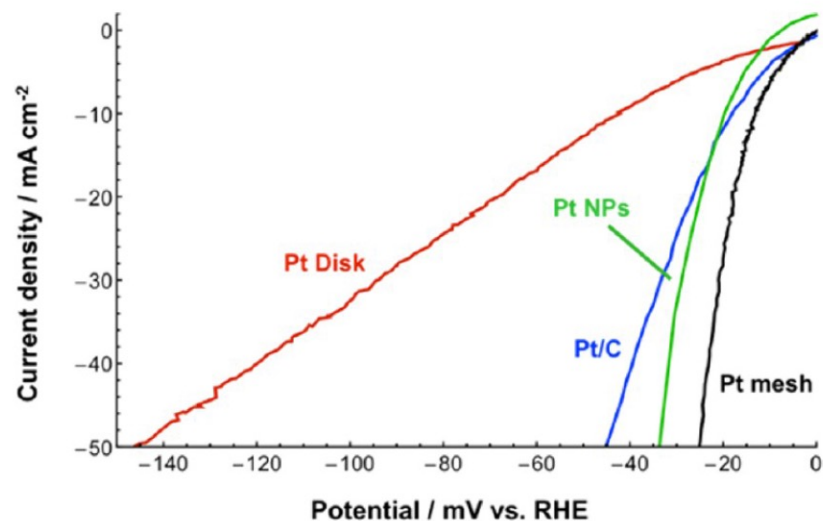
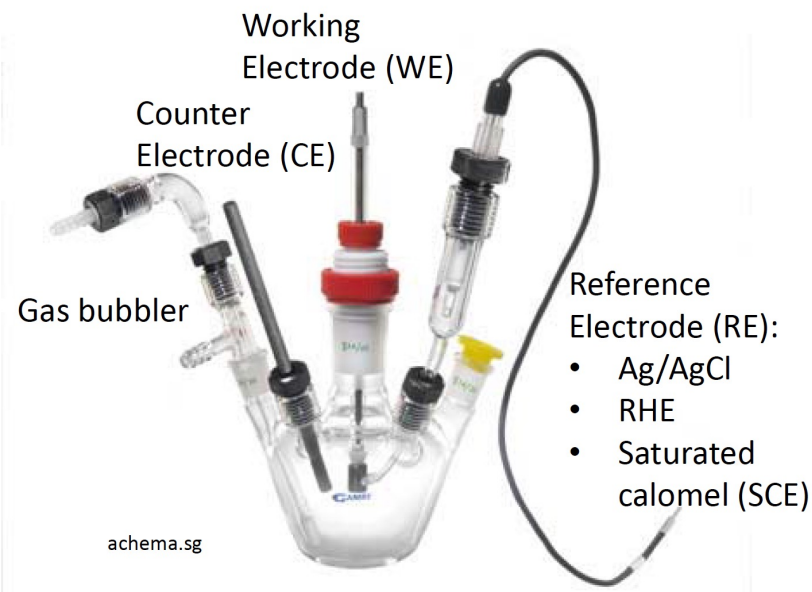


Figure 4. Polarization data for the HER in 0.5 M H₂SO₄ for a series of Pt electrodes, including a Pt mesh, Pt nanoparticles, Pt on carbon black, and a Pt disk.

Colloidal Nanocrystals as Electrocatalysts with Tunable Activity and Selectivity

Yannick T. Guntern, Valery Okatenko, James Pankhurst, Seyedeh Behnaz Varandili, Pranit Iyengar, Cedric Koolen, Dragos Stoian, Jan Vavra, and Raffaella Buonsanti*

✓ **Cite this:** *ACS Catal.* 2021, 11, 3, 1248–1295

Publication Date: January 12, 2021 ▾

<https://doi.org/10.1021/acscatal.0c04403>

Copyright © 2021 American Chemical Society

[RIGHTS & PERMISSIONS](#)

Article Views

2837

Altmetric

7

Citations

10

[LEARN ABOUT THESE METRICS](#)

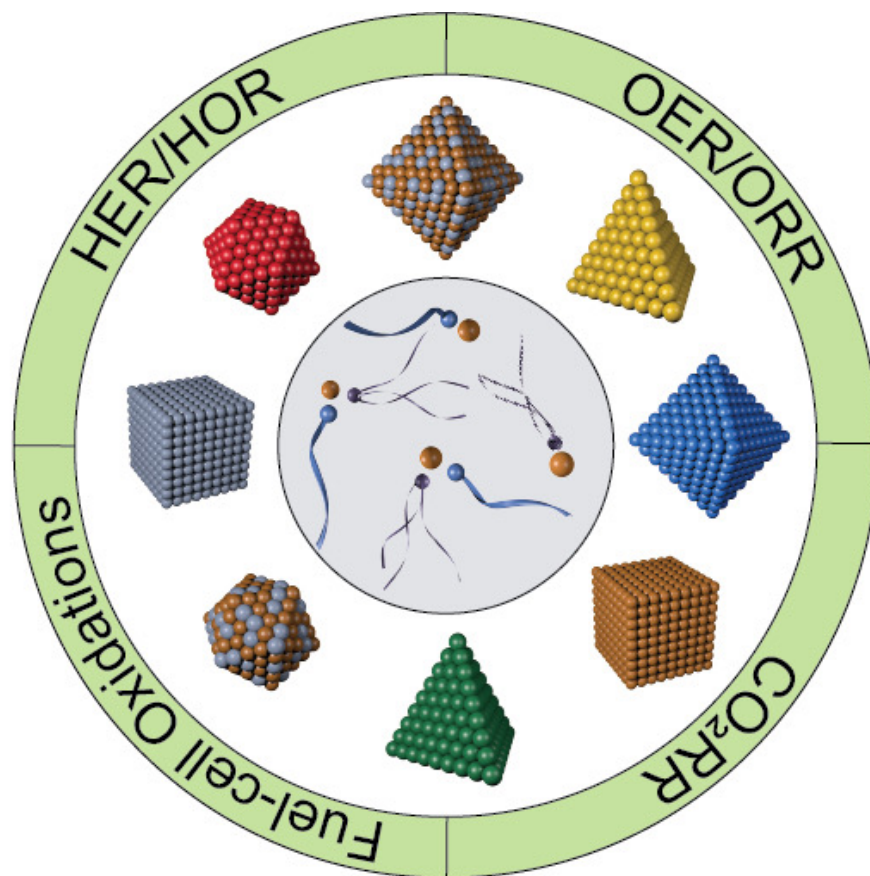
Share



Add to



Export

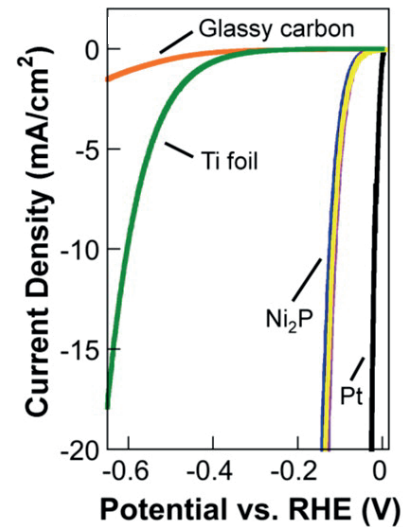
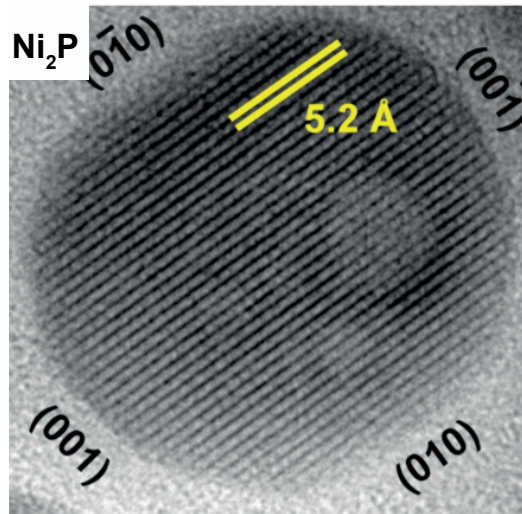


8.2. Water Electrolyzers

METAL PHOSPHIDE NANOCATALYSTS FOR HER*

Nickel phosphide NCs

NCs were synthesized as hollow multifaceted particles with an average size around 17nm and high density (001) facets exposed, which has previously been predicted to be the most active surfaces. The overpotential for these particles to produce current densities of 20 and 100 mA/cm² were -130 mV and -180 mV, respectively.



*Before performing any electrocatalytic measurement on these NCs, ligand removal was performed by annealing 30 minutes at 450C in 5% H₂/N₂ without observing any apparent change in the morphology /composition of the particles used in their studies.

8.2. Water Electrolyzers

METAL PHOSPHIDE NANOCATALYSTS FOR HER*

Nickel phosphide NCs

Table 1. Compilation of HER Performance Metrics for Various Nickel Phosphide Catalysts Synthesized under Different Conditions and Evaluated in 0.5 M H₂SO₄

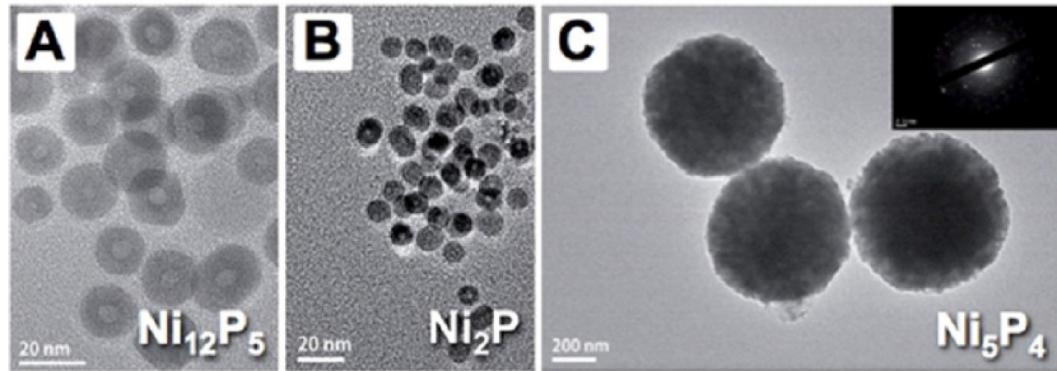
material	$\eta_{-10\text{mAcm}^{-2}}$	$\eta_{-20\text{mAcm}^{-2}}$	Tafel slope (mV dec ⁻¹)	exchange current density (A cm ⁻²)	loading density (mg cm ⁻²)	ref
Ni ₂ P NPs/Ti	~-116	-130	~46	3.3×10^{-5}	1.0	50
Ni ₂ P/Ni	-128	-153	66	-	-	58
Ni ₂ P NS/Ni foam	~-115	~-140	68	-	-	79
Polydispersed Ni ₂ P/GCE	~-125	-140	~87	-	0.38	104
nanoparticle films Ni ₂ P/Ti	~-130	-138	60	-	2.0	107
Ni ₂ P/CNT	-124	-	53	5.37×10^{-5}	-	108
peapod-like Ni ₂ P/C	-87	-115	54	-	0.36	109
Ni ₂ P-G@NF	~-150	-	~30	-	-	110
Ni ₅ P ₄ MP pellet	-23	-	33	-	177	111
Ni ₂ P MP pellet	-42	-	38	-	177	111
Ni ₁₂ P ₅ /Ti	-107	-141	63	-	3	112
NiP ₂ NS/CC	-75	-	51	2.60×10^{-4}	4.3	113
Ni ₂ P NPs	-137	-	49	-	1.99	114
Ni ₅ P ₄ NPs	-118	-	42	-	1.99	114
Ni ₁₂ P ₅ NPs	-208	-	75	-	1.99	114
Ni ₅ P ₄ /Ni	-140	-	40	-	-	115
Ni ₁₂ P ₅ /CNT	-129	-	56	7.10×10^{-5}	0.75	116
Ni ₂ P/GCE	-	-	84	2.90×10^{-6}	0.15	117
Ni ₁₂ P ₅ /GCE	-	-	108	3.70×10^{-7}	0.15	117
MOF-derived Ni ₂ P	~-200	-	62	7.10×10^{-5}	0.35	118
MOF-derived Ni ₁₂ P ₅	~-650	-	270	4.50×10^{-5}	0.35	118
Ni ₂ P/CNSs	-92	-108	47	4.90×10^{-4}	-	119
Ni ₂ P NPs/Ni foam	-136	-	-	-	0.14	120
Ni-P films	-93	-	33 and 98	-	0.35	121
Ni ₂ P-NRs/Ni	-131	-163	106.1	8.62×10^{-5}	-	122
Ni ₅ P ₄	-	-62	46.1	2.75×10^{-4}	0.15	123
Ni ₂ P	-	-228	83.3	2.10×10^{-4}	-	124
Ni ₂ P/NRGO	-102	-122	59	4.90×10^{-5}	-	125
Ni ₂ P-G/NF	-75	-	51	-	-	126
(Ni ₂ P)@graphitized carbon	-45	-	46	-	0.38	127

8.2. Water Electrolyzers

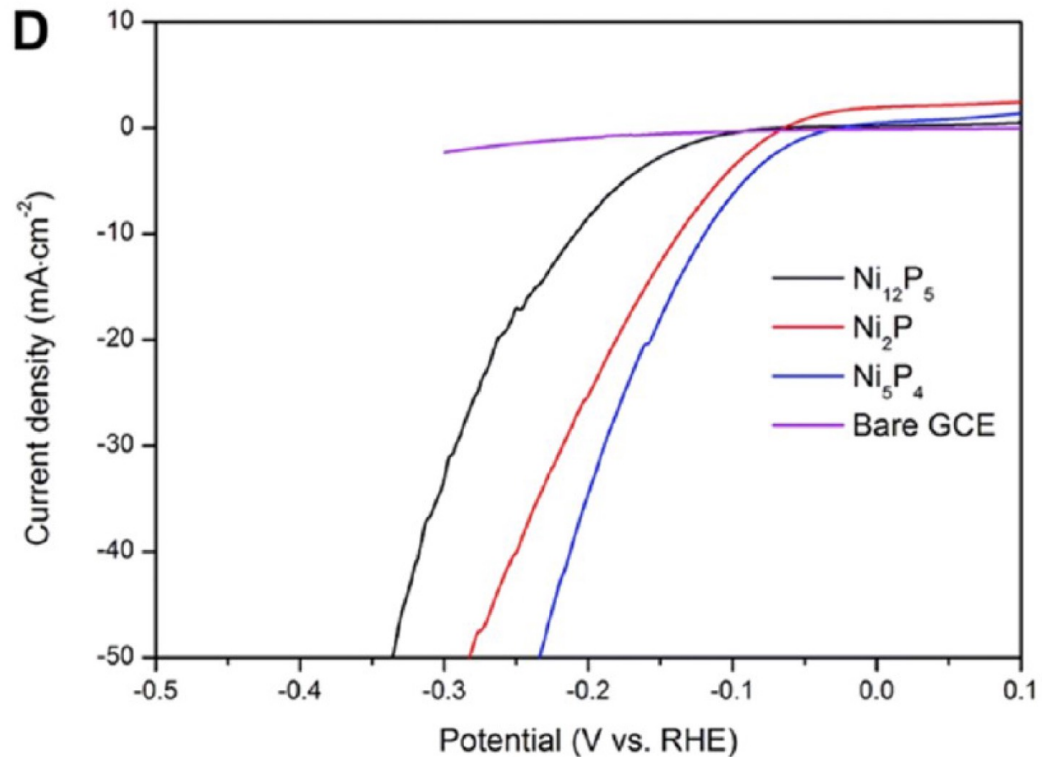
STOICHIOMETRY-DEPENDENT BEHAVIOUR

METAL PHOSPHIDE NANOCATALYSTS FOR HER*

Nickel phosphide NCs



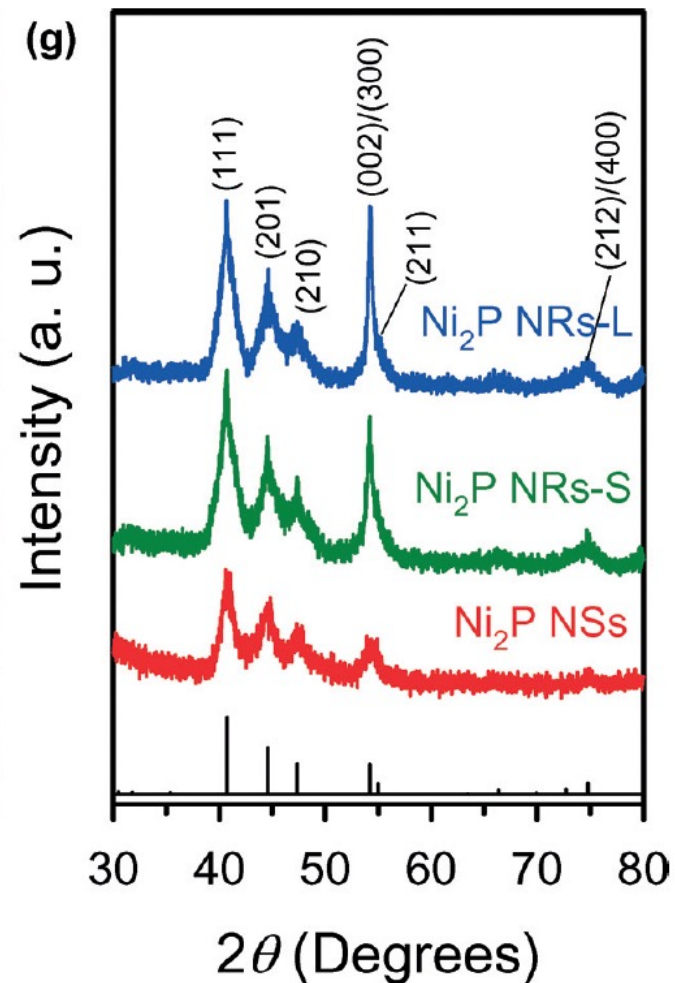
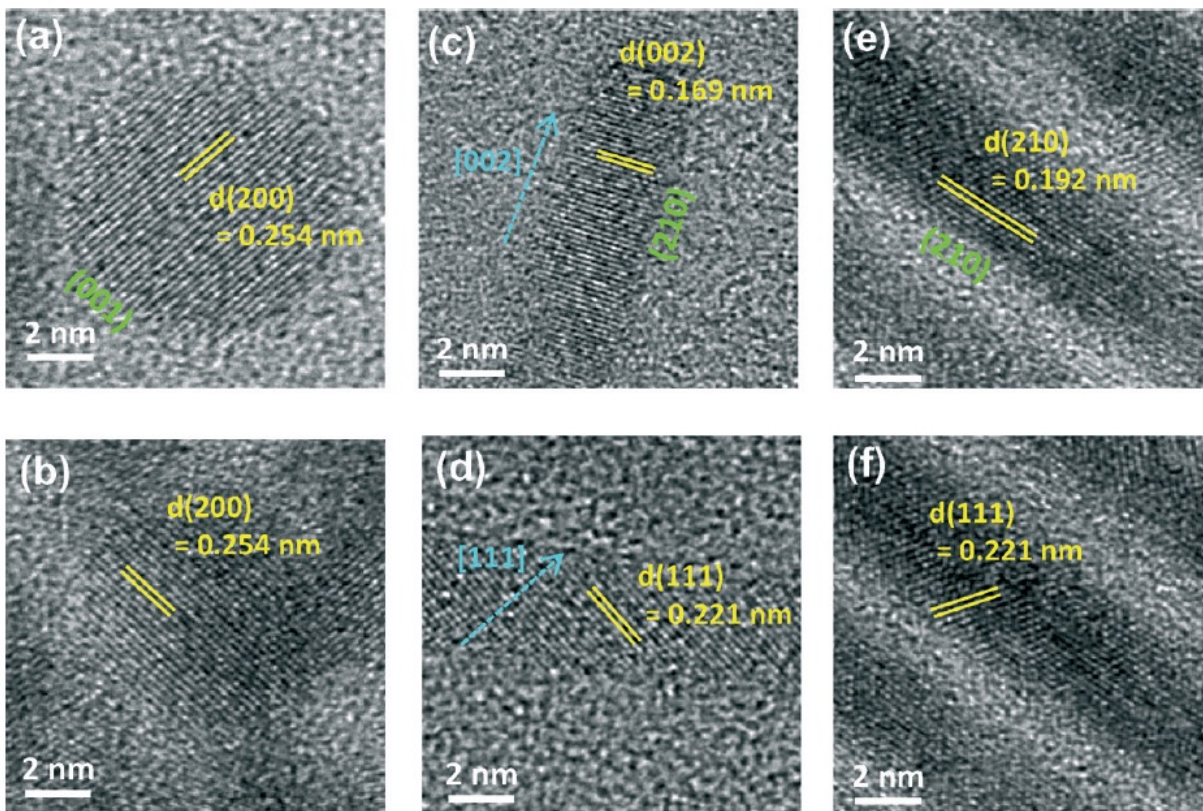
Note: the crystal structure changes with composition so it is not only matter of atomic ratio.



8.2. Water Electrolyzers

METAL PHOSPHIDE NANOCATALYSTS FOR HER*

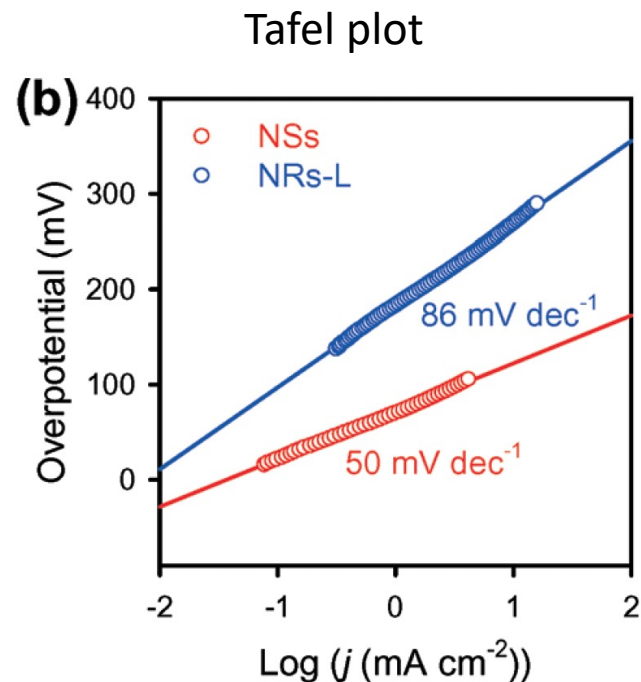
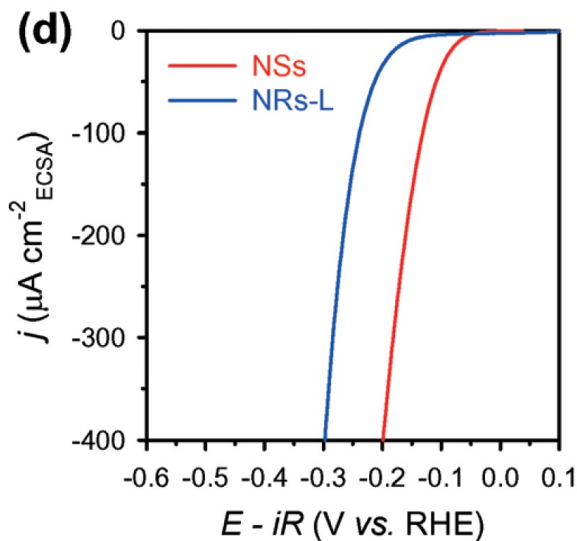
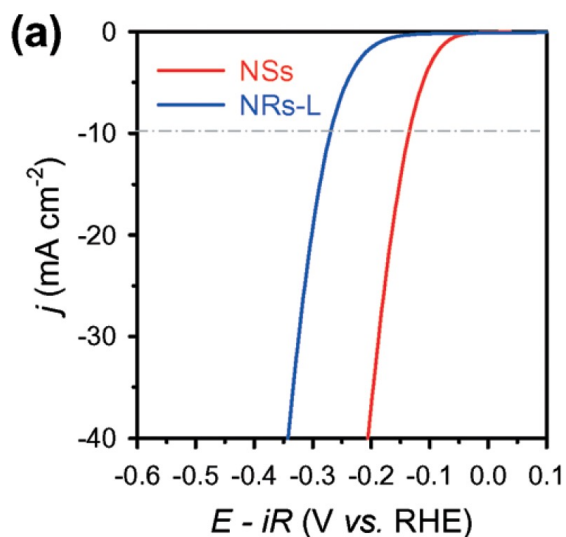
Nickel phosphide (Ni_2P) NCs



8.2. Water Electrolyzers

METAL PHOSPHIDE NANOCATALYSTS FOR HER*

Nickel phosphide (Ni_2P) NCs



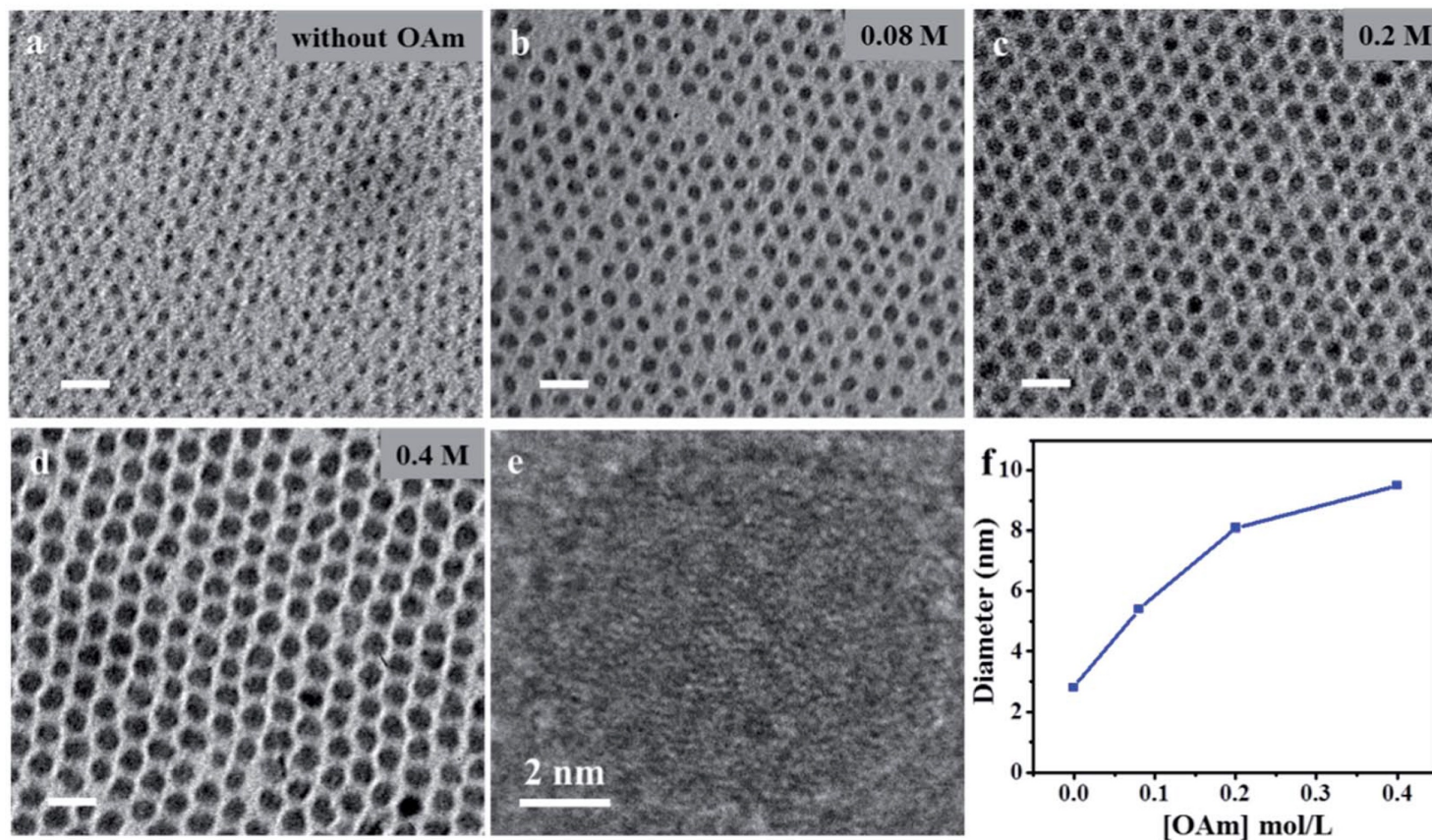
The size and shape-dependence of electrocatalytic activity of the Ni_2P NCs has also been investigated. Electrochemical measurements have revealed that Ni_2P nanospheres (Ni_2P NSs) with predominant (001) surfaces exhibit higher HER activity than Ni_2P nanorods (Ni_2P NRs) with the (210) surface. Ni_2P NSs generated a current density of -10 mA cm^{-2} at an overpotential of 135 mV in 0.5 M H_2SO_4 , whereas Ni_2P NRs produced the same current density at a larger overpotential (270 mV). Furthermore, the turnover frequency of Ni_2P NSs was about thirteen times higher than that of Ni_2P NRs. The results suggest that the crystallographic facets of Ni_2P NCs play a critical role in dictating HER activities.

8.2. Water Electrolyzers

SIZE-DEPENDENT BEHAVIOUR

METAL PHOSPHIDE NANOCATALYSTS FOR HER*

Nickel phosphide (Ni_2P) NCs

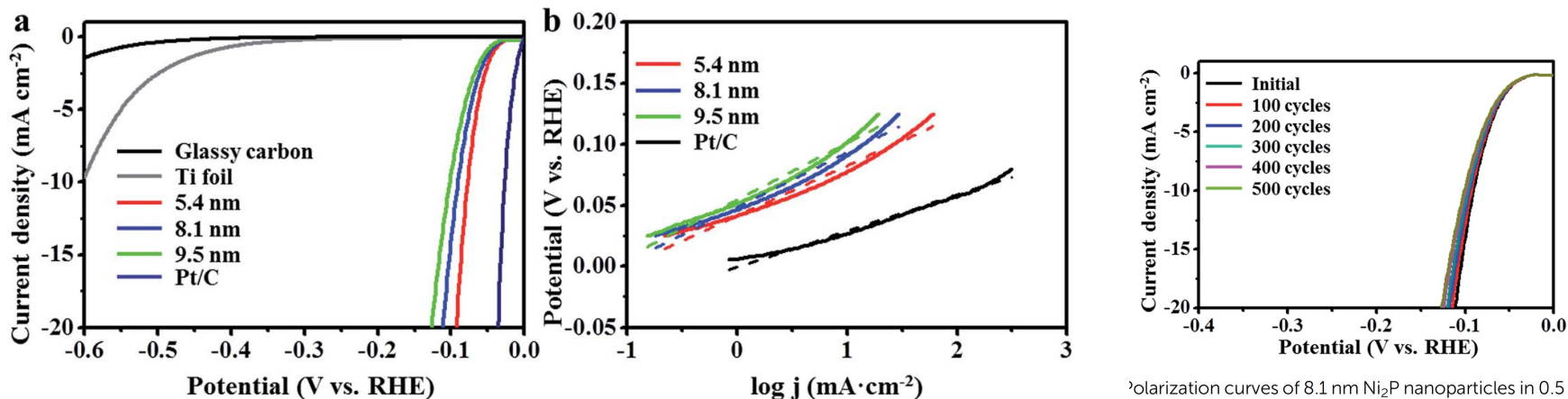


8.2. Water Electrolyzers

SIZE-DEPENDENT BEHAVIOUR

METAL PHOSPHIDE NANOCATALYSTS FOR HER*

Nickel phosphide (Ni₂P) NCs



Polarization curves of 8.1 nm Ni₂P nanoparticles in 0.5 M H₂SO₄ (dotted line) and after 100, 200, 300, 400, and 500 CV sweeps between +0.22 and -0.23 V vs. RHE.

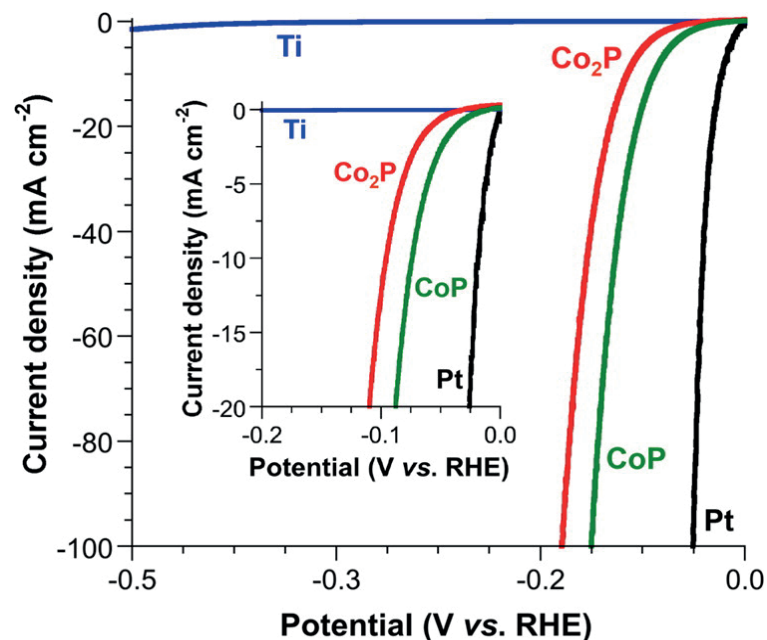
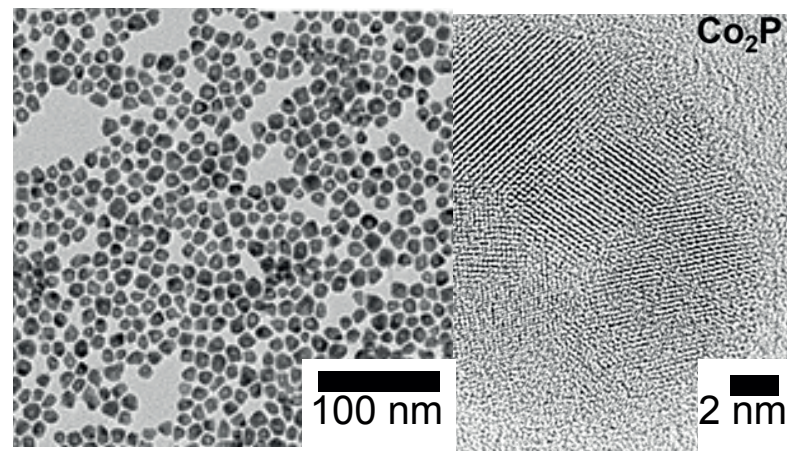
The resulting small-sized product possesses a high accessible surface area and a high density of exposed (001) facets. Experimental results showed that the small-sized Ni₂P NCs not only reduced the overpotential but also decreased the Tafel slope, thus significantly improving HER catalytic performance. The best performance were achieved with 5.4 nm Ni₂P NCs which showed an overpotential of 93 mV at 20 mA/cm² and for a mass loading of approximately 1 mg/cm² onto a 0.20 cm² Ti foil substrate.

8.2. Water Electrolyzers

METAL PHOSPHIDE NANOCATALYSTS FOR HER*

Cobalt phosphide NCs

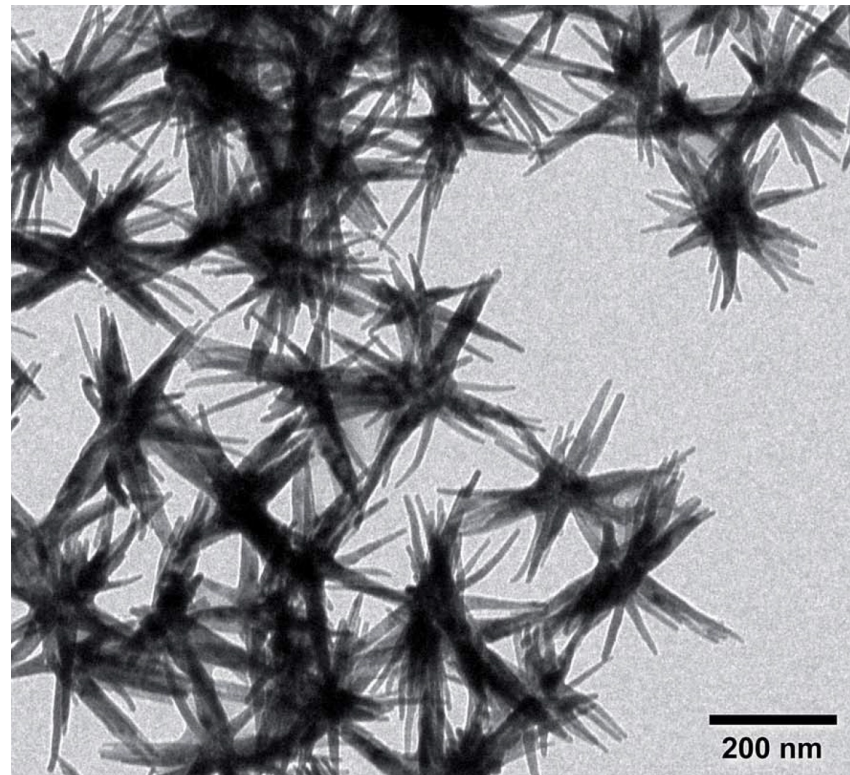
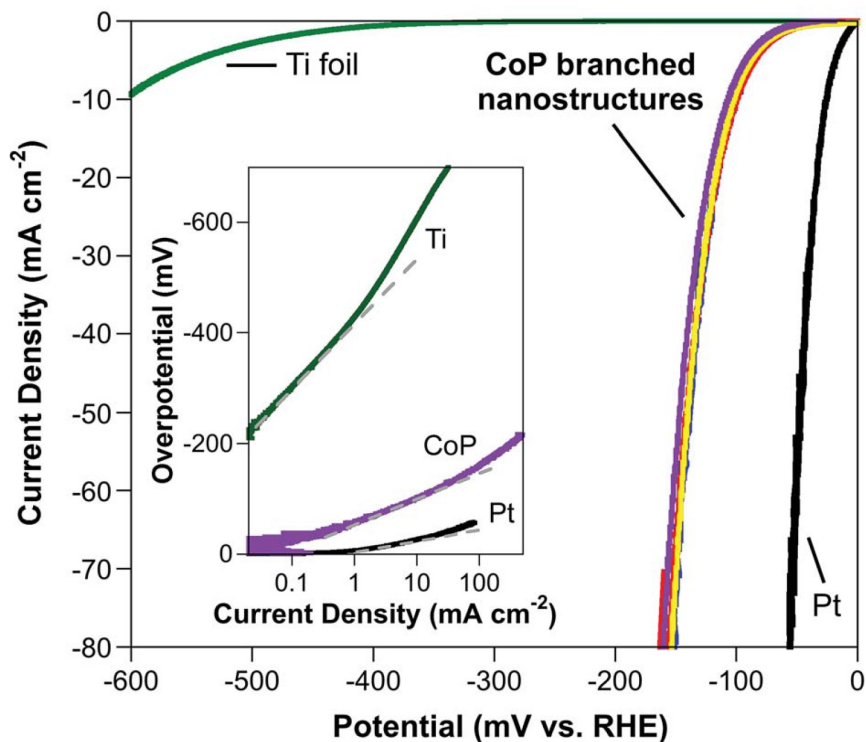
Morphologically equivalent CoP and Co₂P multifaceted and hollow particles were accessed using the same colloidal procedure. This allows similarities and differences in HER activity to be correlated most significantly with composition and structure, while minimizing morphological contributions, such as size, size distribution, dispersability, and faceting. When testing the electrocatalytic activity of CoP and Co₂P NCs, the following activity trend was found Co < Co₂P < CoP. While this result is in agreement with previous literature, much lower overpotential (-95 mV and -109 mV to produce cathodic current densities of -10 and -20 mA/cm², respectively) was found for the Co₂P NCs compared to the ones with different morphology reported in the literature (that falls in a range between -160 mV and -200 mV at -20 mA/cm²), once again it reveals the importance of morphology in catalysis.



8.2. Water Electrolyzers

METAL PHOSPHIDE NANOCATALYSTS FOR HER*

Cobalt phosphide NCs

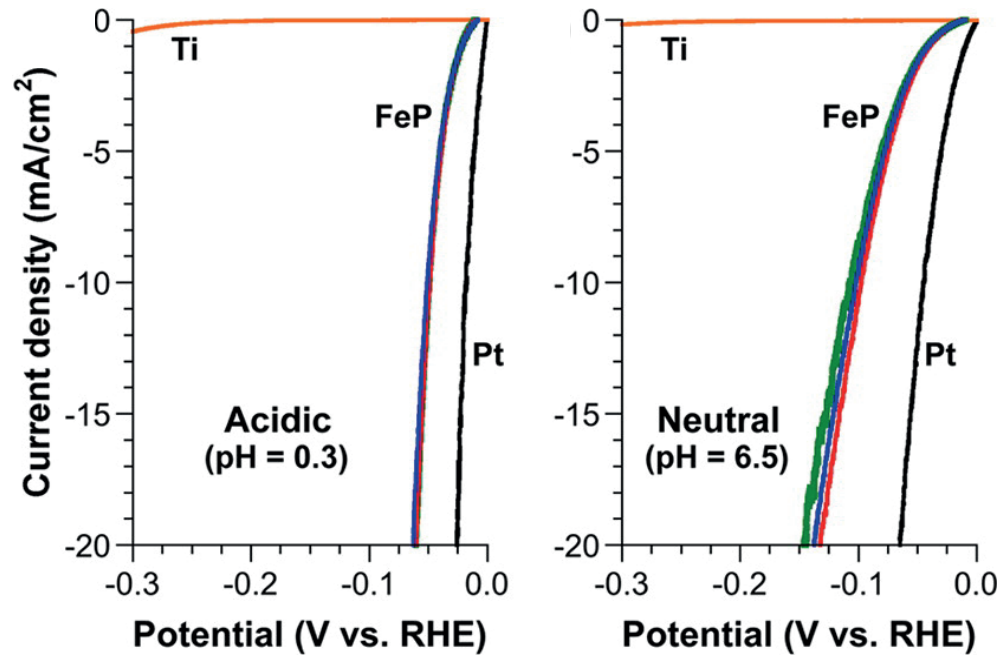
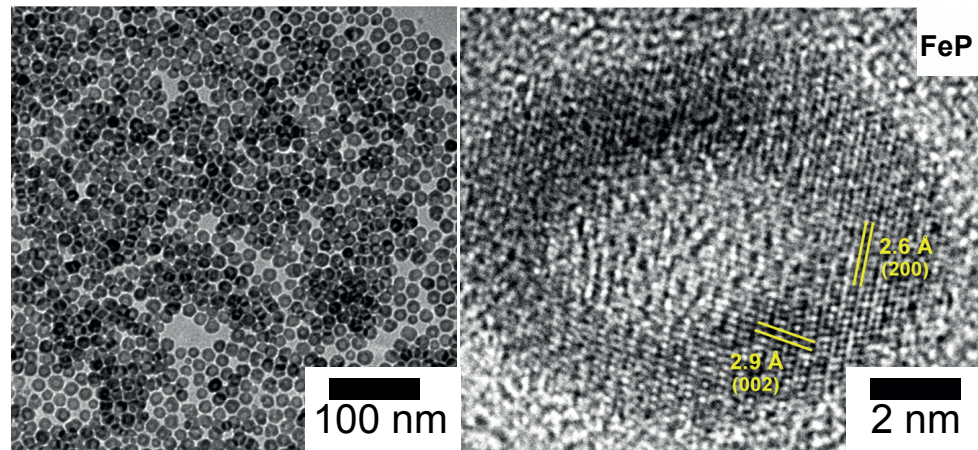


Direct comparisons by the same group of multifaceted CoP nanoparticles with highly branched CoP nanostructures that exposed a high density of (111) facets suggested that the high HER activity of CoP is intrinsic to the system and that, in this case, shape may not play a significant role in defining the magnitude of the overpotentials required to produce operationally relevant cathodic current densities.

8.2. Water Electrolyzers

METAL PHOSPHIDE NANOCATALYSTS FOR HER*

Iron phosphide NCs

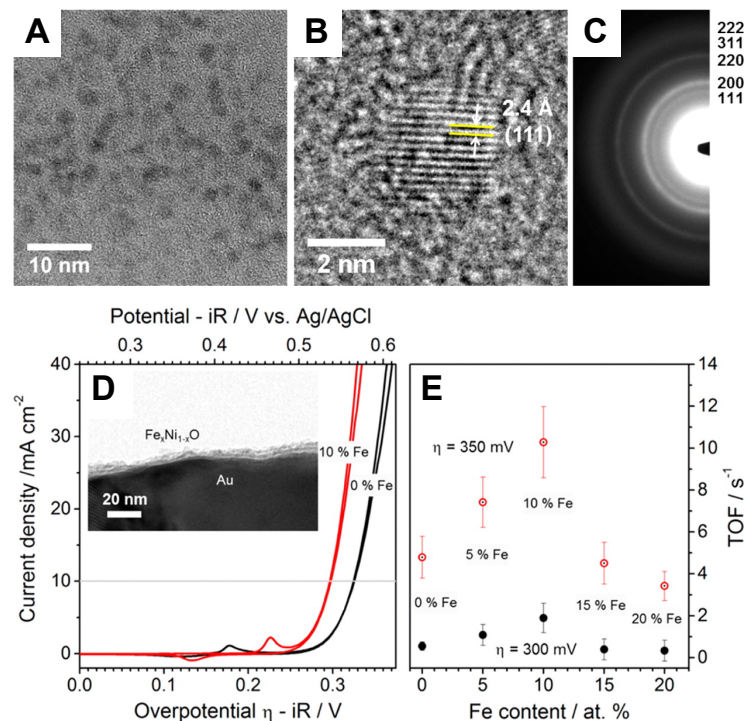
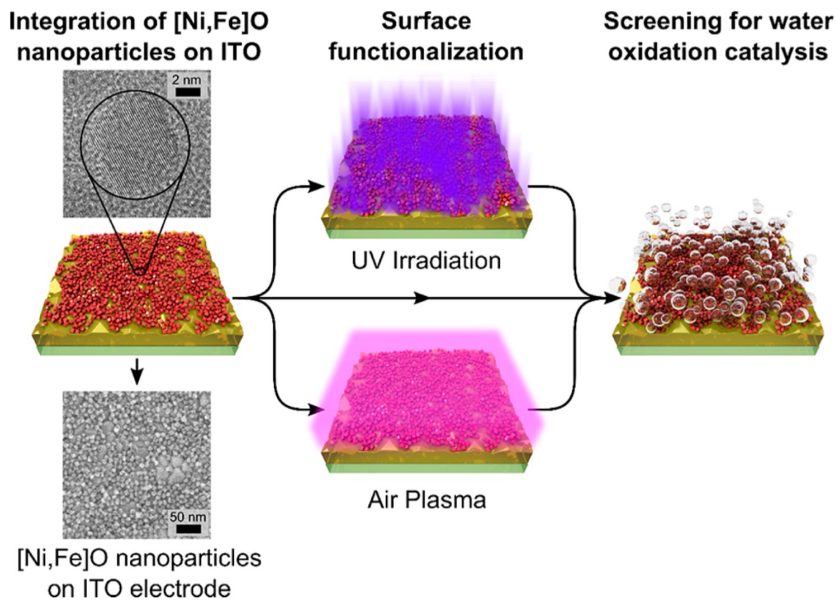


8.2. Water Electrolyzers

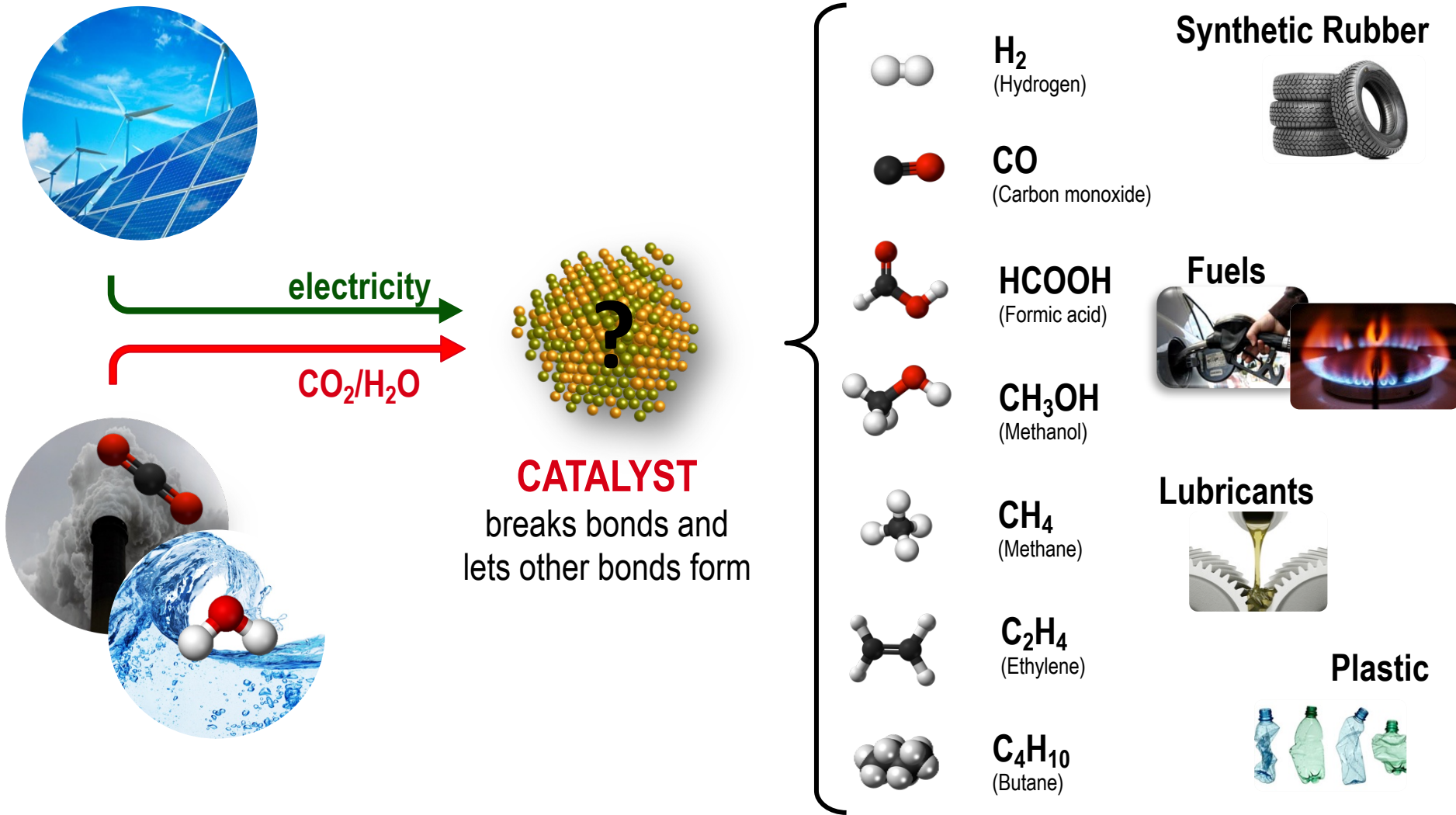
Nickel Iron Oxide Nanocrystals

For context Ni-Fe-O has attracted a lot of interest as OER catalysts. Not too much work has been done in this area with colloidal NCs. Bau et al. have synthesized and tested as OER electrocatalysts 8 nm Ni-Fe-O NCs in a metastable rock-salt phase and variable composition ratios of nickel to iron. The nickel-rich NCs showed the lowest overpotential of around 300 mV at 10 mA/cm² with optimal electrode thickness corresponding to a couple of monolayers. The similar OER performance of the rock salt phase NCs with other Ni-Fe-O based catalysts suggests that the presence of Fe³⁺ centers on the surface plays a bigger role than the crystalline phase itself.

Scheme 1. Functionalization of ITO Electrodes with [Ni,Fe] O Nanoparticles



8.3. CO₂ Electrolyzers



8.3. CO₂ Electrolyzers

CO₂ electrolysis is one technology that utilizes power from renewables and operates at room temperature and ambient pressure

Fischer-Tropsch

300 °C
+ 50 atm
+ H₂



CO/CO₂ to methane
or methanol

Reversed solid oxide fuel cells

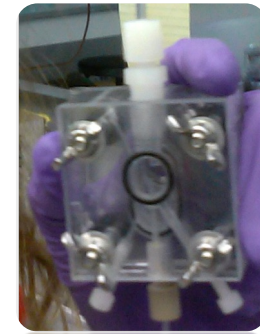
500-800 °C
+ 10 atm
+ Power



CO/CO₂ to methane

CO₂ electrolysis

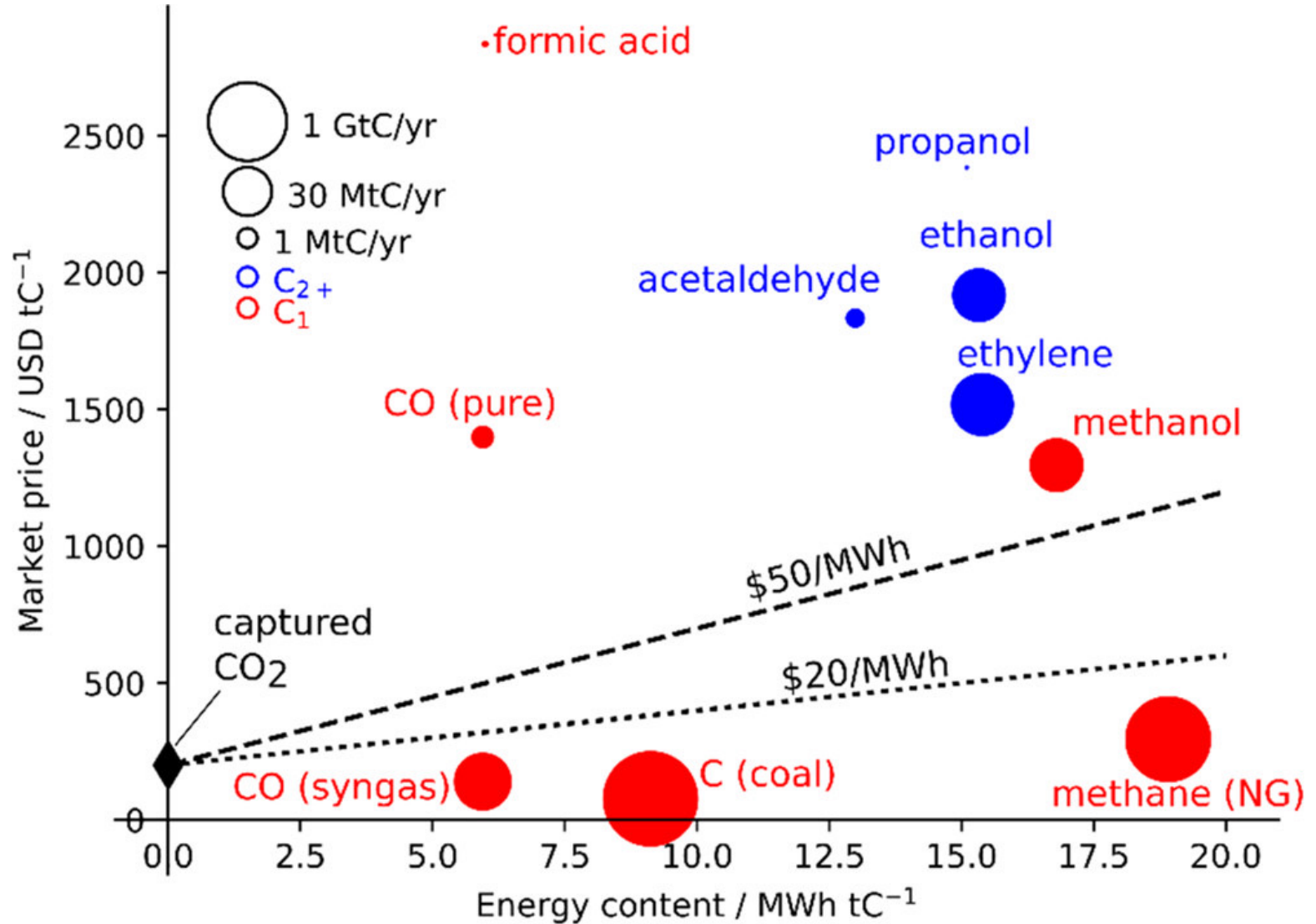
Room temperature +
Atmospheric pressure +
Power



CO₂ to hydrocarbons

8.3. CO₂ Electrolyzers

Which products should be target?

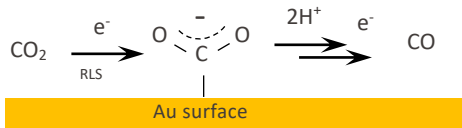


8.3. CO₂ Electrolyzers

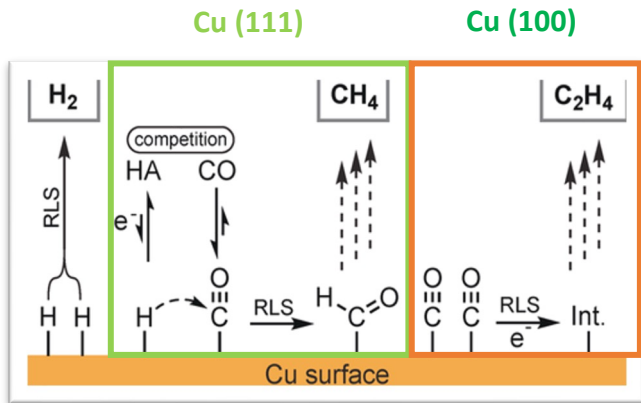
The CO₂ reduction pathway is “quite” complex!

Nitopi, Nørskov*, Jaramillo*, Chorkendorff* et al. *Chem. Rev.* (2019)

Experimental evidences

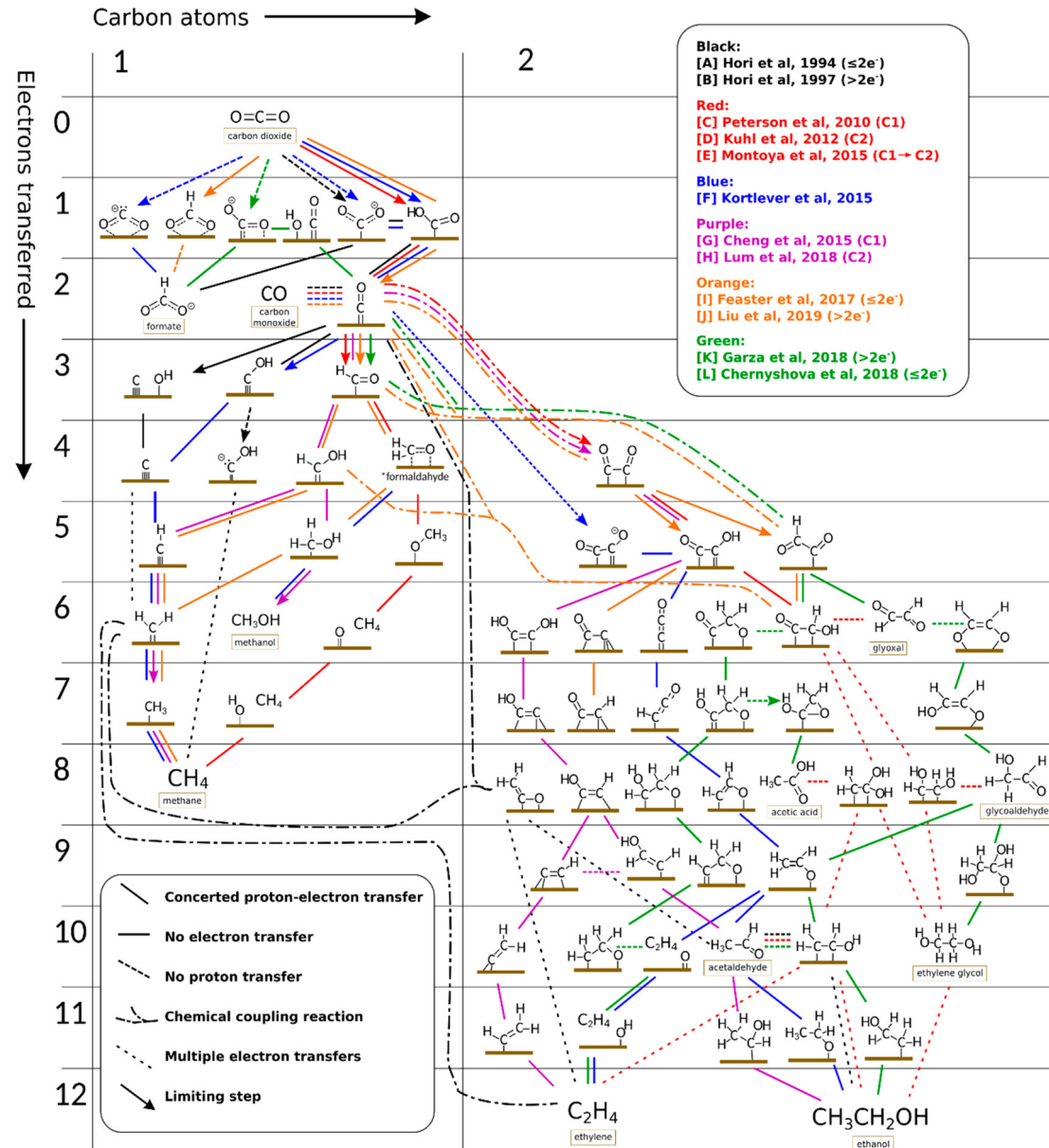


Wutting, Surendranath*, et al. *J. Am. Chem. Soc.* (2017)



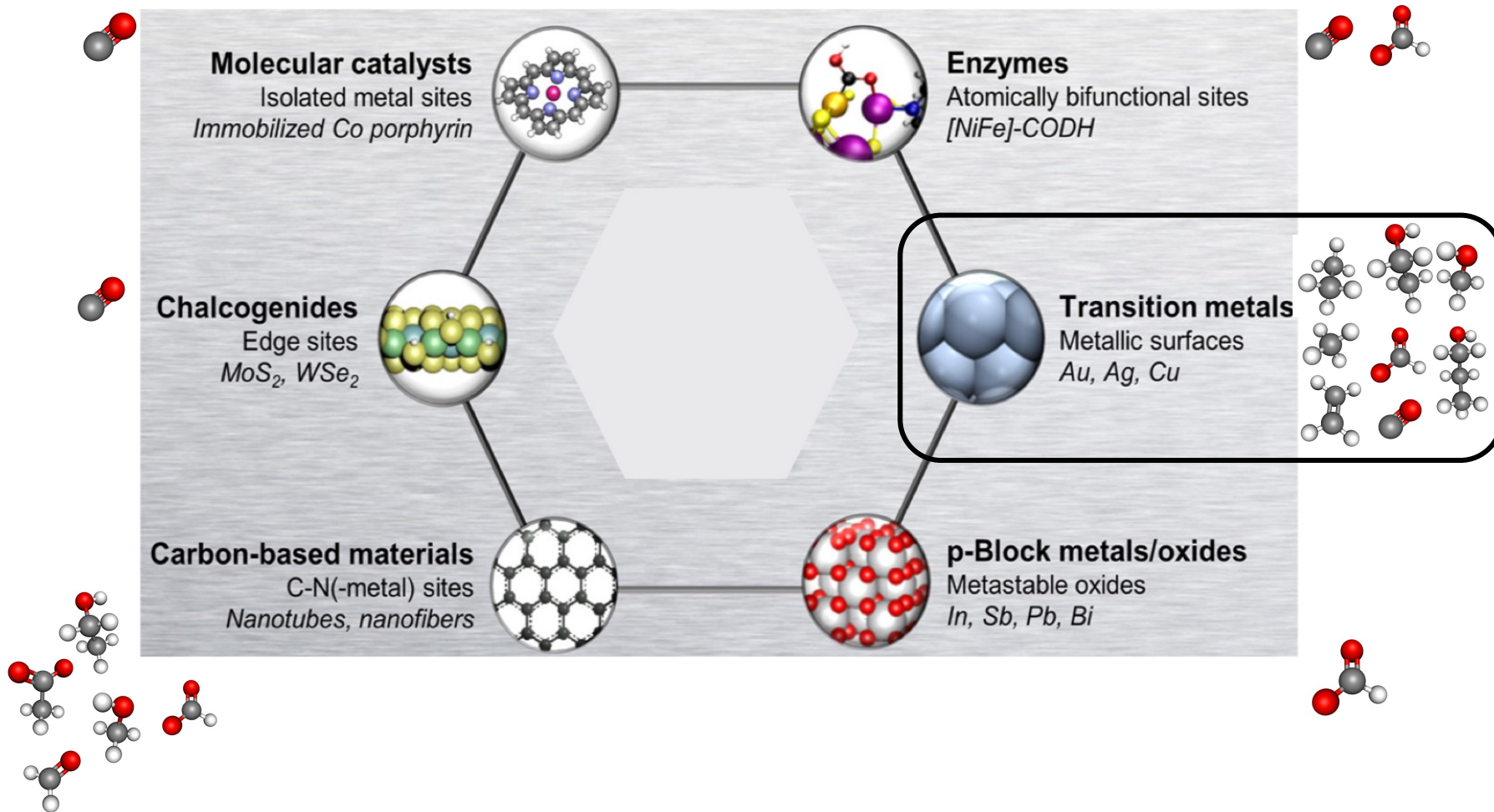
Schreier, Surendranath*, et al. *ACIE* (2018)

Perez-Gallent, Calle-Vallejo*, Koper*, et al. *ACIE* (2017)



8.3. CO₂ Electrolyzers

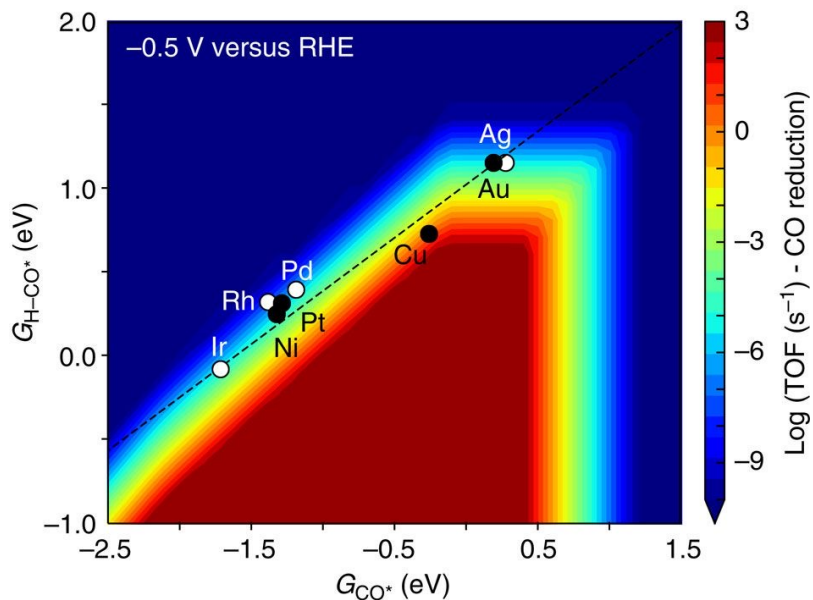
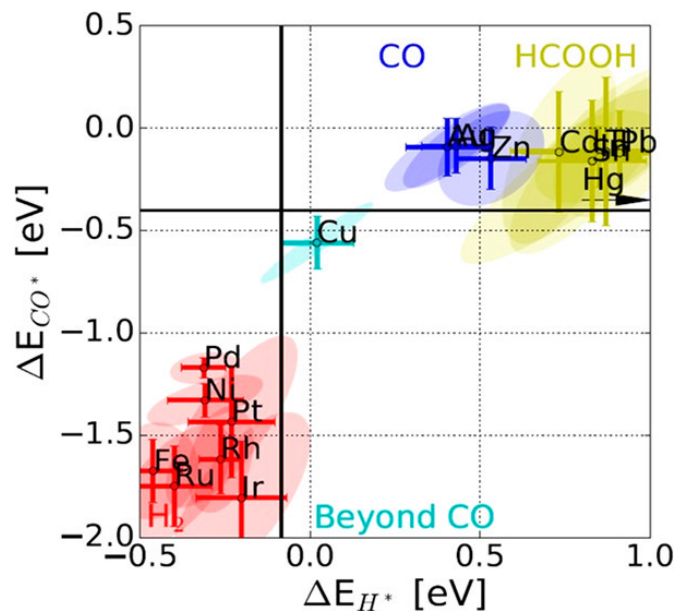
Which catalysts should we use?



8.3. CO₂ Electrolyzers

Copper provides the “right” binding energies to proceed beyond CO products

CO*, H* and H-CO* binding energies have been identified as good descriptors of the catalytic activity of metals



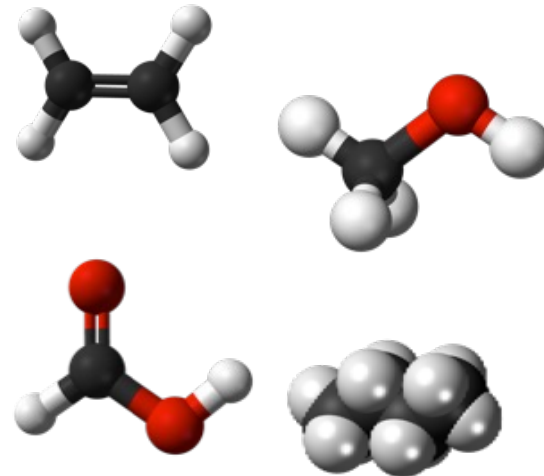
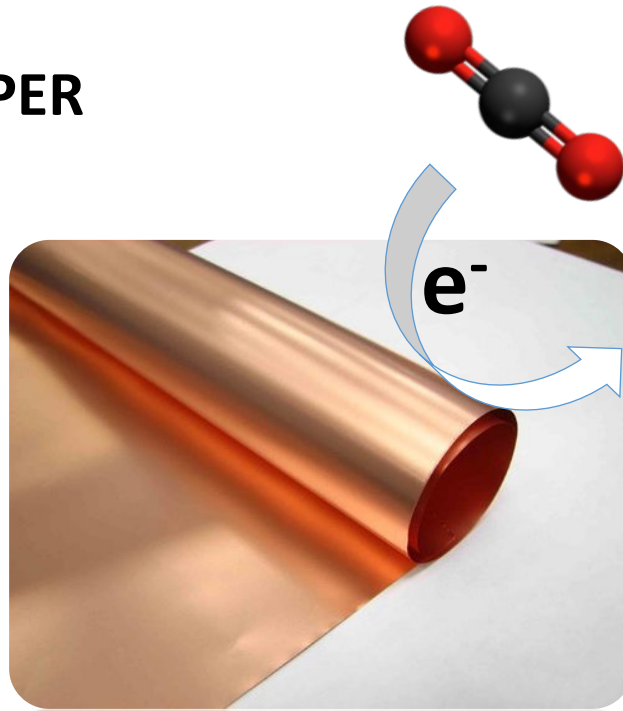
Bagger, Rossmeisler, et al. *Chem. Phys. Chem.* (2017)

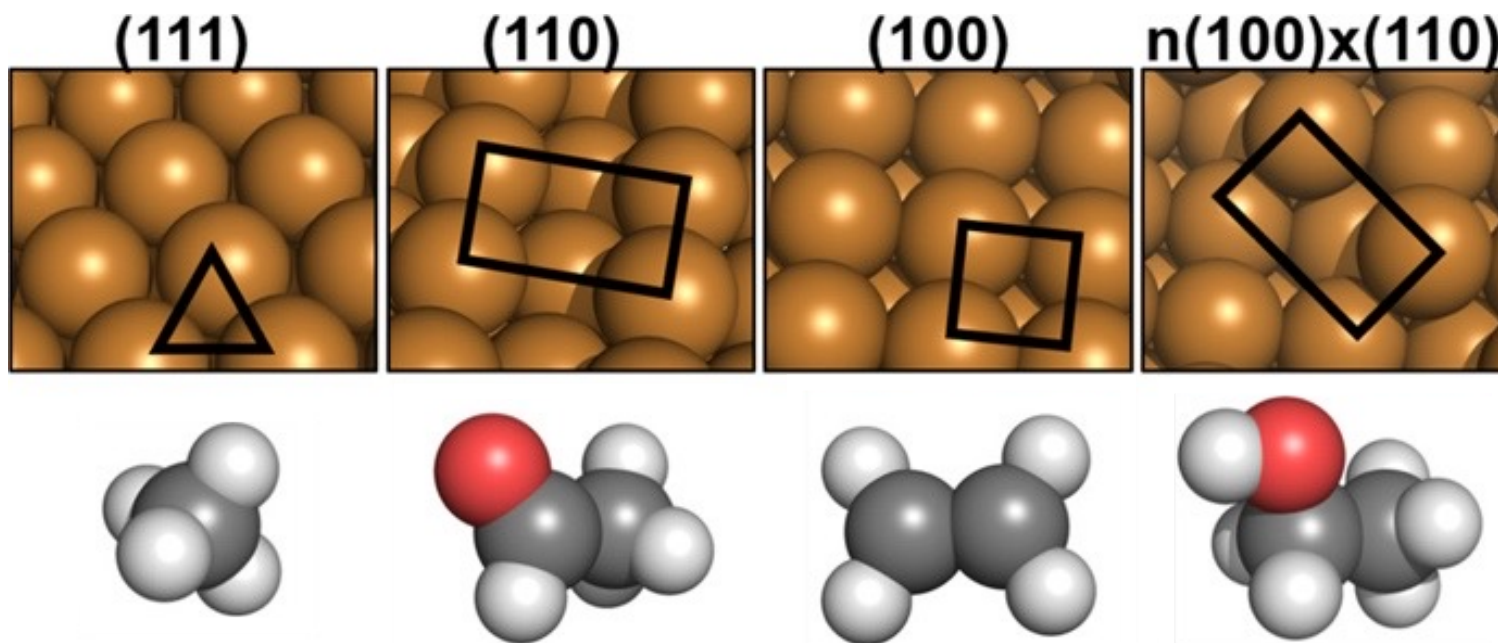
Liu, Nørskov, et al. *Nat. Commun.* (2017)

8.3. CO₂ Electrolyzers

Polycrystalline copper produced 16 different products!

**COPPER
FOIL**

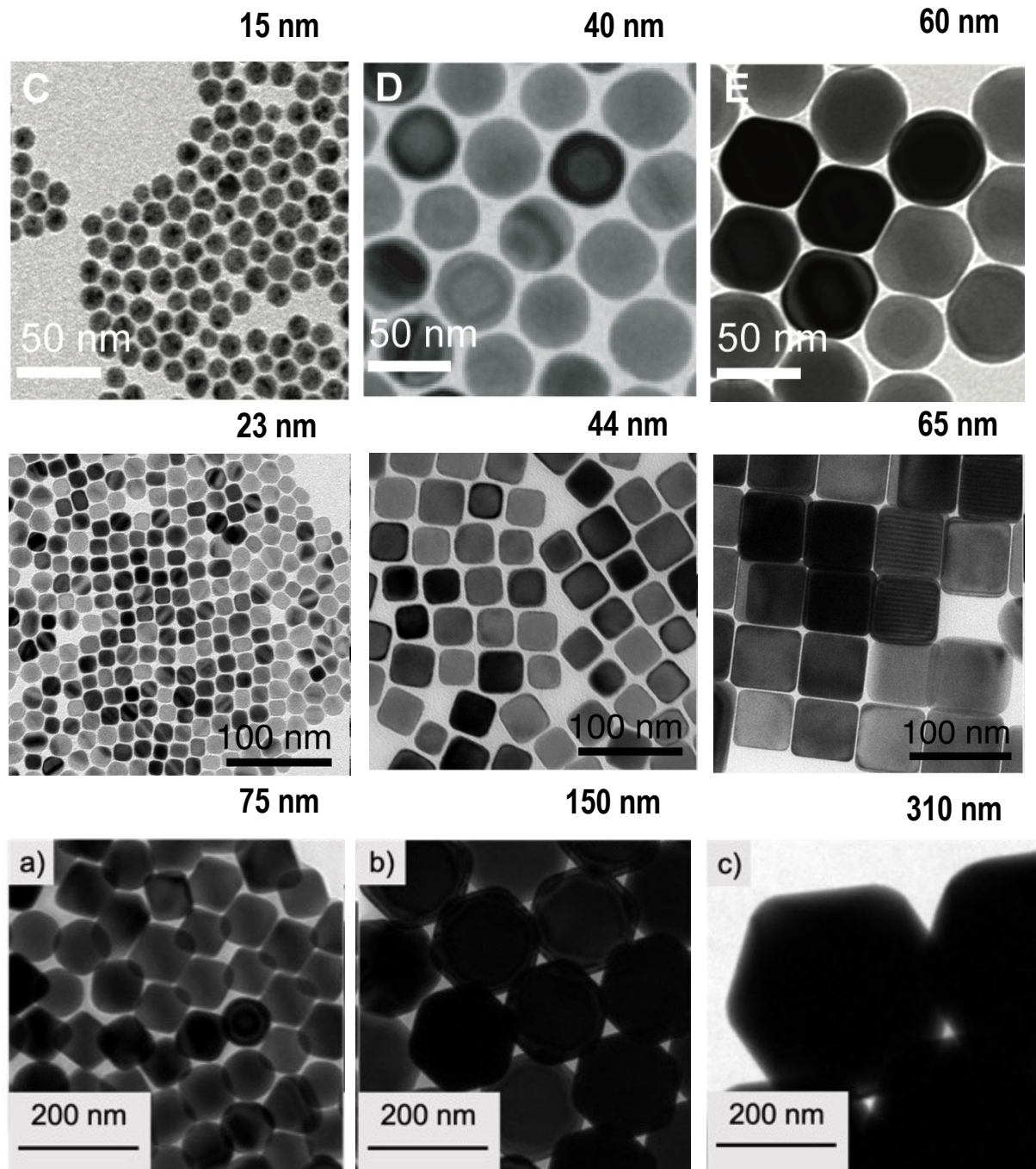




Can we make shape controlled Cu NCs to translate the discoveries from surface science studies to catalyst behaviour under more realistic conditions?

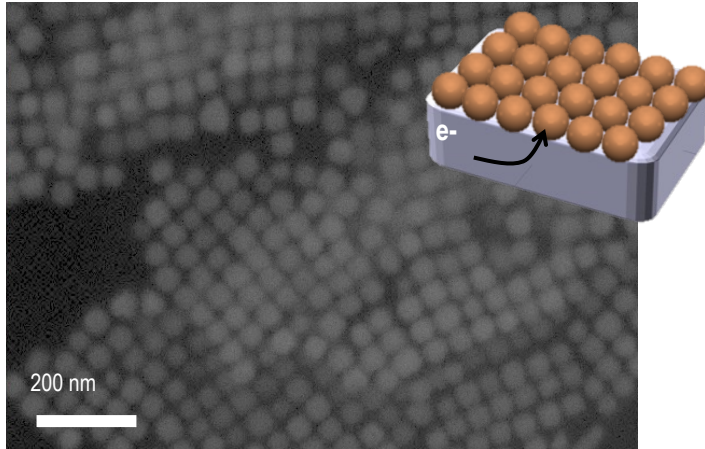
8.3. CO₂ Electrolyzers

Colloidal nanocrystals:
finely tailored catalysts

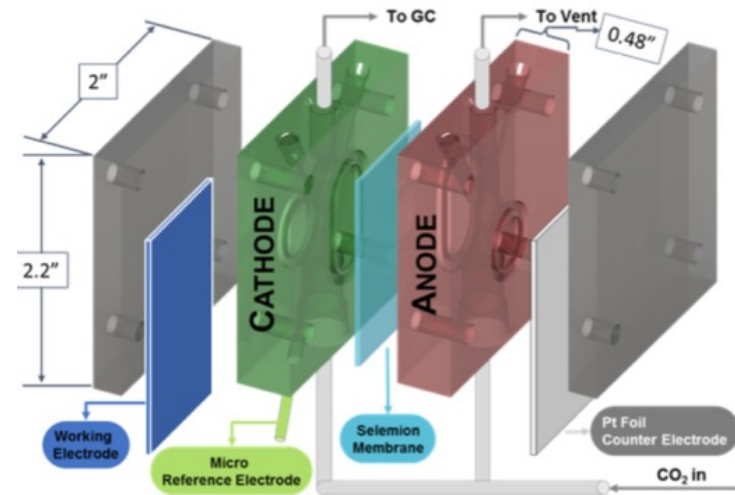
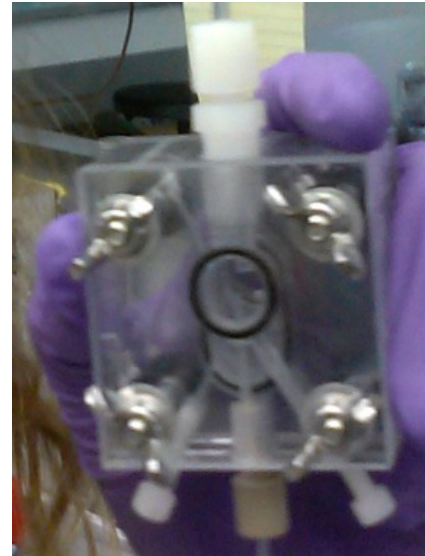


8.3. CO₂ Electrolyzers

H-cell



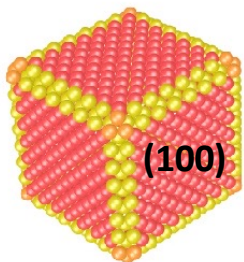
Nanocrystals are deposited on a conductive glassy carbon substrate



8.3. CO₂ Electrolyzers

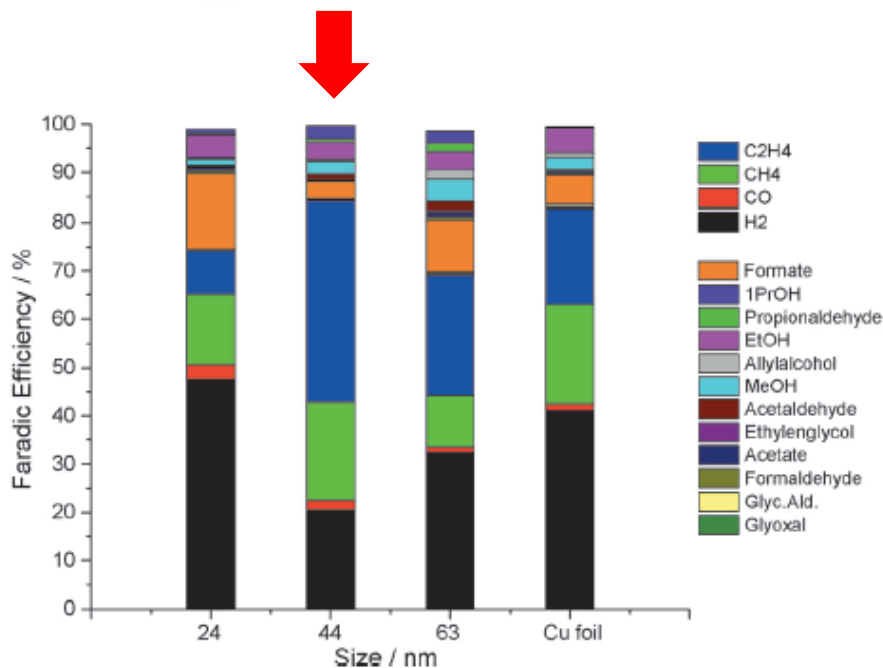
Synergy between size and shape in CO₂RR

Cu_{Cubes} 44nm are the best for ethylene

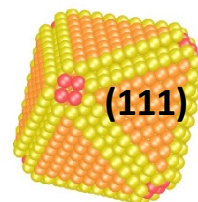


FE (CO₂RR) = 80 %

FE (C₂H₄) = 40 %

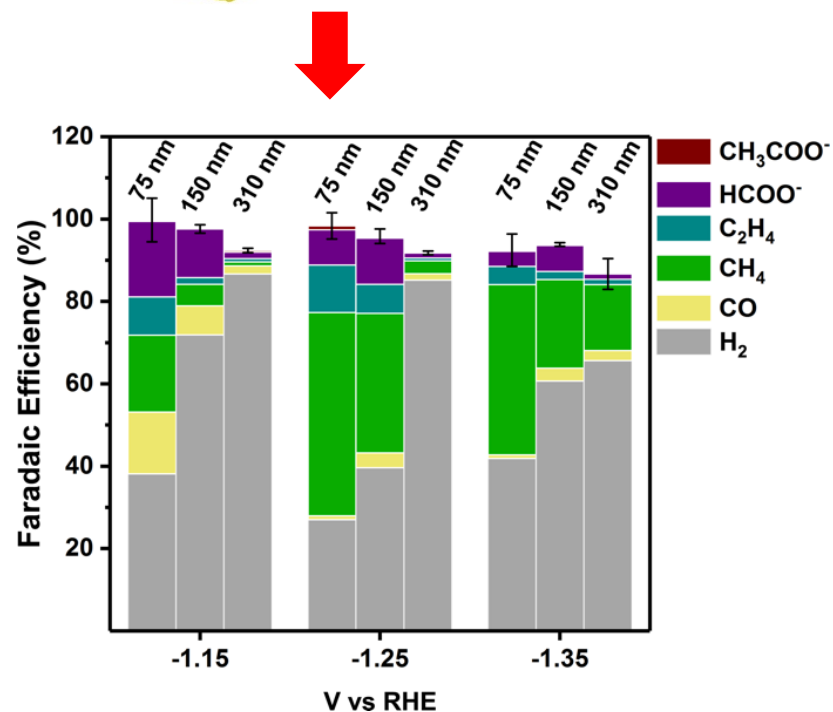


Cu_{Octahedra} 75nm are the best for methane



FE (CO₂RR) = 80 %

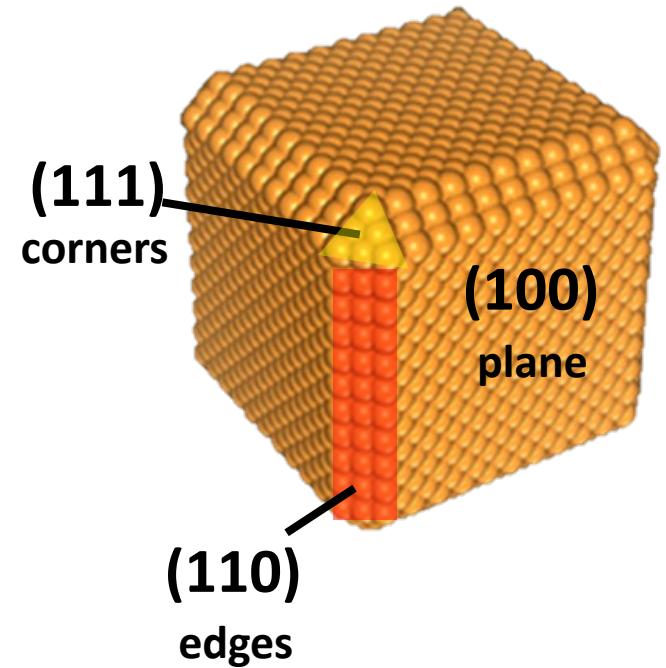
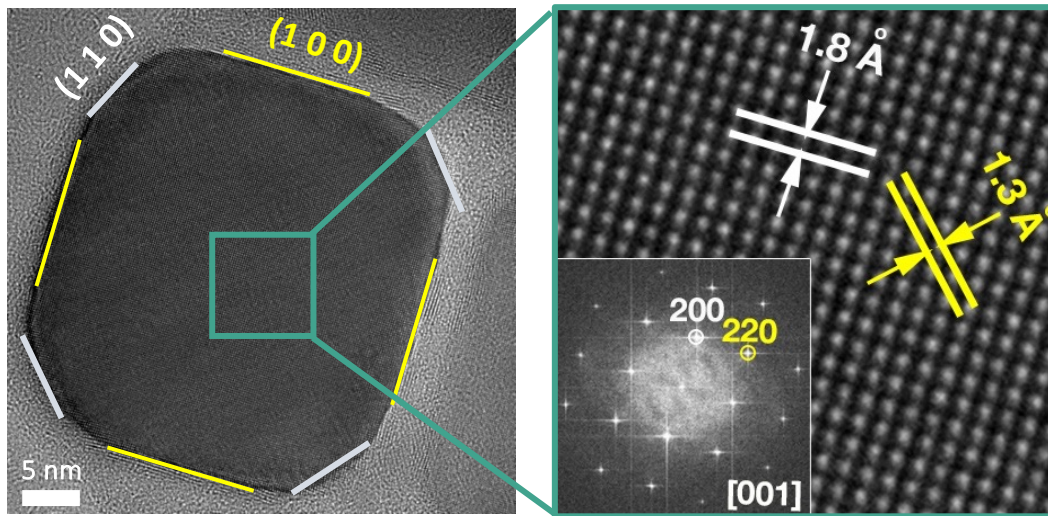
FE (CH₄) = 50 %



Loiudice et al. Buonsanti*, *Angew. Chem. Int. Ed.* (2016); Huang et al., Buonsanti* *Nature Commun.* (2018) Iyengar et al., Buonsanti* *Chem. Commun.* (2019)

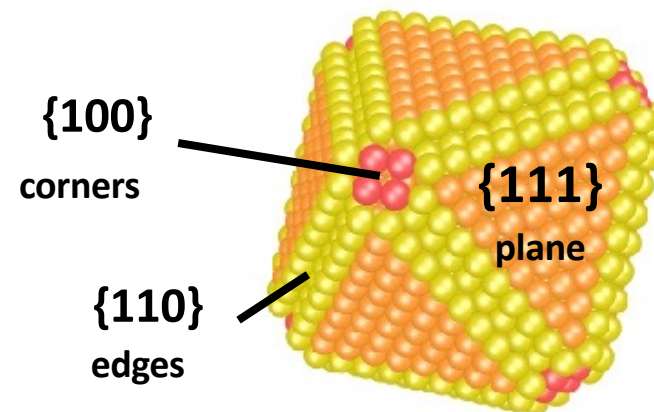
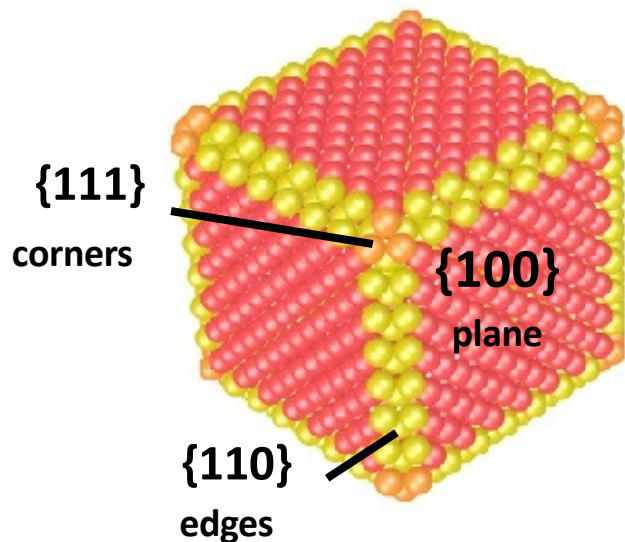
8.3. CO₂ Electrolyzers

Learning about the crystal structure of the cubes



8.3. CO₂ Electrolyzers

The facet ratio is size dependent



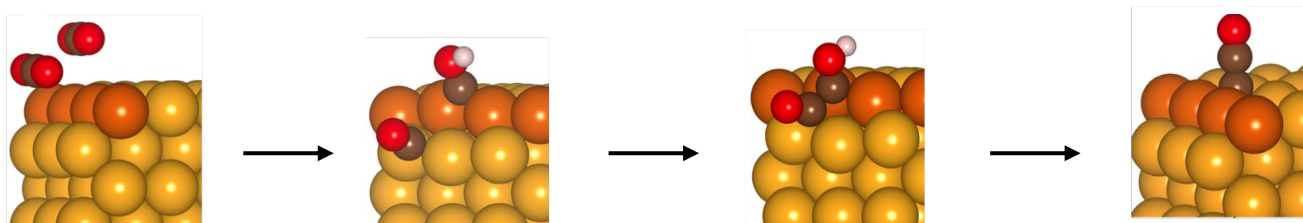
16 nm	{110}/{100}	1.12
41 nm	{110}/{100}	0.75
65 nm	{110}/{100}	0.55

75 nm	{110}/{111}	0.22
150 nm	{110}/{111}	0.12
310 nm	{110}/{111}	0.07

Loiudice et al. Buonsanti, Angew. Chem. Int. Ed. (2016); Huang et al., Buonsanti* Nature Commun. (2018) Iyengar et al., Buonsanti* Chem. Commun. (2019)*

8.3. CO₂ Electrolyzers

Dual-facet mechanism favors C-C coupling

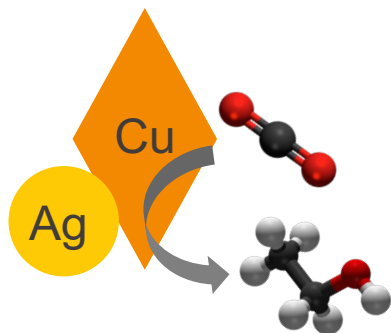


DFT calculations indicate that the $\{110\}/\{100\}$ interface improves the C-C coupling kinetics by favoring the formation of OCCOH*.

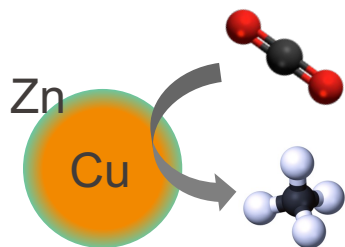
The 44 nm CuNCs give the optimal $\{110\}/\{100\}$ ratio to drive the reaction pathway towards the formation of ethylene.

8.3. CO₂ Electrolyzers

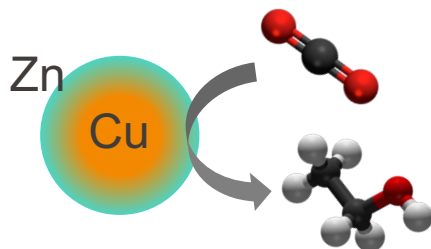
Coupling copper with different materials changes selectivity



Cu octahedra + Ag NCs generate ethanol as the main product



Zn=5%



Zn=19%

Cu@CuZn generate methane or ethanol depending on the Zn amount

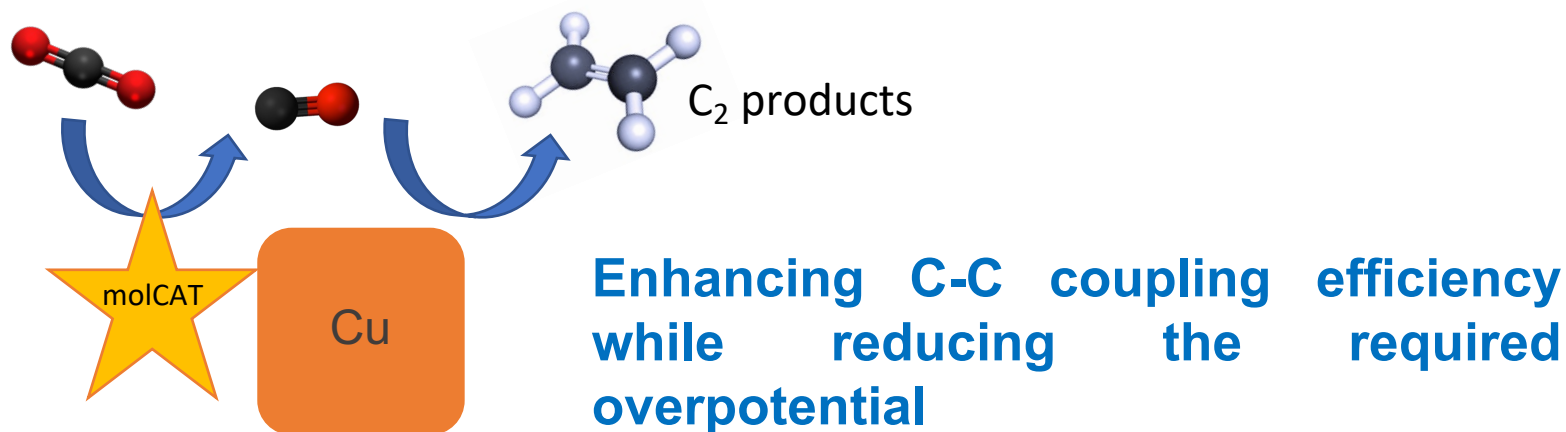
Iyengar et al., Calle-Vallejo, Buonsanti *ACS Catal.* (2021)

Varandili et al., Buonsanti *Chem. Sci.* (2021)

8.3. CO₂ Electrolyzers

Coupling copper with different materials changes selectivity

Tandem catalysts by coupling Cu NCs with molecular catalysts

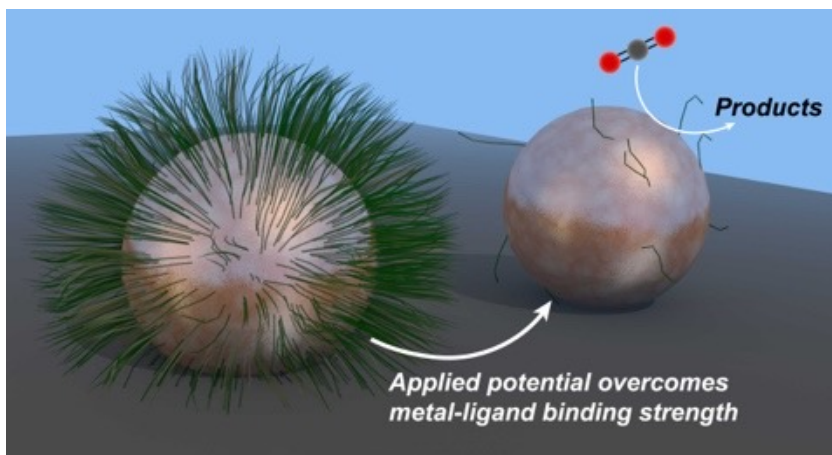


8.3. CO₂ Electrolyzers

What about the ligands during catalysis?

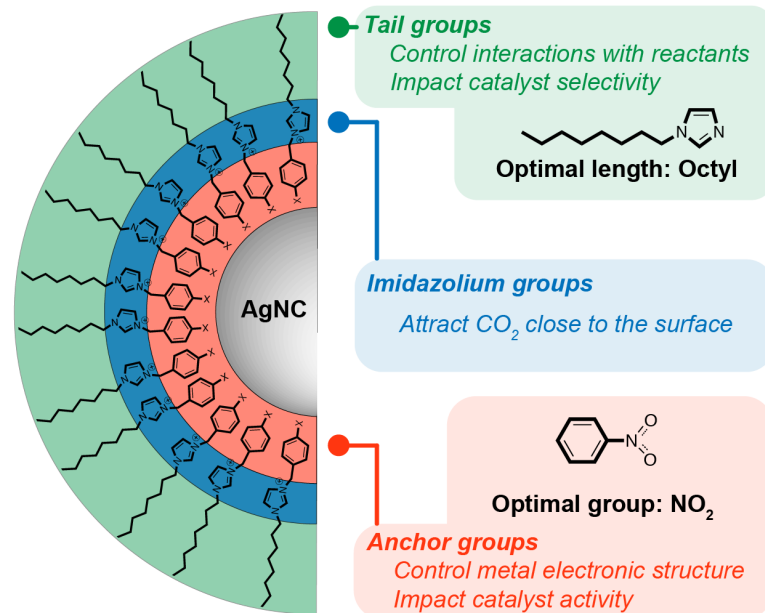
Ligand removal:

- Gentle removal by nitrogen plasma/solvent washing before catalysis
- In-situ electrodesorption



Ligands as promoters

Imidazolium-based ligands tune the intrinsic activity of Ag NCs



Pankhurst et al, Buonsanti* Chem. Sci. (2020)

Huang et al., Buonsanti* Nature Commun. (2018)

Pankhurst et al, Buonsanti* Chem. Sci. (2019)

Pankhurst et al, Buonsanti* Chem. Sci. (2020)

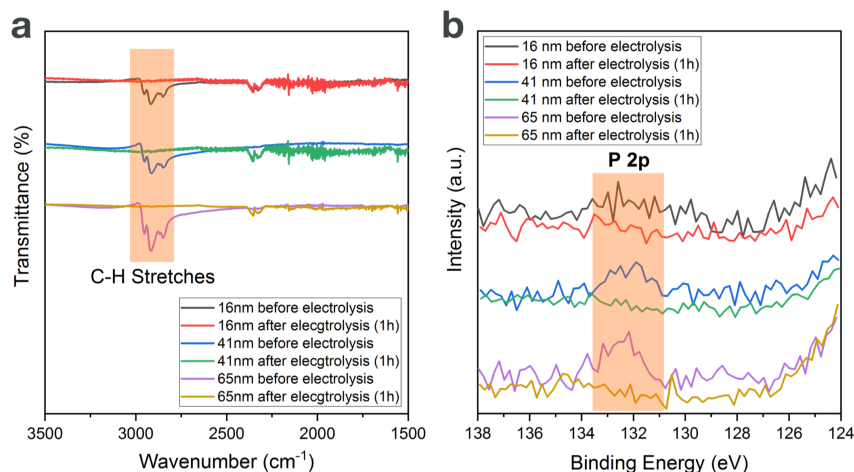
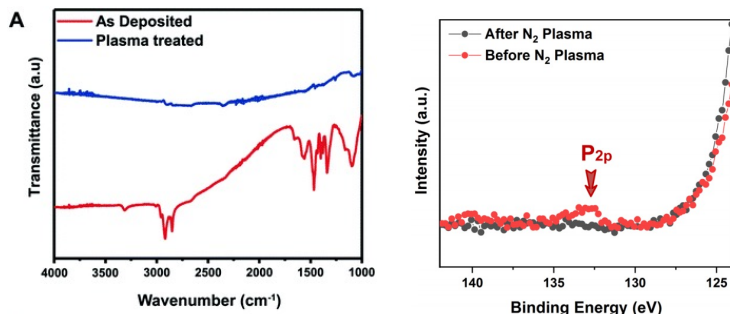
Pankhurst et al, Buonsanti* Inorg. Chem. (2021) 66

8.3. CO₂ Electrolyzers

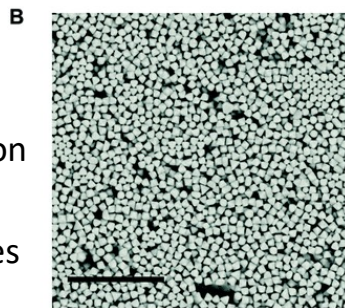
What about the ligands during catalysis?

Option 1: Gentle removal before catalysis
(nitrogen plasma, solvent washing)

Option 2: Ligand electrodesorption
(ligand are removed by the cathodic potential within the first 10 minutes)



- FTIR and XPS confirm ligand removal
- XPS evidences no changes in Cu oxidation state
- TEM shows no changes in morphology



The activity (current) increases after ligand stripping. The selectivity does not change.

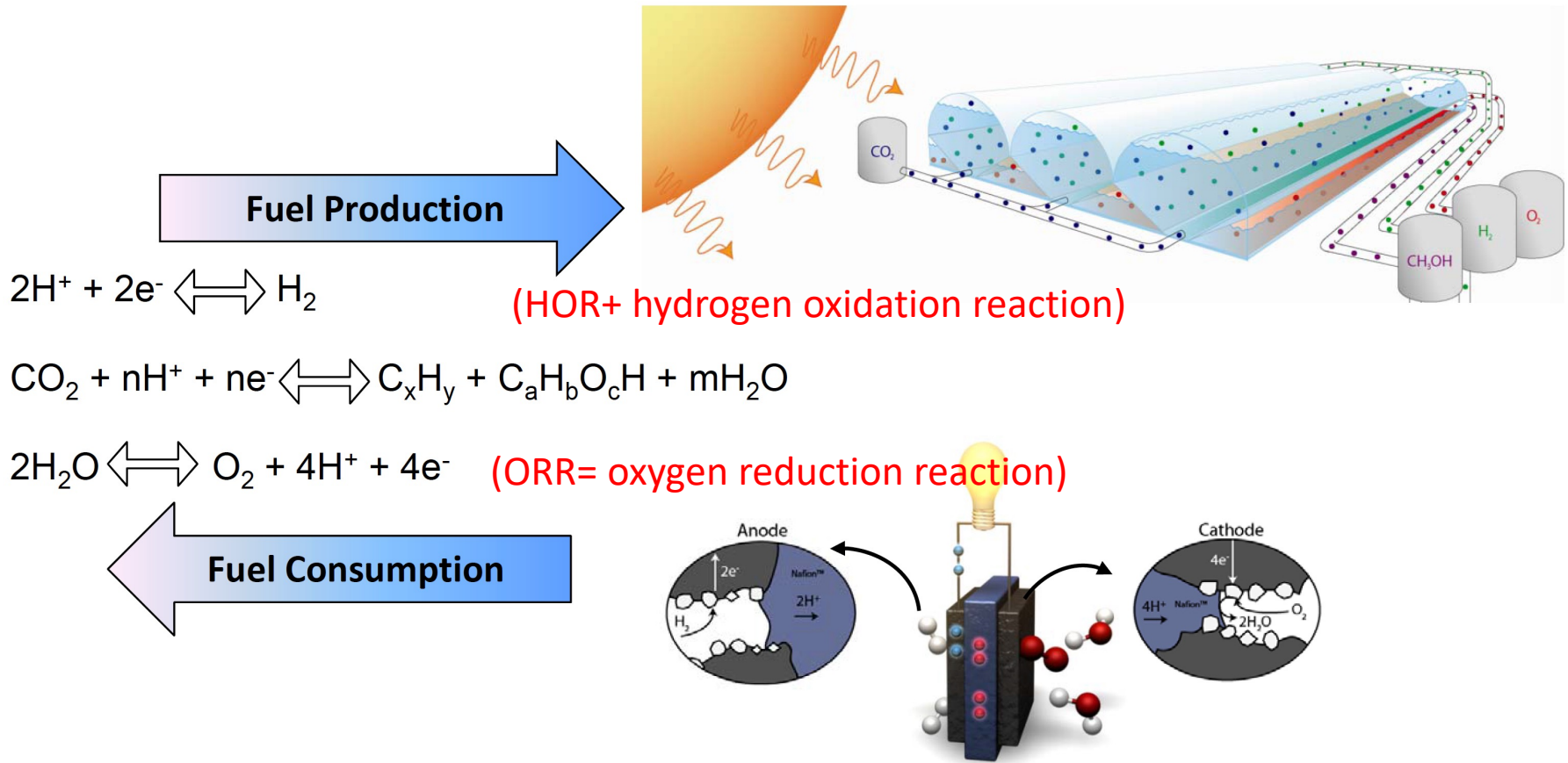
Huang et al., Buonsanti* *Nature Commun.* (2018)

Pankhurst et al. Buonsanti*, *submitted*

P. Alivisatos *JACS* (2014), P. Yang et al. *JACS* (2017)

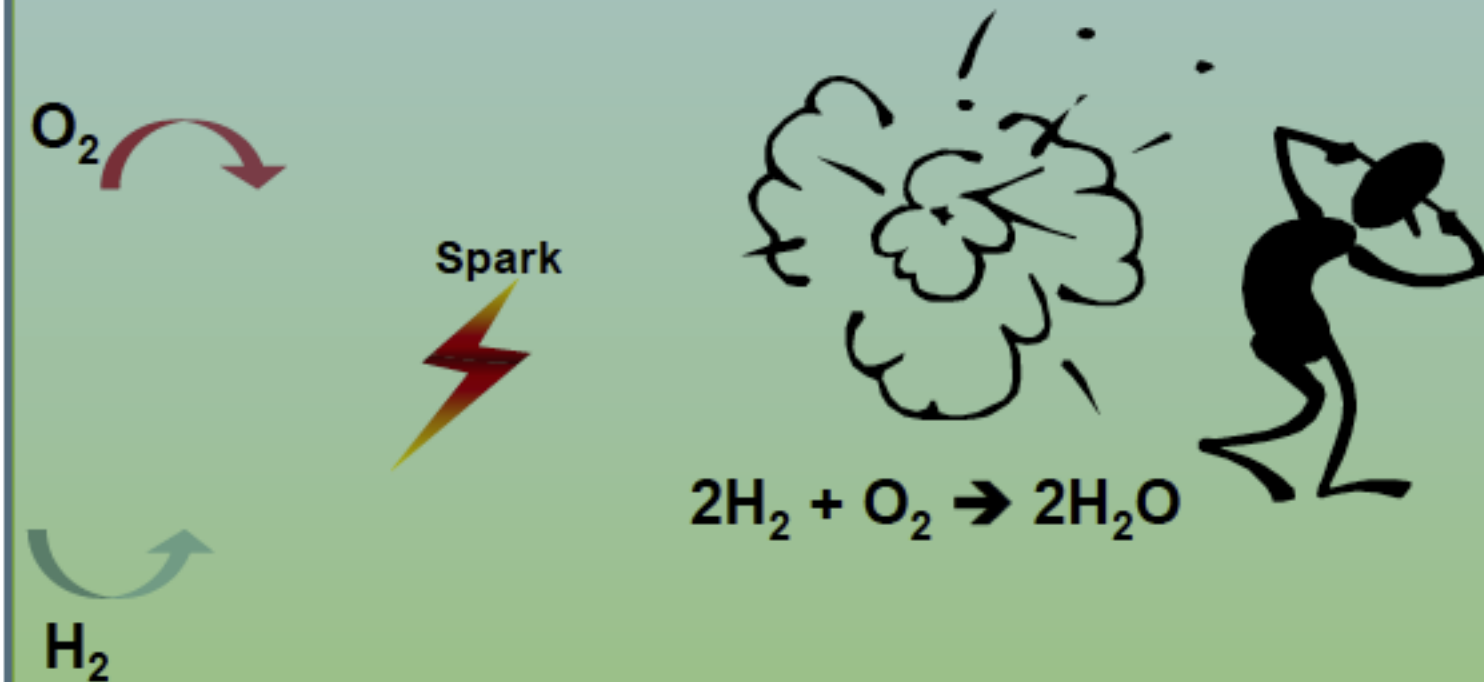
8.4. Fuel cells

Same reactions but opposite direction!



Combustion vs. Fuel Cell

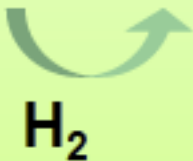
- No fuel cell



8.4. Fuel cells

Combustion vs. Fuel Cell

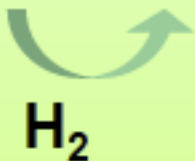
- With fuel cell:
 - Oxygen and hydrogen gas are separated by the electrolyte, the nature of which determines the fuel cell type



Combustion vs. Fuel Cell

- **Solid Oxide Fuel Cell (SOFC) example:**

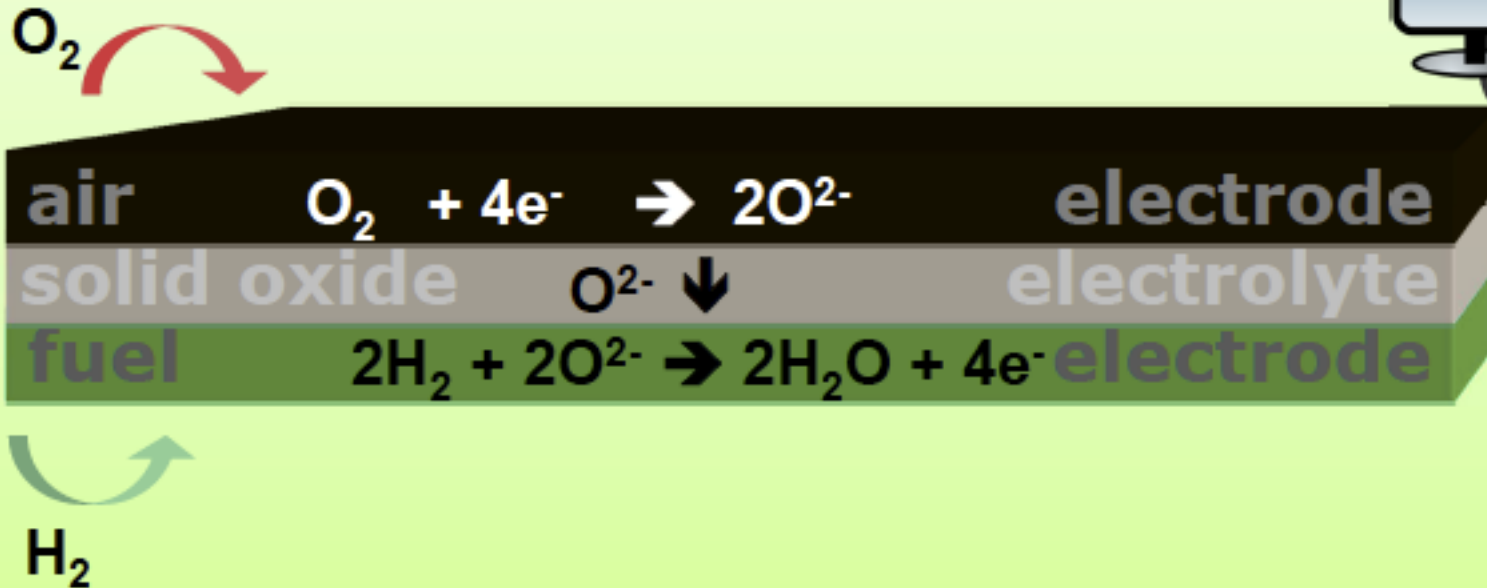
- Oxygen and hydrogen gas are separated by a solid oxide electrolyte



Combustion vs. Fuel Cell

- **Solid Oxide Fuel Cell (SOFC) example:**

- Oxygen and hydrogen gas are separated by a solid oxide electrolyte
- And react on each side of it on the electrodes
- Producing electricity and heat



8.4. Fuel cells

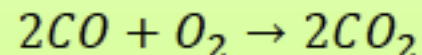
Fuel Cell Types

	Low temperature			High temperature	
Name	AFC	PE(M)FC	PAFC	SOFC	MCFC
Electrolyte	Alkaline	Polymer	Phosphoric acid	Ceramic	Molten carbonate
Charge carrier	OH^-	H^+	H^+	O^{2-}	CO_3^{2-}
T (°C)	80-220	80	200	700-900	650
Fuel	H_2	H_2	H_2	HCs/CO/ H_2	$(\text{H}_2)\text{CO}/\text{CH}_4$
η_{el} (%) *	50-60	40-45	40-45	50-70	50-60

Fuel Cell Key Characteristics

- ✓ High electrical efficiency (40-70%)
- ✓ Low emissions (CO_2), no NO_x , no noise
- ✓ Modular concept (from kilowatts to megawatts)

- ✓ Specifically SOFC:
 - ✓ High tolerance towards fuel contaminants
 - ✓ Fuel derived from conventional and sustainable sources (e.g., natural gas, biogas, hydrogen, liquid hydrocarbons)



8.4. Fuel cells

Electrolysis Technologies

	AEC	PEM	SOEC
Reactant	H ₂ O	H ₂ O	H ₂ O, CO ₂
Overall reaction	H ₂ O → H ₂ +1/2 O ₂	H ₂ O → H ₂ +1/2 O ₂	H ₂ O → H ₂ +1/2 O ₂ CO ₂ → CO+1/2 O ₂
Anode reaction	2OH ⁻ → 1/2O ₂ +H ₂ O+2e ⁻	H ₂ O → 1/2O ₂ +2H ⁺ +2e ⁻	O ²⁻ → 1/2O ₂ +2e ⁻
Cathode reaction	2H ₂ O+2e ⁻ → H ₂ +2OH ⁻	2H ⁺ +2e ⁻ → H ₂	H ₂ O+2e ⁻ → H ₂ +O ²⁻
Charge carrier	OH ⁻	H ⁺	O ²⁻
Electrolyte	NaOH, KOH	polymer	ceramic
Electrodes	Nickel	Pt/C/IrO ₂	Nickel, ceramic
Temperature	80 °C	80 °C	750-900 °C

S.D. Ebbesen, S.H. Jensen, A. Hauch, and M.B. Mogensen, Chem. Rev. 2014, 114, 10697–10734

8.4. Fuel cells

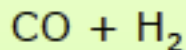
Electrolysis Technologies

	AEC	PEM	SOEC
Reactant	H_2O	H_2O	$\text{H}_2\text{O}, \text{CO}_2$
Overall reaction	Commercially available, cheap cell materials Low efficiencies	$\text{H}_2\text{O} \rightarrow \text{H}_2 + 1/2 \text{O}_2$	$\text{H}_2\text{O} \rightarrow \text{H}_2 + 1/2 \text{O}_2$ $\text{CO}_2 \rightarrow \text{CO} + 1/2 \text{O}_2$
Anode reaction	$2\text{OH}^- \rightarrow 1/2 \text{O}_2 + \text{H}_2\text{O} + 2\text{e}^-$	Commercially available Expensive materials, electrode and electrolyte durability issues, increased hydrogen crossover at elevated Temperatures	$\text{O}^{2-} \rightarrow 1/2 \text{O}_2 + 2\text{e}^-$
Cathode reaction	$2\text{H}_2\text{O} + 2\text{e}^- \rightarrow \text{H}_2 + 2\text{OH}^-$		$\text{H}_2\text{O} + 2\text{e}^- \rightarrow \text{H}_2 + \text{O}^{2-}$
Charge carrier	OH^-		O^{2-}
Electrolyte	NaOH, KOH	polymer	High efficiencies and the possibility to produce synthesis gas, cheap cell materials Not commercially available
Electrodes	Nickel	$\text{Pt}/\text{C}/\text{IrO}_2$	
Temperature	80 °C	80 °C	

S.D. Ebbesen, S.H. Jensen, A. Hauch, and M.B. Mogensen, Chem. Rev. 2014, 114, 10697–10734

Electrolysis Technologies

- Specifics of solid oxide electrolysis cells (SOECs)
 - ✓ Larger efficiencies can be obtained (increase with temperature, close to 100%)
 - ✓ Better economic potential:
 - ✓ No noble metals, cheap materials
 - ✓ Truly reversible operation
 - ✓ Electrolysis of both H₂O and CO₂ yielding synthesis gas



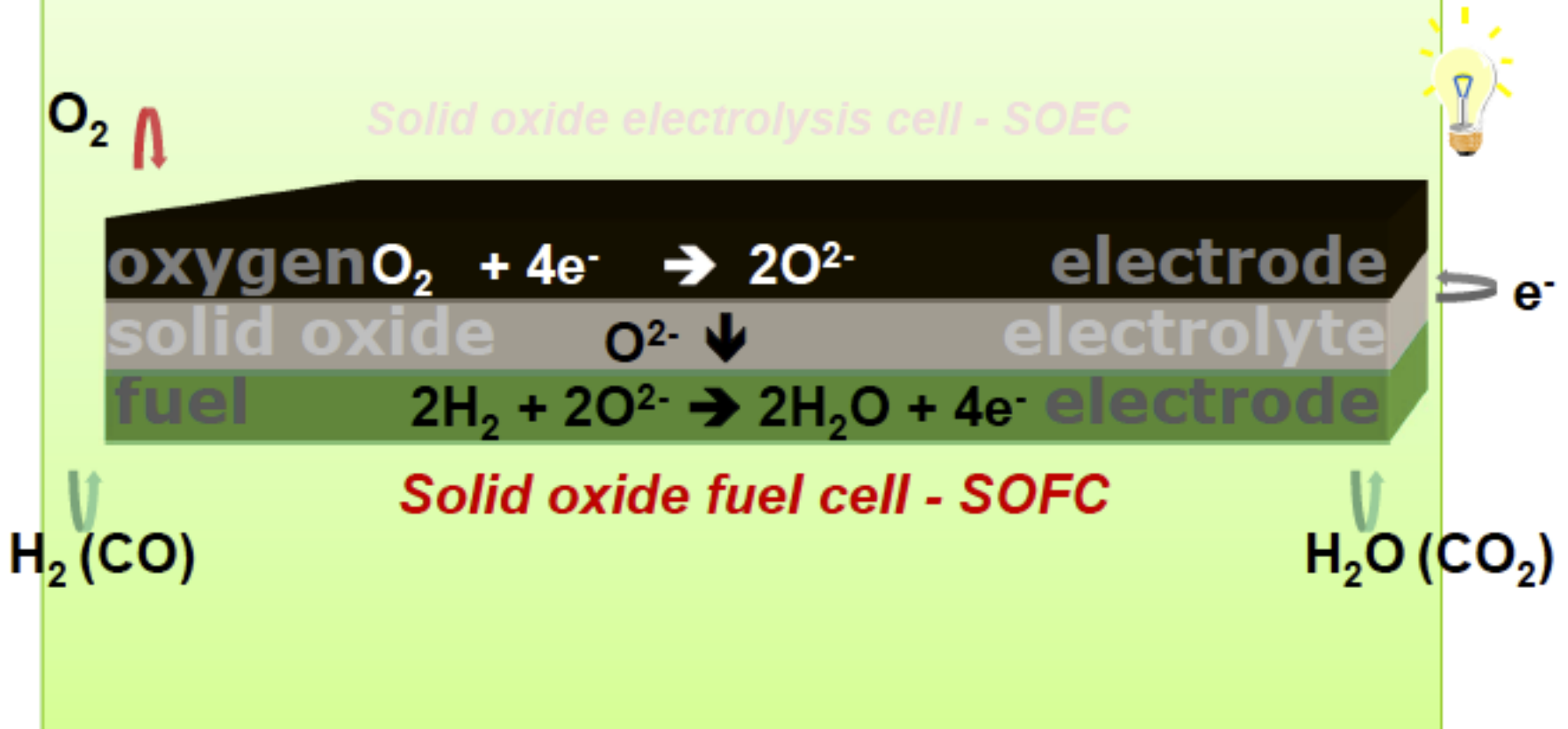
Through known catalytic processes:

- ✓ Fischer Tropsch fuels
- ✓ Methane (synthetic natural gas)
- ✓ Methanol
 - Application in the transport sector and using existing infrastructure

8.4. Fuel cells

Solid Oxide Cells

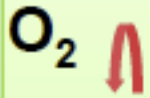
Direct mode of operation



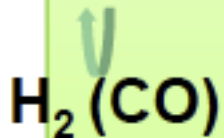
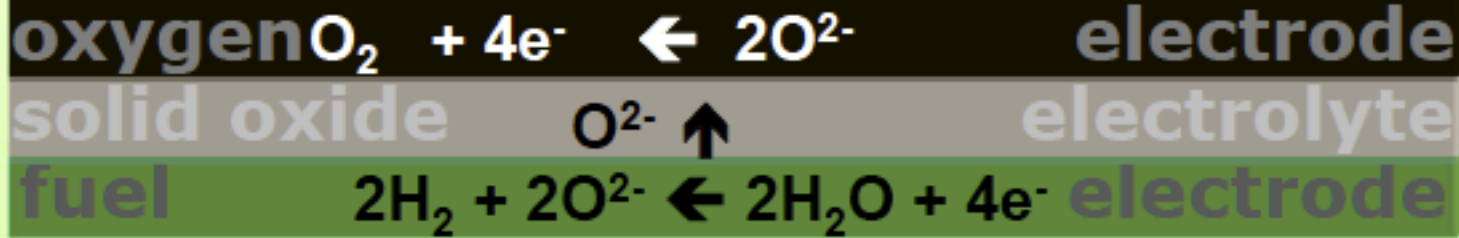
8.4. Fuel cells

Solid Oxide Cells

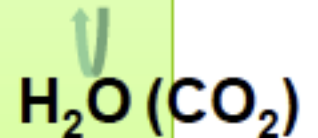
Reverse mode of operation



Solid oxide electrolysis cell - SOEC



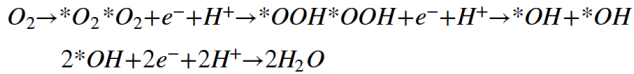
Solid oxide fuel cell - SOFC



8.4. Fuel cells

NCs for ORR: The case of Pt-Ni

Mechanism 1



Mechanism 2

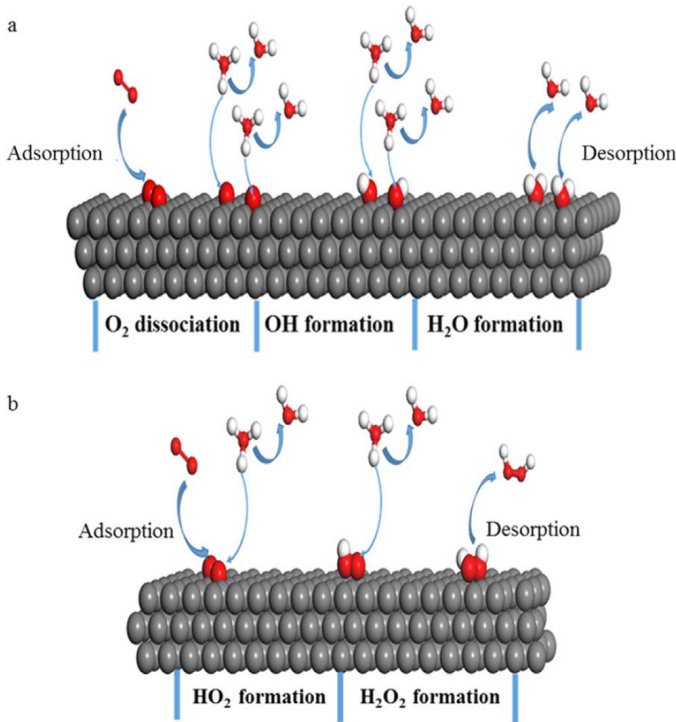
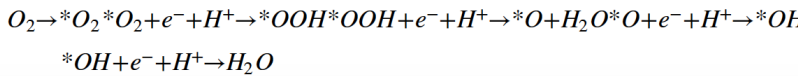


Fig. 1. Mechanism schematics based on the work of Zhang et al. [24] of (a) full reduction and (b) partial reduction of oxygen.

The need: to substitute Pt for OER!

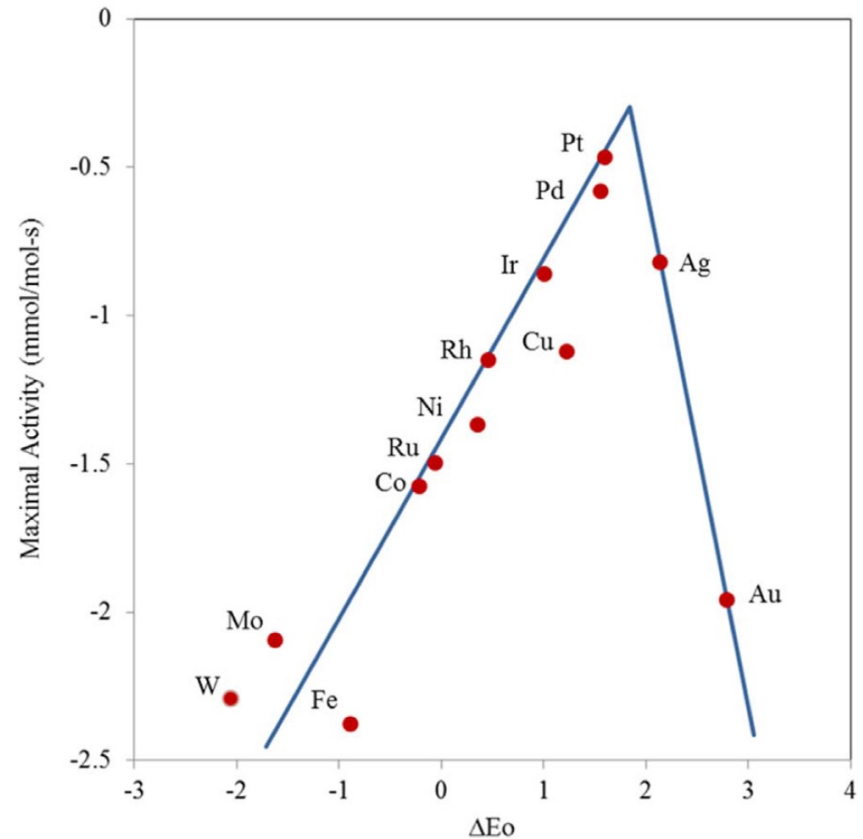


Fig. 2. Volcano plot showing relationship between oxygen binding energy and maximal activity calculated using Sabatier Analysis. Reproduced with permission from Nørskov, J.K., et al., *Origin of the overpotential for oxygen reduction at a fuel-cell cathode*. The Journal of Physical Chemistry B, 2004. 108(46): p. 17886–17892. Copyright 2004 American Chemical Society. [23,29].

8.4. Fuel cells

NCs for ORR: The case of Pt-Ni

Improved Oxygen Reduction Activity on Pt₃Ni(111) via Increased Surface Site Availability

Vojislav R. Stamenkovic,^{1,2*} Ben Fowler,³ Bongjin Simon Mun,² Guofeng Wang,⁴ Philip N. Ross,² Christopher A. Lucas,³ Nenad M. Marković^{1*}

NANO LETTERS

Letter

pubs.acs.org/NanoLett

Synthesis and Characterization of 9 nm Pt–Ni Octahedra with a Record High Activity of 3.3 A/mg_{Pt} for the Oxygen Reduction Reaction

Sang-Il Choi,[†] Shuifen Xie,[†] Minhua Shao,^{*‡} Jonathan H. Odell,[‡] Ning Lu,[§] Hsin-Chieh Peng,^{||} Lesia Protsailo,[‡] Sandra Guerrero,[‡] Jinho Park,^{||} Xiaohu Xia,[†] Jinguo Wang,[§] Moon J. Kim,^{§,1} and Younan Xia^{*†,||,‡}

Highly Crystalline Multimetallic Nanoframes with Three-Dimensional Electrocatalytic Surfaces

Chen Chen,^{1,2,3*} Yijin Kang,^{4*} Ziyang Huo,^{1,2} Zhongwei Zhu,^{1,2} Wenyu Huang,^{1,2} Huolin L. Xin,² Joshua D. Snyder,⁴ Dongguo Li,⁴ Jeffrey A. Herron,⁵ Manos Mavrikakis,⁵ Miaofang Chi,⁶ Karren L. More,⁶ Yadong Li,³ Nenad M. Marković,⁴ Gabor A. Somorjai,^{1,2} Peidong Yang,^{1,2,7,8†} Vojislav R. Stamenkovic^{4†}

ARTICLE

Trends in electrocatalysis on extended and nanoscale Pt-bimetallic alloy surfaces

VOJISLAV R. STAMENKOVIC^{1,2*}, BONGJIN SIMON MUN^{2,3}, MATTHIAS ARENZ⁴, KARL J. J. MAYRHOFER⁵, CHRISTOPHER A. LUCAS⁵, GUOFENG WANG⁶, PHILIP N. ROSS² AND NENAD M. MARKOVIC^{1*}

nature
materials

ARTICLES

PUBLISHED ONLINE: 16 JUNE 2013 | DOI: 10.1038/NMAT3668

Compositional segregation in shaped Pt alloy nanoparticles and their structural behaviour during electrocatalysis

Chunhua Cui¹, Lin Gan¹, Marc Heggen², Stefan Rudi¹ and Peter Strasser^{1*}

ARTICLES

PUBLISHED ONLINE: 15 AUGUST 2016 | DOI: 10.1038/NMAT4724

nature
materials

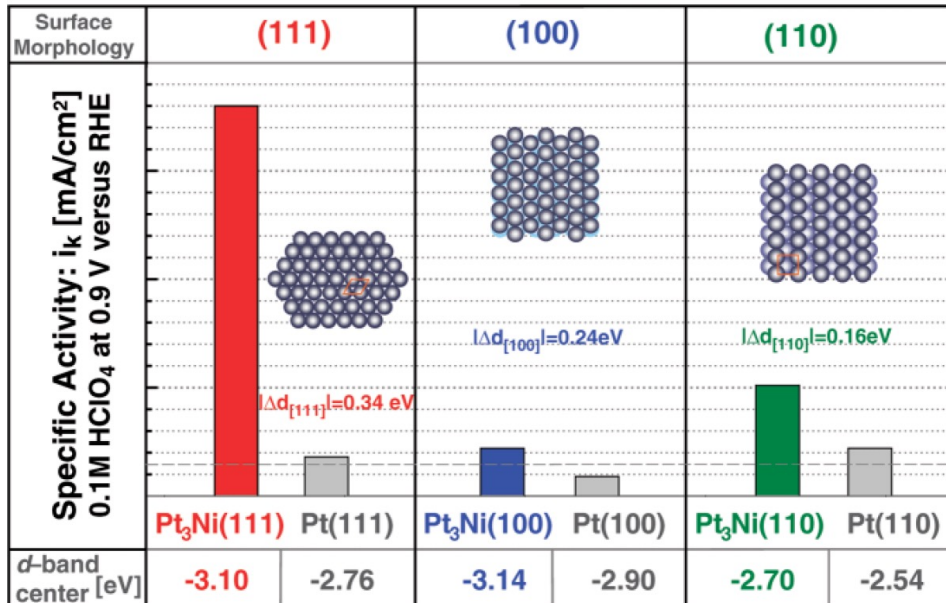
Anisotropic phase segregation and migration of Pt in nanocrystals en route to nanoframe catalysts

Zhiqiang Niu^{1†}, Nigel Becknell^{1†}, Yi Yu^{1,2}, Dohyung Kim³, Chen Chen^{1,4}, Nikolay Kornienko¹, Gabor A. Somorjai^{1,2,5} and Peidong Yang^{1,2,3,5*}

8.4. Fuel cells

NCs for ORR: The case of Pt-Ni

Stamenkovic et al. demonstrate that the **Pt₃Ni(111) surface** is 10-fold more active for ORR than the corresponding Pt (111) surface and 90-fold more active than the current state-of-art Pt/C catalysts. The Pt₃Ni(111) surface has an unusual electronic structure (d-band center position) and arrangement of surface atoms in the near-surface region. Under operating conditions relevant to fuel cells, its near-surface layer exhibits a highly structured compositional oscillation in the outermost and third layer, which are Pt-rich, and in the second atomic layer, which is Ni-rich. The weak interaction between the Pt surface atoms and nonreactive oxygenated species increases the number of active sites for O₂ absorption.

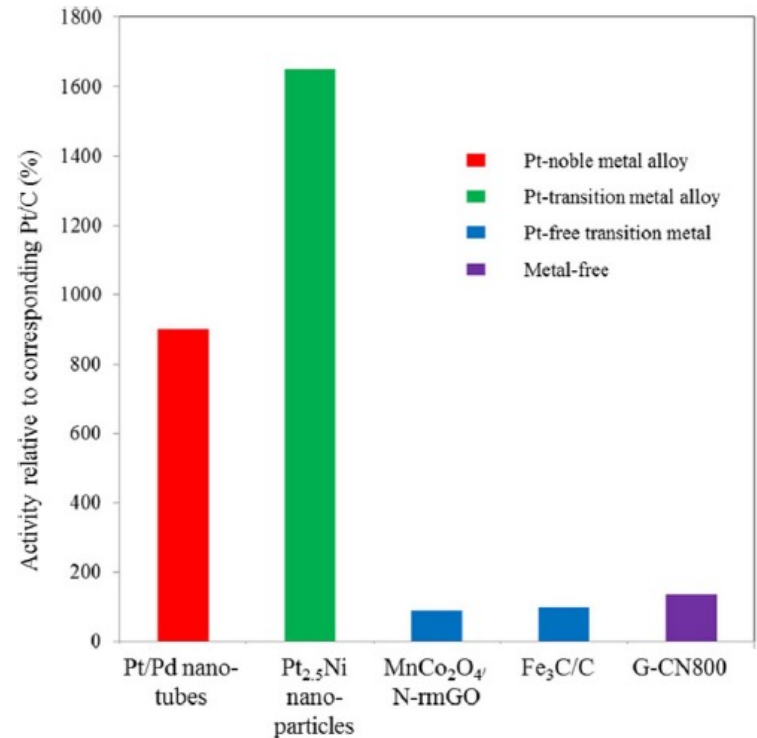
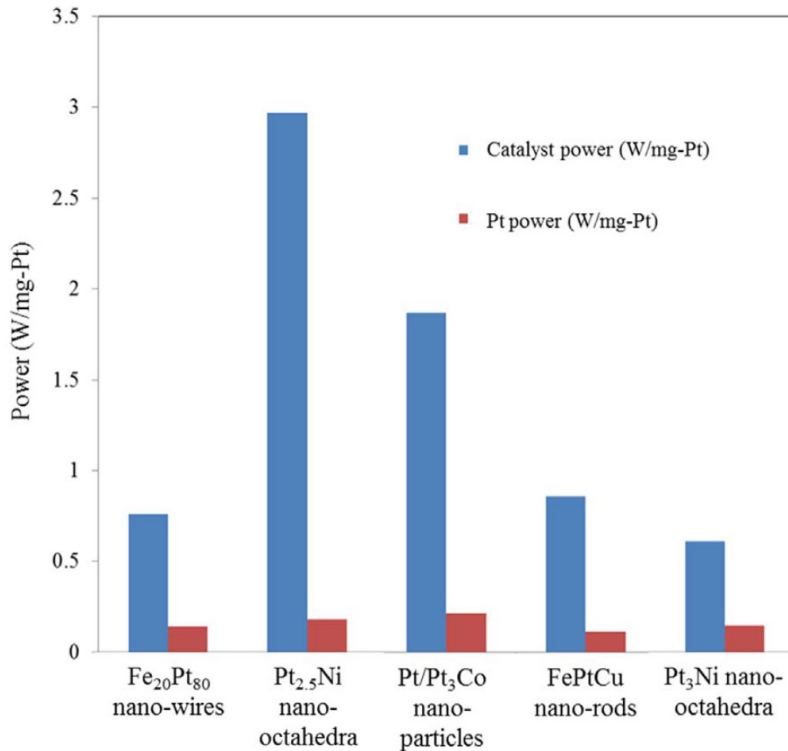


Considering that the Pt₃Ni(111)-skin surface exhibits the highest catalytic activity that has ever been detected, the challenge would be to create a nanocatalyst with electronic and morphological properties that mimic the Pt₃Ni(111) surface. Therefore in the future, a way to reduce the current value (~1.0g of Pt per kW) of Pt-specific power density in a PEMFC without a loss in cell voltage, while also maintaining the maximum power density (W/cm²), would be the engineering of Pt₃Ni(111)-skin-like nanocatalysts.

8.4. Fuel cells

NCs for ORR: The case of Pt-Ni

Following this work, a number of research groups successfully prepared octahedral nanoparticles of Pt-Ni alloys enclosed by {111} facets. However the highest activity was only 10 fold higher than the commercial Pt/C catalyst.



8.4. Fuel cells

NCs for ORR: The case of Pt-Ni

Compositional segregation in shaped Pt alloy nanoparticles and their structural behaviour during electrocatalysis

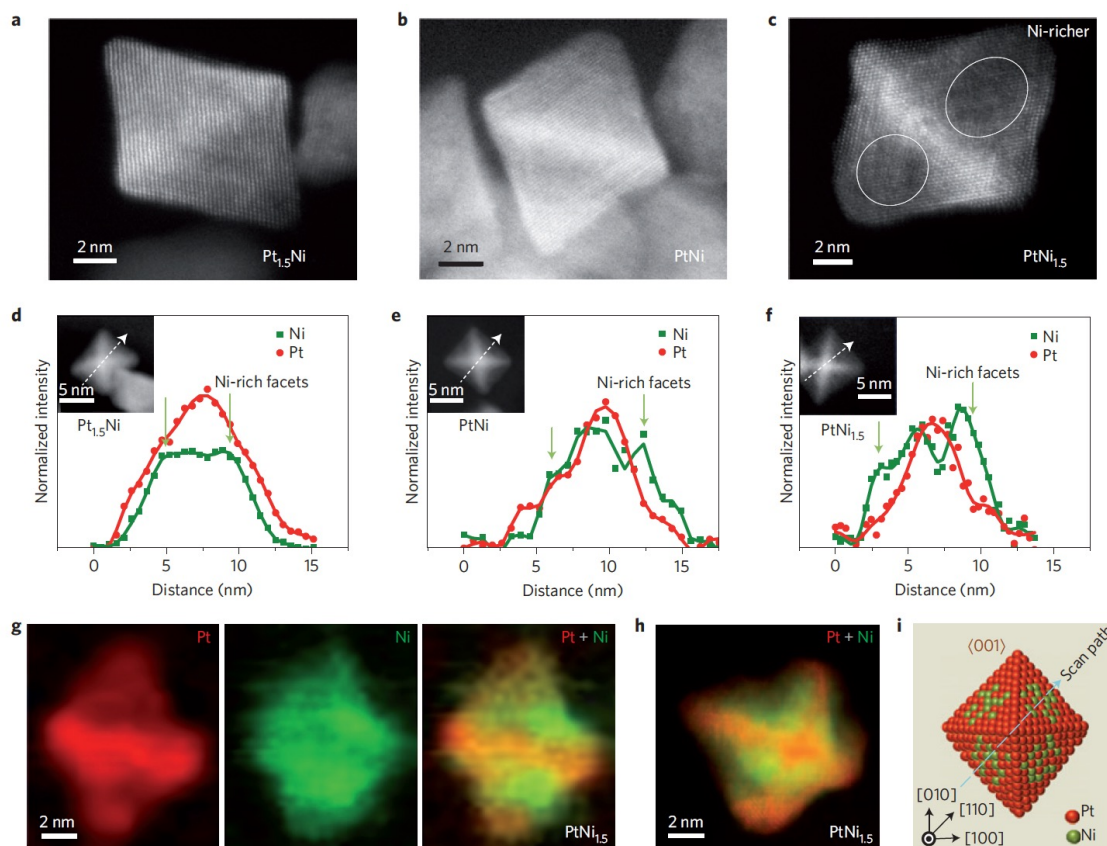
Chunhua Cui¹, Lin Gan¹, Marc Heggen², Stefan Rudi¹ and Peter Strasser^{1*}

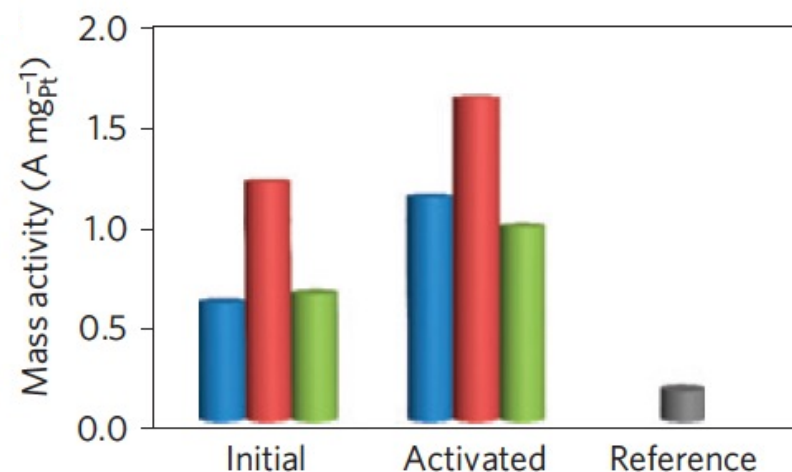
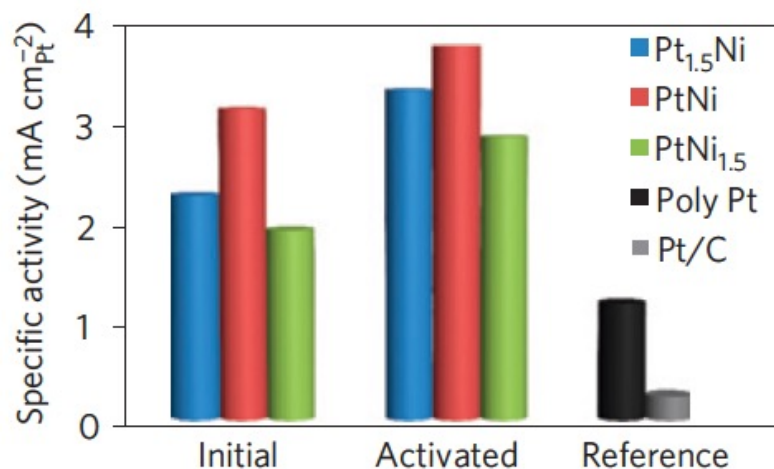
Figure 1 | Atomic-scale Z-contrast STEM images and composition profile analysis of Pt_xNi_{1-x} octahedral nanoparticles. **a-c**, Z-contrast STEM images of Pt_{1.5}Ni (**a**), PtNi (**b**) and PtNi_{1.5} (**c**) octahedral nanoparticles close to the (110) zone axis. **d-f**, EELS line scan analysis of Pt_{1.5}Ni, PtNi and PtNi_{1.5} octahedral nanoparticles close to the (100) zone axis, respectively. The scan path is specified along the [110] direction passing through the longest major axis to track the Ni composition profile. The insets are the Z-contrast images of a corresponding single nanoparticle. Further information can be found in Supplementary Fig. S3. **g**, EELS element map of PtNi_{1.5} shows the segregated distribution of Pt (red) and Ni (green) in a particle close to the (110) zone axis. **h**, Composite image of a HAADF image showing mainly Pt (red) and an EELS map showing Ni (green) in a particle close to the (100) zone axis. **i**, Ball schematic sketch shows the particle model along the (001) zone axis and the Ni-rich facet profile and Pt-rich frame.

8.4. Fuel cells

NCs for ORR: The case of Pt-Ni

Compositional segregation in shaped Pt alloy nanoparticles and their structural behaviour during electrocatalysis

Chunhua Cui¹, Lin Gan¹, Marc Heggen², Stefan Rudi¹ and Peter Strasser^{1*}



“Activated” represent the carbon-supported octahedra after 25 potential cycles in the potential region 0.06-1VRHE at a scan rate of 250 mV s⁻¹

8.4. Fuel cells

NCs for ORR: The case of Pt-Ni

Ni^{2+} leaches out of the structure during ORR because Pt is much more stable to oxidation.

Compositional segregation in shaped Pt alloy nanoparticles and their structural behaviour during electrocatalysis

Chunhua Cui¹, Lin Gan¹, Marc Heggen², Stefan Rudi¹ and Peter Strasser^{1*}

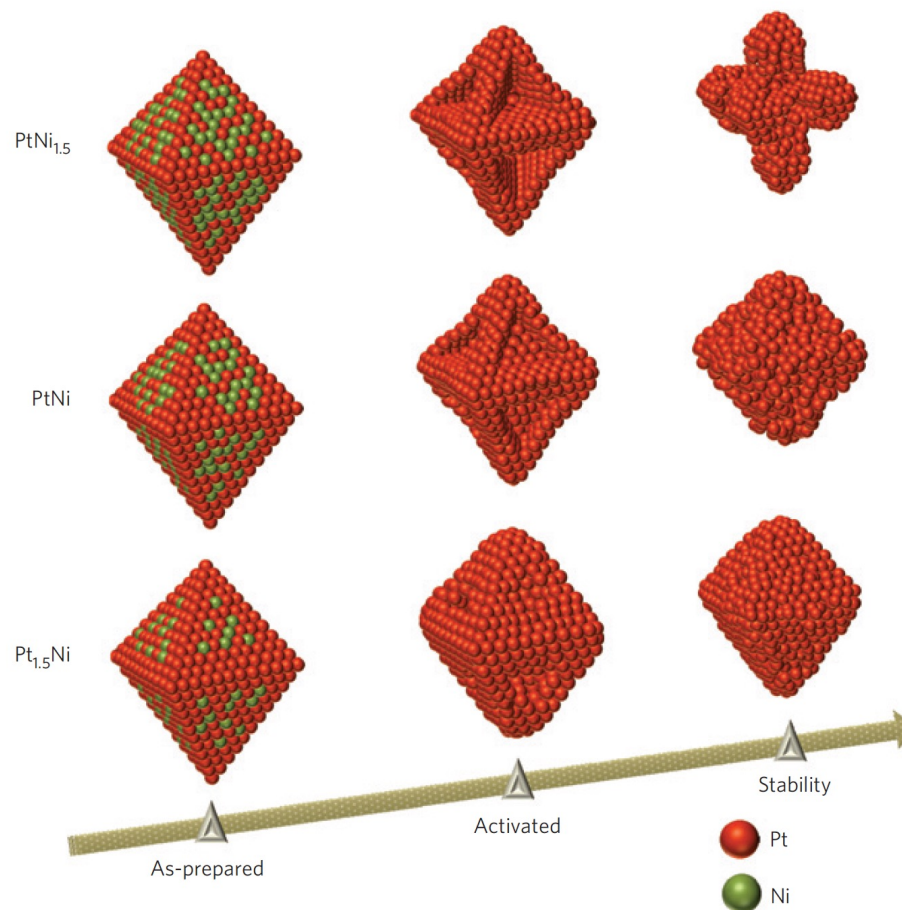
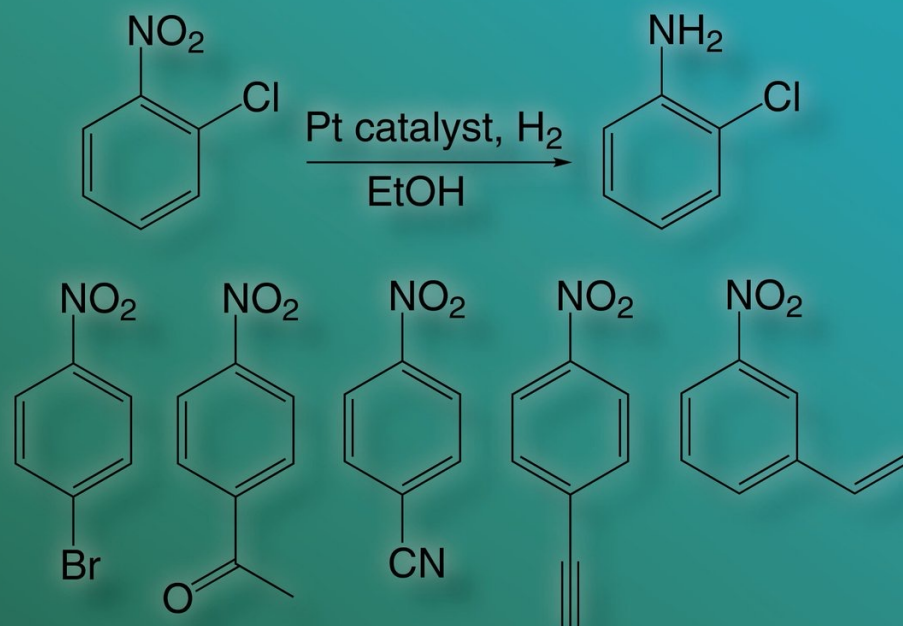


Figure 5 | Morphology and surface structural changes of Pt_xNi_{1-x} octahedra. Schematic representation of the Pt_xNi_{1-x} nanoparticle morphology and surface structure changes after electrochemical surface activation (25 potential cycles) and electrochemical stability tests relative to as-synthesized nanoparticles.

Colloidal NCs have demonstrated improved mass activity and selectivity to the point that industry commercializes colloidal catalysts

*Innovative
Pd and Pt
NanoSelect™
catalysts sold
in collaboration
with BASF*

STREM
CHEMICALS, INC.
ESTABLISHED 1964



Substituted nitroarene substrates for selective hydrogenation to the corresponding anilines using NanoSelect Pt-100 (78-1630) or Pt-200 (78-1635)